Washington University in St. Louis
Washington University Open Scholarship

All Theses and Dissertations (ETDs)

8-31-2012

Reading Your Own Mind: Dynamic Visualization of Real-Time Neural Signals

Zachary V. Freudenburg
Washington University in St. Louis

Follow this and additional works at: http://openscholarship.wustl.edu/etd

Recommended Citation
Freudenburg, Zachary V., "Reading Your Own Mind: Dynamic Visualization of Real-Time Neural Signals" (2012). *All Theses and Dissertations (ETDs)*. 954.
http://openscholarship.wustl.edu/etd/954

This Dissertation is brought to you for free and open access by Washington University Open Scholarship. It has been accepted for inclusion in All Theses and Dissertations (ETDs) by an authorized administrator of Washington University Open Scholarship. For more information, please contact digital@wumail.wustl.edu.

WASHINGTON UNIVERSITY IN ST. LOUIS
SCHOOL OF ENGINEERING AND APPLIED SCIENCE

Department of Computer Science and Engineering

Dissertation Examination Committee:
Robert B. Pless, Chair
Ron K. Cytron
Caitlin Kelleher
Eric C. Leuthardt
Joseph A. O'Sullivan
William D. Smart

Reading Your Own Mind:
Dynamic Visualization Of Real-time Neural Signals

by
Zachary Voges Freudenburg

A dissertation presented to the
Graduate School of Arts and Sciences
of Washington University in
partial fulfillment of the
requirements for the degree
of Doctor of Philosophy

August 2012
Saint Louis, Missouri

WASHINGTON UNIVERSITY IN ST. LOUIS
SCHOOL OF ENGINEERING AND APPLIED SCIENCE

Department of Computer Science and Engineering

ABSTRACT

Reading Your Own Mind:
Dynamic Visualization Of Real-time Neural Signals
by
Zachary Voges Freudenburg
Advisor: Robert B. Pless
August 2012
St. Louis, Missouri

Brain Computer Interfaces (BCI) systems which allow humans to control external devices directly from brain activity, are becoming increasingly popular due to dramatic advances in the ability to both capture and interpret brain signals. Further advancing BCI systems is a compelling goal both because of the neurophysiology insights gained from deriving a control signal from brain activity and because of the potential for direct brain control of external devices in applications such as brain injury recovery, human prosthetics, and robotics. The dynamic and adaptive nature of the brain makes it difficult to create classifiers or control systems that will remain effective over time. However it is precisely these qualities that offer the potential to use feedback to build on simple features and create complex control features that are robust over time. This dissertation presents work that addresses these opportunities for the specific case of Electrocorticography (ECoG) recordings from clinical epilepsy patients. First, queued patient tasks were used to explore the predictive nature of both local and global features of the ECoG signal. Second, an algorithm was developed and tested for estimating the most informative features from naive observations of ECoG signal. Third, a software system was built and tested that facilitates real-time visualizations of ECoG signal patients and allows ECoG epilepsy patients to engage in an interactive BCI control feature screening process.

Acknowledgements

I would like to thanks Eric Leuthardt, who invited me into his lab and introduced me to BCI, and all the members of his lab who helped me assemble and interpret ECoG data. I would also like to thanks my advisor who allowed me to make the jump to the other side of the park and then the other side of the Atlantic but didn't let me lose site of the goal line.

Zachary Voges Freudenburg

Washington University in St. Louis
August 2012

To my wife and parents

Contents

List of Tables

List of Figures

Chapter 1

Introduction

1.1 Introduction

The study of Brain Computer Interfaces (BCI) is a rapidly expanding field that seeks to directly measure brain signals well enough to control devices. With recently developed tools to measure electrical signals in the brain, both monkeys and humans have shown the ability to control simple video games, based only on these measured signals. These successes have led to excitement about a vast range of BCI applications. The main challenge limiting these potential applications is the acquisition of control signals based on brain activity.

One dream of BCI would be to use internal speech to create a simple, intuitive, and rich control strategy. A user could directly think of an enormous number of possible commands, such as: "I'd like to watch Matlock PI on TV". Complete measurement of the electrical signals in the brain could conceivably differentiate the presumably unique thought patterns of different sentences. However, current measurement and understanding of brain signals is rather more limited, and the current closest approach to detecting language is recognizing a subject's desire to move tongue or their hand.

The alternative approach is to focus on a small set of simple brain signal features that can be reliably controlled by a user and detected by a BCI system. Because this approach may be able to extract only a few reliable control signals, BCI applications are limited, and application designers are asked to get the most out of a small set of control signals. Most BCI control achieved so far has used this strategy. This thesis tries to extend and improve this second approach. We seek to develop a system that allows for the selection of intuitive and robust control features. We aim for minimal training requirements so that a system can quickly be tuned to a new user. The system we envision has three basic components.

1) The system adaptively defines a set of brain signal features that are robustly responsive to changes in the user's thoughts without pre-screening of the brain signal.

2) The system generates continuous feedback that conveys the dynamics of the brain signal features so that the user can detect features that correspond to thoughts they can control.
3) The system supports the user's ability to select and practice with the specific controllable features, and map those control features to interface elements in a BCI application.

Collectively, these components provide a user with flexibility in finding a set of features that maximizes the efficiency of a brain-computer interface. The challenges to creating such a system are in defining potential brain signal features without extensive pre-screening based on online learning of brain signal dynamic, and generating suitable online feedback about these features to a user.

The remainder of this chapter provides an overview of the context of BCI applications, some of the neuroscience concepts and brain signal acquisition methods that frame our work, the feature characteristics of the brain signals that are used, and the specific contributions of this thesis to the field of BCI. Chapter 2 present a simple approach to defining features based on global patterns of brain signal activity (rather than activity measured at just one electrode location), and gives evidence that these features are more robust and appropriate for BCI. Chapter 3 explores the use of Deep Belief Networks to define independent patterns of brain signals, demonstrates that patterns learned while the patient is resting define a basis to differentiate different signals measured during different activities, and demonstrates that measured signal patterns are consistent over multiple days. Chapter 4 builds the basics of an interactive user interface called the Brain Mirror, allowing one to visualize the activity of different signal patterns to allow a user to automatically select those that they can control. These contributions are reviewed and discussed as a whole in the larger context of brain electrophysiology and BCI feature selection in chapter 5.

1.1.1 Challenges of BCI control feature selection

While BCI has many exciting possible applications, its practical applications remain limited. Exciting recent advances in the ability to measure electrical brain signals have pushed the challenge to finding, within those measurements, useful and reliable brain signal features. This is difficult because of the large volume, high dimensionality and noisy nature of brain activity, where particular thoughts or actions are manifested in highly dynamic and complex patterns. Moreover, these patterns are highly individual and influenced by sensory input, emotional state, past experience and other environmental factors.

BCI control features must meet three main requirements to be suitable for practical use. First, a BCI control feature needs to be reliably induced through intentional mental task performance; otherwise the patient may not be able to produce the feature when desired. Second, the features should be functionally specific to a mental task that can be practically avoided during normal behavior; otherwise the patient may produce the feature accidentally. Third,

practical control features must be robust to the overall variability in the brain signal patterns; otherwise the user and/or the system will be required to frequently rediscover new features.

The brain has evolved to be complex and dynamic because these qualities allow it to be good at learning things and adapting to its environment. While this makes it difficult to find robust and consistent signal patterns, it is possible to also take advantage of these qualities to find control features that meet the above criteria. As an example, mouse control of a cursor might be very un-natural; the 2-dimensional computer screen lies in a different plane than the mouse pad, slight hand motions can create large cursor motions, and even cursors that disappear and re-appear at a different location cause little trouble. In many cases, this ability to link task intentions with the complex behavioral control needed to achieve them requires feedback through sensory inputs. For this reason the focus of this thesis research is centered on developing a reliable real-time visual feedback system that captures the dynamics of complex brain signal patterns and displays them as easily perceivable dynamics on a 2D monitor.

This introduction started with three requirements for a BCI system; these all seek to use this adaptability to make it faster and easier to achieve BCI control. By allowing a subject to 'see' her own brain activity directly we hope to facilitate quick learning of consciously controlled brain signals. This helps to avoid time-consuming pre-screening protocols, and the interactive nature of the system works with the adaptability of our brains to improve the robustness and number of different control features.

1.1.2 ECoG as a BCI data source

To realize the vision of interactive control feature selection suitable for long term BCI, we focused on a specific brain signal recording technology. The measured brain signal should be capable of capturing a rich representation signal patterns that can differentiate a wide variety of thoughts/cognitive tasks, and should be suitable for long-term continuous recording. Electrocorticography (ECoG) is a promising technology with these properties and is currently used in a procedure for treatment of epilepsy.

ECoG is a technology for recording the electrical fields on the surface of the brain induced by brain activity. These signals are recorded from many electrodes placed over a broad range of locations on the brain surface in parallel. The time-varying electrical signals are often analyzed in terms of the spectral components (i.e. the power at different frequencies in the signal), and the dynamic of these spectral components.

Evidence that BCI is possible from ECoG signals comes from current approaches that find a single electrode whose response at a single frequency correlates with some mental task. These successes in BCI control have been limited to short periods of control in closely monitored research environments. While ECoG implant technology is well suited for long-term application, it is not clear that these simple features remain consistent over long time periods.

Thus, this thesis considers three investigative steps explore BCI control feature selection with ECoG data. First, we explore representations of ECoG responses that capture correlated changes across both different electrodes and

different frequencies, which we call a spatio-spectral feature. Second, we explore the use of deep-learning to robustly extracting spatio-spectral features from the ECoG signal. Third, we develop and test an interactive control feature selection system that can run in real-time based on spatio-spectral ECoG features.

1.2 Context

To give context for this work, this section introduces the surprising breadth of BCI applications and the varied alternatives to ECoG that are used to measure brain signals. We then highlight some particular advantages of ECoG and discuss the clinical context that facilitated this research and some limitations this imposed. Finally, we discuss the current state of the art in BCI and ECoG based real-time feedback systems.

1.2.1 Applications for BCI Control

BCI device control systems seek to directly measure and use brain signals to control prostheses or robotic devices. This may serve the purpose of directly giving someone additional capabilities, or can be part of protocols for neuro-rehabilitation.

Most BCI research is currently focused on applications to neural prosthesis control. Spinal cord injuries, Amyotrophic Lateral Sclerosis (ALS), amputations, and stroke can all be causes of motor impairment [1-2]. However, the clinical needs of patients with these disabilities do not require the same degrees of freedom (DOF) of control or impose the same control restraints on BCI systems [1]. A spinal cord injury patient may benefit from BCI control of a motorized wheelchair or the ability to control of their bowel and bladder sphincter, while an ALS patient may benefit more from BCI control that improves their ability to communicate. A quadriplegic may have equal need for both. A locked-in patient would benefit from even the simplest BCI control since it is their only channel for interaction with the outside world. On the other hand an amputee may need to have very fine control of a prosthetic limb to justify the use of a BCI system.

In all cases, the BCI systems are driven by measured brain signals. These signals are created by users having a particular thought or executing a mental task, for example, thinking about moving their hand. The degree to which the mental task or thought control should mirror that of the overt action is dependent on the application. Amputees, for instance, may find it very hard to control a complex neural prosthesis if the BCI does not respond to neural signals that strongly resemble the neural signals responsible for the limb control before it was amputated. In cases such as stroke, where a motor disorder may be due to damage of the brain itself, it may be necessary to map a very different mental task in order to control some motor prosthesis.

BCI generated control can also be used to systematically induce neuroplastic changes [3], and has applications in neuro-rehabilitation as well as functional recovery. Induced neuroplastic changes can also be used to learn regulation of emotional disorders [2]. The point is just that neuroplasticity is likely to be important to learning to optimally use a BCI. I don't have a ref for this because no BCI has been used long enough to study neuroplasticity.

BCI device control can be used to augment the physical abilities of humans and the cognitive abilities of machines. Many limitations in robotic device control are not due to physical limitations of the machinery, but due to limitations on the amount of complexity that can be automatically controlled. Human operators are used to extend the cognitive abilities of machines while the machines increase the physical abilities of the operator. Thus, the interface between humans and machines is key to increasing their joint functional abilities. BCIs offer one path that may allow humans to achieve robust control of complex machines with fewer mental resources than other overtly controlled interfaces such as joysticks or voice commands. Overtly controlled devices present a bottleneck between the vast DOF of brain dynamics and the ever-increasing DOF of mechanical devices. While the control that can be accomplished with BCIs today is limited the field is still very new and it is hoped that they will present a way around this bottleneck in the future.

1.2.2 Basic structures in cortical organization

Here we review several basic concepts in neuroscience that are fundamental to the work in this thesis. The reader with a basic understanding of neuroscience may comfortably skip this section.

The electrical 'spiking activity' of neurons is the basis for information processing in the brain. This spiking is a result of rapidly migrating ions across electrically insulating cellular membranes. This process can trigger a neuron to release neurotransmitters along synaptic pathways which connect neurons within a complex network. These neurotransmitters, in turn, trigger spiking activity in other neurons causing the spiking response to propagate through neural tissue. Spiking activity is generally seen as the information output of a neural population or group of neurons.

Intercellular electrodynamics is affected by the local the chemical concentrations in the tissues immediately surrounding the neurons, and affects the tendency of neurons to spike. This modulation of the spiking contributes to the information processing of the neural tissue and is regulated by the excitatory or inhibitory input to a neural ensemble.

The cerebral cortex, or cortex, is the outermost layer of neural tissue in the brain, and is where most information processing is thought to takes place. The populations of neurons that are involved in a particular neural computation are called neural ensembles. In order to talk about neural ensembles across with established functional properties across many people, the folding and grooves (sulci) and bumps (gyri) in the cortical surface are used as anatomical landmarks.

The human cortex is characterized by a high degree of cortical folding or amount of grooves (sulci) and bumps (gyri) in the cortical surface. These sulci and gyri are often used as anatomical reference points which indicate neural ensembles with established functional properties when studying the brain. See Figure 1.1.1 for an overview of the functional division of the cortex.

At a smaller scale, a cortical column is defined as the area of cortex responsive to a particular stimulus, movement, or behavior. Cortical columns are about 0.5mm in diameter, and are formed because neural connections "up" and "down" within the thickness of the cortex are much denser than connections from side to side. Cortical columns have been mapped in somatic sensory and visual cortex based on correlations of firing rates with cognitive tasks and reported sensation; they are less well defined for other cortical areas such as the frontal cortex. In this thesis we will consider electrical recordings both at the scale of functional areas as well as smaller scales of one or a few neighboring cortical columns.

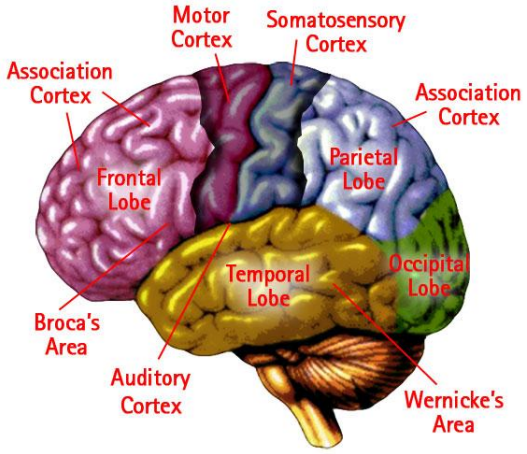

Figure 1.1: Functional division of the human cortex [4].

Functional areas are closely associated with Brodmann Areas, which are brain regions defined solely on differences in structure and organization of cells. While the influence of the structure and organization of cells within a neural ensemble on its functional response remains a topic of study, these anatomic differences may lead to differences in the frequency and amplitude of the electrical signal that we will measure and interpret in this work.

1.2.3 Brain signal Acquisition Methods

Brain activity can be measured at four levels: the activity of chemical signaling pathways, the electric field activity from the spiking activity of single or multiple neurons or the intercellular electrodynamics, the magnetic fields induced by neuronal electrical activity, or physiological changes such as water diffusion or blood flow that occur with neural activity. The following section reviews brain functional activity measurement methods at each of these levels starting

from the physiological level. The focus of this thesis will be on Electrocorticograph (ECoG), which is one of the ways of measuring the electrical field activity.

1.2.3.1 Brain recording device overview

The non-invasive nature and many clinical applications of Magnetic Resonance Imaging (MRI) has made MRI machines commonplace in clinical settings despite their large size and high cost. Because it is non-invasive, MRI is used for the majority of functional brain imaging studies. The most common of these techniques is functional-MRI (fMRI) that uses the Blood Oxygen Level Dependent (BOLD) signal to infer functional brain activity from shifting blood concentrations. Diffusion Tensor Imaging (DTI), modifies conventional MRI to measure how water is diffusing, and is especially useful in studies that are concerned with neural pathways in deep brain structures, such as the study of functional abnormalities associated with schizophrenia [5]. However, both fMRI and DTI require prohibitively large machines for practical BCI applications and are used only for proof-of-concept studies for BCI.

Near-infrared Spectroscopy (NIRS) has also been used to measure BOLD signal activation [3]. fMRI and NIRS have been used in the context of learned regulations of emotional disorders based on brain signal feedback [3]. However, the BOLD signal is a measure of brain activity that is sluggish in its response to cognitive tasks and as such not well suited for BCI.

Like MRI, Positron Emission Tomography (PET) is an anatomical imaging technique that has been modified to do functional imaging and used to study differences in diseased brains, such as schizophrenia [6]. While PET is non-surgical it does involve the risk associated with the injection of tracers that emit radiation. This radiation is then measured and the absorption pattern of the tracers can be used to infer brain activity. Again this measure of brain activity is seen to be too slow for BCI.

Magnetoencephalography (MEG) is another non-invasive method that measures the weak magnetic fields produced by the electric currents flowing in neurons [7]. MEG has also seen wide spread clinical use, and it gives a more direct measurement of neural electrical activity then fMRI, NIRS and PET, making it a useful tool for functional brain studies as well. However, MEG requires a large machine with very sensitive instruments that need to be placed in a special room that is heavily shielded from environmental magnetic fields. As such, like fMRI, MEG is suitable for proof of concept BCI studies, but not practical BCI applications.

More portable and suitable for BCI are several electrode-based methods that can directly measure the electrical fields produced by brain activity. Because they are lightweight and portable, they represent the dominant platform for BCI applications. The electrode-based methods provide good temporal resolution and have been used extensively for functional brain studies. They range from non-invasive Electroencephalograph (EEG) scalp electrodes to minimally invasive ECoG electrodes to highly invasive intraparenchymal (Single Unit) electrode arrays. Figure 1.2 depicts the relative placement of each of the three electrode-based brain activity measurement methods.

Finally, microelectrode biosensors arrays have recently been developed that can record real-time chemical signaling data [8], which may provide the most direct measurement of brain function. However, this functional imaging method is relatively new, it is highly invasive, and comparatively little functional brain imaging work has been done at this level, so the rest of this section focuses on measurements of the electrical field.

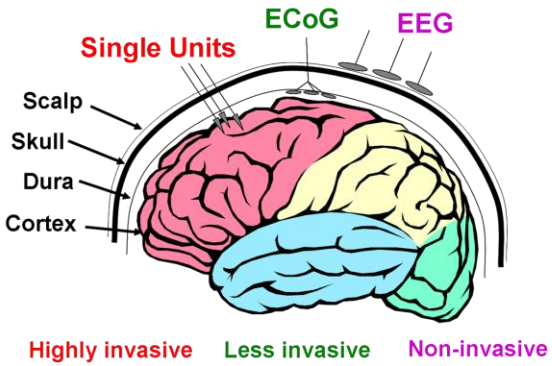

Figure 1.2: Electrode-based electrophysiological brain activity recording platforms [modified from the original figure provided by the Dan Morran Lab].

1.2.3.2 Intraparenchymal (Single Unit) brain recordings

Intraparenchymal, or sub-cortical, electrode arrays, measure brain activity data at a very direct level with very high anatomical resolution. They are often referred to as 'Single Units' because they are sensitive to the electrical activity of single neurons. However, they are also sensitive to very local variations in the intercellular electrodynamics. As such, single units are very anatomically specific measure of neuronal output and input electrodynamics. Their sensitivity to neuronal spiking activity has led to understanding basic neurological information processing concepts such as receptive fields [9], population coding [10], and place cells [11]. Single unit studies continue to lead the way in functional research.

However, single unit electrodes are not optimal for long-term human BCI use. They need to penetrate the cortical tissue and this can lead to scar tissue formation and electrode encapsulation. Scar tissue encapsulation can render the electrodes insensitive to neural electrical activity and limit the useful life the implant. Also, to avoid large scale tissue damage, the area that can be covered by arrays of single units is limited to 1 cm. Thus, most single unit studies have been done in animals. While some efforts to avoid triggering an encapsulation response in rat cortical tissue have been successful [12], these implants are far from being used in humans.

1.2.3.3 Electroencephalograph (EEG) brain recordings

EEG electrode arrays are placed on the scalp, and they are non-invasive and provide complete anatomical coverage of the brain. However, EEG electrodes give a much less direct measurement of neural electrical activity, measuring the Local Field Potentials (LFPs) resulting from the summed activity of billions of neurons. While single units also measure LFPs, their anatomic resolution captures single neuron firing patterns. In contrast, EEG electrodes are sensitive to the electrical activity of a cortical area of 3-5 cm projecting down from the skull [1].

Despite this limitation, the non-invasive nature of EEG makes it the predominant electrode-based method for human functional brain studies. Event Related Potential (ERP) changes on the human scalp were used to detect evoked brain events in real-time as early as 1977 [13]. EEG studies have characterized frequency bands associated with neural oscillations in normal and abnormal brain function. Some of these cortical spectral patterns have been well defined; the delta band (0.5-4 Hz) associated with sleep, theta band (4-7.5 Hz) associated with the hippocampus and memory [14], alpha or mu (8-14 Hz) and beta bands (15-25 Hz) associated with Event Related Desynchronisation (ERD) of motor movements [15], and gamma bands (>30 Hz) associated with Event Related Synchronization [16]. The general consensus is that these frequency bands reflect oscillations in intercellular electrodynamics or are due to synchronized neural spiking caused by these oscillations. Hence they are most associated with the input signals of a neuronal population. However, a broadband effect in higher frequency ranges well above 30 Hz are also thought to reflect a general unsynchronized increase in spiking activity of a neural population [17] and thus reflect neuronal output signals. Recent work has also fundamentally linked ERPs to phase properties of neural oscillations [18-19].

1.2.3.4 Electrocorticograph (ECoG) brain recordings

A compromise between EEG and Single Units is the intracranial EEG or Electrocorticograph (ECoG) platform. ECoG signals are not sensitive to single neuron spiking activity, but they are sensitive to much higher frequency electrical signals than EEG. This makes ECoG a compromise in terms of invasiveness and anatomical resolution (see Figure 1.2) which is sensitive to electrophysiological features of both input and output signals of a neural population. This is the focus platform of this thesis; it is covered in detail in the next section, and the following section describes some limitations that arise from the clinical context in which the data was captured.

1.2.4 ECoG brain recordings

As depicted in Figure 1.2, ECoG electrodes are implanted intracranially (inside the skull) and make direct electrical contact with the surface of the cortex. This gives ECoG several advantages with respect to both single units and EEG. First, ECoG electrodes do not penetrate the cortical surface (as single units do) so cortical scarring does not take place and large areas of cortex can be covered for extended periods of time without disrupting normal cortical

function. Second, ECoG electrodes have the advantage over EEG electrodes of being in direct electrical contact with the cortex surface, and are partially shielded from outside electrical noise by the skull. Thus, ECoG signal is typically on the order of 0.05-1.0 mV verses 0.01-0.2 mV for EEG [1]. Third, ECoG electrodes provide superior anatomical resolution and spectral bandwidth compared to EEG; each electrode measures data from a smaller cortical region and is able to detect higher response frequencies. The ECoG electrodes themselves can be smaller; due to the increased signal to noise ratio electrodes as small as tens of microns are still able to record neural signals [20].

Surgery is needed to implant ECoG electrode grids and significant risk is involved. For this reason ECoG use in humans is limited to clinical settings and coverage and implantation duration is dictated by clinical considerations. The most prevalent use of ECoG implants today is in patients with serious epilepsy who require invasive monitoring for localization of an epileptic focus [1]. A single patient will only have partial coverage of one hemisphere for a period of 1 to 2 weeks. In addition, because ECoG electrodes are constrained to lie on the surface of the brain they are mainly insensitive to activity in sulci. Also, neighboring electrodes may record from neural populations that are not neighboring on the cortical surface.

These limitations have not prevented ECoG from being used to study electrical signals in the brain.. The variance in candidate seizure foci locations across patients means that coverage of all four brain lobes in both hemispheres is obtained within a small patient population. Chronic ECoG electrode implants are also used for treatment of several chronic pain disorders [21-22], giving evidence that ECoG can be a long term data source for BCI. In addition, recently there has been experimentation with temporary instrasulcal ECoG electrodes for chronic pain treatment [23], highlighting the potential to study cortical electrophysiology within the sulci.

ECoG is an especially good way to investigate electrophysiological phenomena because it has good anatomic resolution and is sensitive to low and high frequency signals. It is believed that lower frequency brain rhythms in the delta, theta, and even alpha and beta bands are regulated by deep brain structures, while gamma rhythms are due to synchronization among cortical assemblies. This is significant because cortical ensembles tend to produce synchronized activity over much smaller cortical areas and studies report an inverse trend between the frequency of synchronous activity and the size of the cortical area involved [1]. ECoG has shown patterns in the alpha, beta and low-gamma (30-40 Hz) bands that parallel EEG studies [15-16]. However, no significant results above 40 Hz have been shown in EEG studies, while ECoG studies have revealed gamma spectral patterns near 100 Hz. Electrode sites with significant gamma response to motor tasks match the anatomical locations of stimulation functional mapping results for motor tasks [1]. Also, increases in electrode responses at 200Hz are more tightly correlated to anatomical locations than correlated lower frequency patterns in the theta band (Figure 1.3). [1, 17, 24-25]. At the extreme, ECoG recordings have shown significant functional modulations in amplitudes up to 500 Hz [26]. A good review of the contributions to electrophysiology from the ECoG platform is provided by Jacobs and Kahana [27], we highlight below some of the concepts that arise in our later analysis and discussion below.

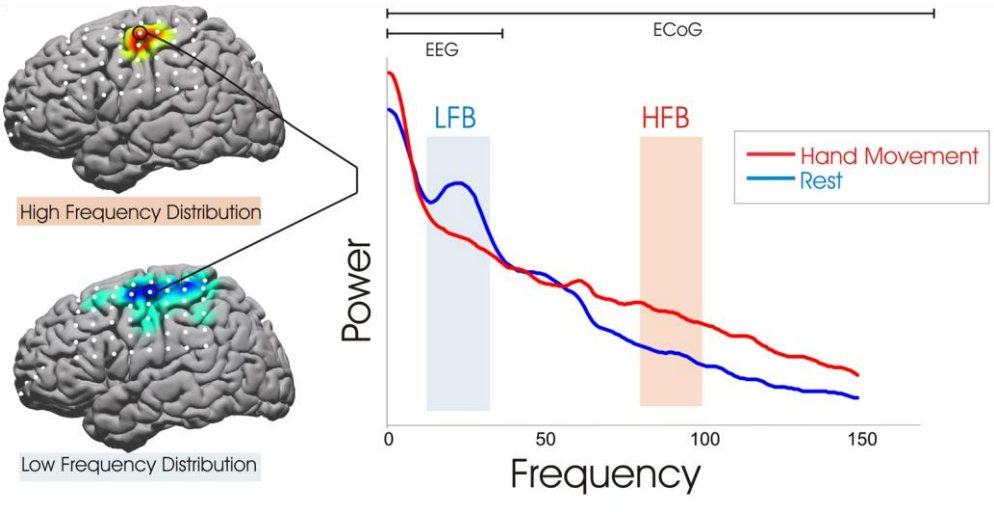

Figure 1.3: Characteristic ECoG spectral response patterns in the beta band (15-25 Hz) and high gamma band (>60 Hz) for the non-active (rest) condition and hand movements [28]. Left column: Anatomic locations of electrodes with statistically significant differences in the high gamma (top brain plot) and beta (bottom brain plot) responses. Right column: Average spectral pattern for rest (red) and active motor (blue) conditions. The average power spectrum during hand movements shows a decrease in beta and an increase in high gamma compared to rest trials. The gamma increase (from 80-100 Hz) is shown to be more anatomically focal to the hand area of the motor cortex (indicated by the red shaded area on the top left brain plot) than the beta decrease (indicated by the blue shaded area in the bottom left brain plot). The horizontal bars at the top of spectral plot in the right column indicate the frequencies in which EEG and ECoG are sensitive to power changes. Only ECoG is sensitive to the decrease in the high-frequency, localized response during motion actions.

Different frequencies of electrical brain activity have been associated with different mental functions. It has been shown that a working memory task gates theta band oscillations [29] and visual attention modulates Gamma band responses [30-35]. When subjects imagine movement, the amplitude of alpha and beta oscillations is observed to diminish while gamma oscillations increase [25, 36-40]. During the activation of working memory, decreases in responses in the theta range are coupled with an increase in the gamma range. [41-45].

Measurements at different frequency bands arise from different electrophysiological phenomena. Frequencies below 30Hz often reflect interactions between cortical columns, or larger scale interactions in or between functional areas [46] Very low frequencies may suppress spiking of individual neurons [47-50], and frequencies around 30Hz have been associated with synchronizing the firing of groups of neurons [51-52]. Broadband increases in frequencies above 30Hz have been observed in ECoG data [17, 53-55] and in cortical population simulation [56], and are believed to arise from non-synchronized neuronal spiking. Recent studies have also observed specific high-frequency firing patterns; Gaona et al. find structure in the frequency responses between 60 Hz and 500Hz [26]. Using ECoG as a measurement tool, they distinguish different cognitive tasks (hearing, reading and speaking) based on the response at specific frequencies in this range.

Studies have also explored patterns of frequency responses, finding sets of anatomical sites whose amplitude fluctuations over time are correlated. These anatomical locations of these networks are similar networks of correlated BOLD fluctuations in the 0.1 Hz range found with fMRI. The Slow Cortical Potential, a band of frequencies below

4HZ found in ECoG data, have been proposed as a possible neural substrate of conscious awareness [57-58], and can be used to map the sensory motor cortex [59]. These patterns that have been discovered to date all correspond to consistent increases or decreases in the response at difference frequencies within a brain region. Little is known about the co-varying across regions or across frequencies during active tasks.

Another property of oscillations in electrical signal is phase, and ECoG has been used to investigate the relationship between phase and the timing of mental tasks. Phase reset, or the tendency of the phase of oscillation of a frequency band to be reset by a mental event, has been demonstrated in the alpha band during a working memory task [60]. Phase locking, or degree to which two anatomic sites show synchronized oscillations at a particular frequency, has been observed between distant cortical sites during visual short-term memory maintenance [61-63]. Phase-amplitude coupling, or the tendency for the amplitude of a certain frequency (generally in the low gamma ranges) to be modulated by the phase of a lower frequency (generally in the theta band) in response to a mental task, has also been reported in numerous ECoG studies [64-66]. Non-linear phase-phase cross frequency coupling between distant neocortical sites was also found in four ECoG subjects during a motor task [67].

A final results emphasizes that these signals have rich and not yet completely understood properties. He et al. have recently shown that the phase-amplitude coupling extends beyond regular oscillations and is present within arrhythmic ECOG activity [68]. They further showed that this phenomenon is modulated by task performance and varies across brain regions.

1.2.5 Specific Clinical Context of the Thesis

The work in this thesis is based on ECoG recordings from intractable epilepsy patients. These patients undergo invasive surgical implantation of multi-electrode ECoG grids for the purpose localizing seizure foci prior to surgical resection. The patients are monitored for a period of several days to two weeks. During this time they are removed from seizure suppression medications. Typically, after a two day surgical recovery period they are cognitively alert and willing to participate in interactive research tasks. The participation is strictly voluntary and written informed consent is obtained. Up to two two-hour research recording sessions can be performed each day. Both adult and pediatric patients have participated in this research. Clinical ECoG electrodes are several millimeters in diameter and are often implanted as grids with 1 cm spacing between electrode centers [1]. A typical clinical ECoG implant is depicted in Figure 1.4. In addition to the clinical implants, smaller implants with higher electrode densities are occasionally used for research purposes.

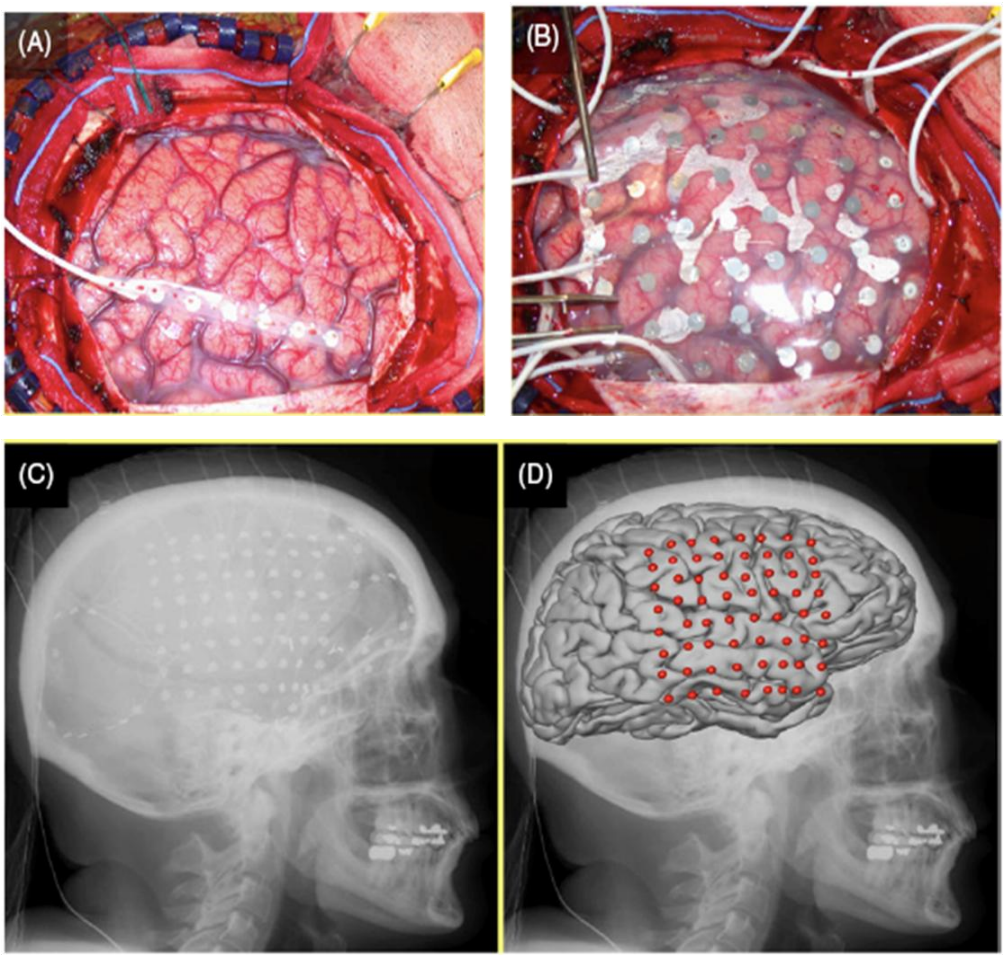

Figure 1.4: Depiction of the implantation of a clinical ECoG grid [69]. A: Exposed cortex before implantation. B: ECoG implant placement on cortex. C: CT scan showing ECoG implant location. D. Reconstruction of ECoG implant on the cortical surface.

As part of the clinical procedure the Cortical Stimulation Mapping (CSM) procedure is used to locate areas of so called 'eloquent cortex,' that need to be avoided during the resection. CSM is the gold standard used to map functional areas of the cortex with ECoG. The procedure involves generating a current between two ECoG electrodes, which creates a brief lesion in the cortical area between them. These lesions can evoke motor or sensory responses or disrupt normal mental task performance [70].

It is also often part of the clinical routine to make Computed Tomography (CT) scans of the patient's brain anatomy after ECoG implantation. Lateral radiographs from these scans can then be used to locate the implanted ECoG electrodes in the standard Talairach stereotaxic coordinate space of the brain [71] using the getLOC MATLAB package [72]. The Talairach coordinates are used to define the function regions of the brain when evaluating recordings from each electrode.

The clinical context of human ECoG research introduces considerable noise into the research data. There are many known sources of signal noise in the hospital setting. These can be put into three categories; electrical noise, medical

electrophysiological noise, and cognitive electrophysiological noise. Electrical noise refers to ECoG signal characteristics that reflect the environmental electric field and not electrophysiological signal. Medical electrophysiological noise refers to the aspects of the ECoG signal that reflect the patient's medical condition such as the effects of changes in medication or epileptic activity. Cognitive electrophysiological noise refers to electrophysiological phenomena such as drowsiness and diverted attention, which cause cognitive states to vary from normal alert brain function. All three forms of noise complicate the analysis of ECoG signal. Because robust electric shielding in the clinical setting is not possible, electrical noise is often the dominant component of the ECoG signal.

There are two main forms of electrical noise within clinical settings. First, sudden movement of the recording wires within the environmental electric field, caused by patient head movement or researcher contact with the wire, cause sharp discontinuities in the ECoG signal that manifest as sharp peaks in amplitude across the entire spectrum of frequencies. Second, electric field sources in the environment such as the incandescent lights and electrical motors in the hospital equipment cause modulations in the environmental electric field at specific frequencies (for example 60 Hz from the standard AC power supplies in the US). This effect can partially be corrected for in the spectral domain by band pass filtering the signal. However, this inevitably leads to a loss of electrophysiological information at these frequency bands. For example, several ECoG studies done in the US note a distinction between the low gamma band (30 to 60 Hz) and the high gamma band (>60 Hz) [25, 28, 73]. This is because there is no observed cognitive task induced signal change around 60 Hz, which is most likely due to 60 Hz filtering effects.

The standard method to correct for electrical noise is to re-reference the ECoG electrode channels to an electrode recorded in-parallel with the clinical electrodes but which is not sensitive to brain activity. This (baseline) signal is subtracted from signal of each ECoG electrode. Since there is no electrode location in an EcoG implant, there are several schemes to generate this signal. These include using a common average signal of all electrodes or making a local average using a Laplacian spatial filter. The quality of contact of electrodes with cortical surface will affect sensitivity to electrical environmental noise. Factors such as air bubbles or defects in the silicon grid can cause the quality of contact to very substantially over electrodes. This makes it harder to re-reference the electrodes, and often leads to such electrodes being removed from consideration in data analysis. In practice it is not possible to create a re-reference signal that fully captures the noise characteristics of each ECoG electrode and is silent to all non-noise electrophysiological content. In practice this re-referencing removes much of the impacts of environmental noise, but the confounding factors make the remaining signal differ from patient to patient and session to session. This drives us to base our approach on learning patient specific patterns of activity that do not depend on accurate estimates of signal strength and rather capture variations in signal strength under different conditions.

1.2.6 The BCI2000 System

This thesis implements ECoG signal analysis and real-time control based on the BCI2000 [74] software package. This package supports signal capture and recording as well as real-time signal analysis. In ECoG BCI, it is often used run feature screening tasks, in order to find features in the ECoG signal that can be used for control. It has also been used to detect those features in real time to perform 2 or 4 target control, allowing simple video games to be played based entirely on ECoG signals [28].

In chapters 2 and 3, this thesis uses standard BCI package for signal pre-processing, including a package that computes the time-varying frequency response of each of the ECoG electrodes, based on a maximum entropy method (MEM) of autoregressive spectral estimation [75]. Chapter 4 modifies the BCI2000 software to implement our real-time feedback scheme.

1.3 Current BCI Achievements

This section will present the highlights of BCI device control achieved with EEG and single unit electrode arrays, then give a more comprehensively review of device control demonstrated thus far with ECoG. To help in discussing and comparing these results, we first introduce a common measure used to evaluate demonstrations of BCI control.

1.3.1 BCI bit rate

Speed and accuracy can be incorporated into a single value known as bit rate. In the context of BCI, bit rate (bpm) can be viewed as measure of correct control decisions carried out per minute [76]. This bit rate depends on the time T (in minutes) it takes to make a control decision, and the degrees of freedom N of the control task, which is the number of different decisions that are possible. With a success rate of S (and error rate of 1-S) the bpm is:

$$bpm = \frac{bits}{T}, \text{ where,}$$

$$bits = \log_2 N + S\log_2 S + (1-S)\log_2\left(\frac{(1-S)}{(N-1)}\right),$$

The bit rate of a BCI system increases when it can differentiate between more different decisions (ie. when the DOF increase), and with increased success rates. A BCI system that is 90% accurate with two DOF conveys roughly the same amount of information as a four DOF system with 65% accuracy, although how useful this is for real BCI tasks may depend on the creativity of the interface that is being controlled.

Despite the many challenges to BCI, preliminary practical demonstrations of BCI device control have been achieved with all three of the electrode-based brain signal acquisition methods. For a continuously controlled device such as a prosthetic limb or wheel chair, a reasonable goal is to achieve a rate of 600 bpm (10Hz) which is often used as a

threshold for real time response. However, currently a control at a rate of 25 bits per minute (0.4 Hz) is common [1]. Hence, most current BCI applications use the strategy of only requiring BCI control decisions to be made at critical points and relay on automated device control to carry out practical tasks, such as selecting from the commands 'turn right', 'turn left', 'move forward', and 'stop' to control a wheelchair.

The current focus of BCI research is not on increasing the speed of the BCI response, but in improving the accuracy and the DOF of the BCI response. While the inherent limits of how fast a user can learn to modulate a BCI control signal likely depend on the type of brain signal recorded and cognitive task being used, to date there has not been enough sufficient long term BCI control to allow this aspect of the bite rate to be adequately explored.

1.3.2 EEG-based BCI control

Of the brain signal acquisition methods used for BCI device control so far, EEG has been the most wide-spread in humans due to its non-invasive nature. While significant training was needed, two separate reports of BCI-based spelling paradigms were reported in 2000. In one report, five homebound severely motor disabled patients were able to spell words by moving a dot over letters on a computer screen by learning to modulate the amplitude of very low frequencies (slow cortical potentials or SCPs) [77]. In a second report, the P300 EEG response, which is a unique ERP response that occurs 300 ms after a stimulation event, was used to choose letters from an alphabet matrix and achieved an average bit rate of 7.8 characters per minute across ten healthy subjects [78]. In 2003 a study of five adults without disabilities achieved 40-70% accuracy at sample rate of 0.1 to 0.25 Hz in a four target task [79]. Also in 2003, a study of 99 subjects showed that 93% of novice BCI users achieve 60% accuracy in a 1-D BCI control task using mu and beta band responses from imagined motor movements [80]. In 2006 results using an Expectation-Maximization algorithm with 9-31 Hz spectral features from EEG data recorded during a four target 1-D trajectory control task achieved an average accuracy on 70% and bit rate of 0.6 bits/trial across 3 healthy subjects [81]. In 2007 the Berlin Brain-Computer Interface method, was able to learn Common Spatial Patterns of ERS and ERD responses to motor tasks to achieve a maximum bit rate of 35 bpm (0.58 Hz) across three subjects in a 1-D, two target, control task [80-83]. In each of these previous cases, the systems were calibrated with one or two 20-30 minute calibration sessions.

1.3.3 Single Unit based BCI control

The most impressive control has been achieved with single unit electrodes. Using single unit recordings and the weighted sum of firing pattern filters on monkey motor neurons, 3D prosthetics control has been achieved [83]. In addition, 2-D cursor control was achieved with bit rates that rivalled that of the monkey using a joystick alone [84]. In

both of these studies the linear firing pattern filters were calculated while the monkeys were using overt movements for control, then the control was switched to BCI control while the monkeys continued to make overt hand movements and the monkeys were eventually able to achieve control without overt movements. Thus a cognitive remapping of the motor neuron firing from overt motor control to BCI task control took place.

In exceptional cases, these electrode arrays are used in humans despite their invasive nature. These have led to the best human BCI control results thus far. A quadriplegic patient with a 100 electrode implant was able to achieve continuous 2-D control of a computer mouse [85]. Considerable smoothing of the 2-D trajectories was used to stabilize the control, and the task was based on the mouse reaching an end target not specific trajectories. This makes it hard to compute a true bit rate, but mouse movement response was in real-time (>10 Hz). However, cortical scarring eventually reduced the signal quality and therefore the level of achievable control, the system required frequent recalibration, and was only used under the supervision of a research team [86]. One encouraging key finding of this study was the fact that the patient was able to converse, and thus focus on other tasks, while achieving BCI control. The same group recently reported that two quadriplegic patients were able to control 2-D movements of a robotic-arm using a 96 single unit array implanted in the motor cortex [87]. In a three target task the subjects were able to reach the correct target 62% and 42% of the time within the 30 second time limit (giving a maximum bit rate of 0.5 bpm). One subject also demonstrated control during an untimed drinking task that required her to bring a bottle to her mouth. A combination of two-dimensional robot arm movements across a tabletop plus a "grasp" command to either grasp and lift or tilt the robotic hand was used and a 66% success rate was achieved.

1.3.4 ECoG-based BCI control

Using the BCI2000 system, Leuthardt et al. first reported successful closed loop ECoG BCI control in 2004 [28]. They achieve control of left-right movement of a circle on a screen using separate overt hand and tongue movement features for left and right. This control was then extended to two dimensional left-right and up-down control in several patients based on overt hand and tongue movements and shown to also work with imagined movements [25]. Usually contralateral (opposite side of body as ECoG grid brain hemisphere) movements are used for movement based BCI control. However, Ipsilateral (same side) vs. contralateral hand movements have also been used for more intuitive left-right control [88].

Recent BCI control results have expanded the achievements of ECoG-based BCI control to include imagined and overt speech activities, with electrode implants covering anatomic locations in the speech region [73]. Both overt and imagined speech phoneme features in the speech cortex have been used in 3 subjects to achieve two dimensional movement control based on 2 DOF. 1 DOF control with overt phoneme pronunciation has been achieved in a subject with a micro scale (16 micrometer electrodes covering 1 square cm) ECoG grid implant over mouth motor cortex. Overt and imagined motor movements can also be used by paediatric patients for BCI [89].

A proof of concept demonstration was also done with a paediatric subject who controls the closing of a robotic hand with both an overt ipsilateral hand movement feature and an imagined contralateral hand movement feature. The same subject was also able to get 3-D control with 3 DOF (an overt ipsilateral hand movement, overt contralateral hand movement, and a click signal controlled by an overt tongue movement) that allowed the subject to move a ball left and right and click to indicate that the left and right side of the movement field had been reached.

Remapping of higher cognitive concepts to lower functional cortical features was demonstrated in a subject playing a very simple version of Space Invaders [90]. While control of the spaceship was achieved with ECoG signal features found from a hand movement screening task, the subject reported that after playing the game for a short period of time, he was able to control the spaceship by thinking about moving it and not his hand. It has also been reported that participation in closed loop BCI control can increase the anatomical areas that have significant response in the control frequency band [25]. In addition Miller et al. found that three subjects were able to learn, through feedback, to decouple hand movement and tongue movement control signals that were initially highly correlated, which precluded successful two-dimensional cursor control, and achieve successful control [91].

1.3.5 ECoG-based classification and detection results

When the goal is not closed-loop control, more sophisticated offline analysis techniques have explored a wider range of analysis techniques on ECoG data. Nonparametric statistical modelling was shown to improve gross motor task classification [92]. Linear Discriminant Analysis has been used to reduce a large set of spectral features encoded in a wavelet dictionary to a combination of just three features that give 93% accuracy on an imagined hand vs. tongue movement task [93]. Non-standard ECoG electrode configurations, such as small scale electrode grids have been shown to have spectral features correlate with EMG signals measured from forearm muscle movements [94] Small scale ECoG grids have also been shown to support discrimination of different phoneme pairs with greater than 70% accuracy [95]. Intrasulcal electrodes placed within the sulci, as opposed to gyri of the brain, have been shown to give better classification results with a support vector machine with overt movement features than electrodes placed on the nearest gyri [23].

However, standard ECoG electrode configurations and techniques have now been used across many patients which has allowed for the establishment of more general ECoG brain activity classification features [96]. Features that were consistent across 12 patients have been shown to differentiate expressive and receptive speech areas [97]. In 2007 Schalk et al. defined a new ECoG feature called Local Motor Potentials (LMPs) and used them to decode two dimensional joystick movement directions [98]. Pistohl et al. followed this up in 2008 with prediction of complete 2D motion paths [99].

Much work has also been done to distinguish finger movements with ECoG. Shenoy et al. first demonstrated ECoG based finger movement classification in 2007 [100-101]. In 2009 Wang et al. achieved individual finger classification

among all five fingers with 73% accuracy using a micro-ECoG grid (4x4 grid with 1.5mm disc electrodes and 4mm center-to-center spacing) and the 60-120 Hz frequency band [102]. Spectral changes associated with ipsilateral finger movements were detected in a single patient by Zanos et. el. [103] and in 6 patients by Wisneski et al. [88]. Recently Miller et al. improved on these results and demonstrated a spectral pattern decoupling method that provided good finger discrimination results with a macro ECoG grid [101].

Recently ECoG has also been shown to be able to decode vowels and consonants and the temporal dynamics of a spoken and imagined speech task. Pei et. al showed that spoken and imagined vowels and consonants could be decoded with ECoG [104]. In a spoken and imagined speech task, they found the amplitude of the response in the high gamma range (65-95 Hz) to have good temporal resolution in tracking the neural changes associated with stimulus presentation and verbal response [105].

The majority of research thus far has focused finding spectral features that correlate with behaviors. The studies that have been successful in decoding finger movement kinematics [25, 28, 69, 90-91, 100, 102, 106] and speech articulations [73, 95, 97, 104, 107] have all employed differences in the response of a single electrode at a single frequency.

1.4 Real-Time Visual Feedback of ECoG signals

BCI systems that offer feedback to the subject are an approach to improving the feature selection process, by allowing a subject to immediately observe their ability to control specific features. The success of a feedback system depends on the quality of the generated feedback. The two key aspects to the quality of feedback are how clearly changes in signal features are displayed to the user, and how much the features that are displayed are something the user can control. Feedback needs to be of high quality in both of these aspects if an interactive control feature selection system is to be successful. ECoG is a well suited technology platform for BCI in that it captures signals related to many relevant electrophysiological processes. In this section we describe previous approaches to visualization of these signals, then discussing the target of the work in this thesis; that different types of features may be even better representation of relevant brain signals, and possible ways to visualize these features to create a high quality feedback system.

Several ECoG-based realtime visual feedback systems have been developed already. These systems are the SIGFRIED [108-109] system that is based on the BCI2000 software and the Brain TV system developed by Jerbi et al. [110]. Both systems are very limited in terms of the parts of the ECoG signal used to generate the feedback and the scope of feedback features that can be comprehensibly displayed for the user. The brief review of these systems will motivate the approach we take with our real-time feedback system.

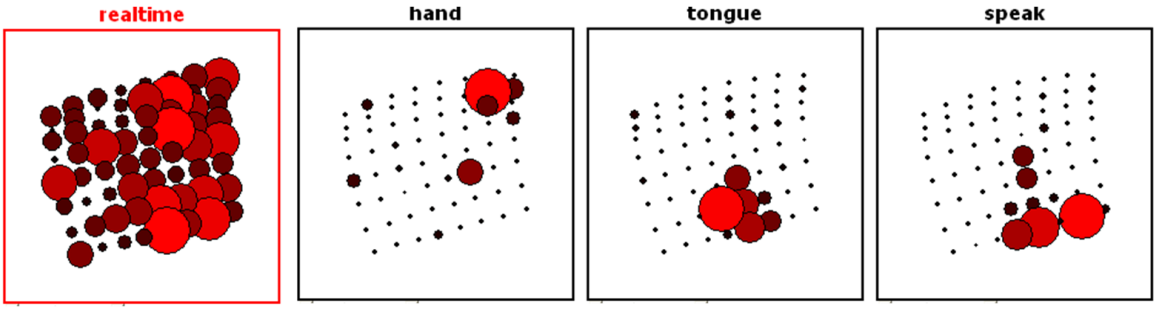

Figure 1.5: Screen shot from the SIGFRIED real-time functional mapping system.

The SIGFRIED system produces real-time feedback based on the ECoG spectral response to brain activity. The system works by building a Gaussian Mixture Model of the distribution of the amplitude response of a defined frequency band during a period when the subject is resting and not actively inducing a mental activity. When the subject is cued to perform a task, this distribution is then used to calculate a probability that the responses of a set of ECoG electrodes are affected by that task. The correlation between the probability of active brain state and the task cues is then used to generate a real-time display of which electrode sites are most activated by the mental task. The system allows for two displays showing the amplitude response of two different frequency bands. Figure 1.5 shows an example screen shot from the SIGFRIED system.

The Brain TV system is intended as a real-time feedback system that allows both the BCI user and researcher to search different cognitive strategies for optimal BCI control. With the system the amplitudes of up to two predefined frequency bands for four electrodes can be displayed in real-time as colored traces on a screen. The BCI user and researcher can then collaborate to search for mental activities that show clear temporal correlations with changes in the four displayed traces.

There is increasing evidence that brain activity comprises correlated changes across anatomical regions and in different frequencies, and the ECoG spectral amplitude response measured across a grid of electrodes captures these complex patterns. However, thus far ECoG-based BCI control features have not reflected the multifaceted nature of the ECoG spectral response. This is reflected in the limited spectral and anatomic content of the current two ECoG-based real-time feedback systems discussed above. In this work we try go beyond the limited window that current ECoG-based real-time feedback systems give, by exploring, defining and visualizing features that summarize larger patterns of activity.

Our first aim is to characterize ECoG signal features that can be used to generate feedback with a robust functional response. We focus our analysis on spectral features that are distributed in terms of frequency band and anatomic representation. Three main factors motivate this decision. First, it has been shown that spectral amplitude response features in single ECoG electrodes contain considerable information with respect to many mental tasks, but the traditional band limited anatomically features require extensive screening to find a robust set that differentiates multiple mental tasks. Second, ECoG spectral amplitude response reflects a rich multifaceted complex of electrophysiological phenomena which are expressed in a diversity of anatomic activations across a multitude of

frequency bands. Third, little work has been done exploring the use of features that reflect the multifaceted nature of ECoG spectral response for BCI control.

Our second aim is to develop an algorithm capable of reducing the high dimensional ECoG spectral amplitude response across many anatomic site and frequency bands into a low dimensional basis set. We evaluate one choice of this basis set to measure its sensitivity to mental task performance. A small, relevant basis set is essential to reducing the high-dimensional nature of the multifaceted ECoG spectral response down to a visually comprehensible feedback.

Our third aim in this work is to develop an interactive feedback system that allows a user to choose control features from a small set of spectrally distributed features and fine tune them.

1.5 Specific Contributions and Thesis Roadmap

The main aim of this work is to develop an interactive ECoG-based visual brain activity feedback system. In chapter 2 we show that diffuse spectral amplitude response features are a better feature basis of such a feedback system than spectrally and anatomically local features. Specifically, this includes:

- a method for ECoG analysis that allowed us to directly compare the functional contrast of distributed vs. local spectral features,
- the first demonstration that distributed spectral features in ECoG spectral response are more sensitive to cognitive tasks than the local spectral features,
- contributions to a fundamental debate about the electrophysiological architecture that supports brain function.

We show in chapter 3 that these features are inherent to ECoG signal and a basis set of these features can be derived from the ECoG spectral response. This includes:

- a demonstration that distributed patterns in spectral response that significantly discriminate mental tasks can be naively learned (without labeled training data) from ECoG spectral response,
- a method to compare naively learned distributed spectral patterns from resting ECoG data to those of active state ECoG response in terms of correlation to cognitive tasks,
- the first demonstration that discriminant distributed patterns are present in resting state spectral response.

We show in chapter 4 that this work supports an online feedback system that successfully reduces the complex electrophysiological dynamics recorded with ECoG to a small set of functionally relevant feedback features. Included within this are:

- the Brain Mirror system for real-time interactive control feature selection,
- an algorithm to derive, online and in real-time, a basis set of distributed spectral features used to generate feedback traces,

- a demonstration that these feedback features can be used to actively choose multiple independent control features corresponding to independent cognitive tasks.

Chapter 2

Functional Spectral Networks

2.1 Introduction

Traditional ECoG analysis considers the response of each frequency band at each electrode individually, even though responses across frequency bands and across electrodes are highly correlated or anti-correlated. Here we develop approaches to investigate the response distributions across many frequency bands and multiple anatomic sites; what we call spatio-spectral patterns. We compare the responses of distributed spatio-spectral patterns to the response at a single site within a limited frequency band. Making this comparison while subjects are performing different tasks allows us to characterize task based activity and to describe if it is distributed across many brain regions or more focussed within a small region. Additionally, this helps determine if these patterns may offer improved discriminative power for use as novel BCI control features.

This chapter proceeds by first introducing terminology in section 2.1.1, then presenting overall goals and the methods we derive to create and analyze the distributed patterns in section 2.1.2. These patterns are characterized for a set of clinical patients and section 2.2.2 details the ECoG signal acquisition tools, subject tasks and algorithmic methods that are compared. We report the results of our analysis in section 2.3, and discuss the implications of our results to ECoG electrophysiology, BCI control, and basic functional brain properties in section 2.4.

2.1.1 Spectral Features (SF) and Functional Spectral Networks (FSNs)

Our analysis of ECoG signals focuses on using them to discriminate between different mental states. Because the experimental protocol creates these states by asking the subject to perform different cognitive functions, we term the ability to differentiate between states "functional contrast". To more easily discuss the comparison of the functional contrast of individual locations and larger patterns, we introduce the terms Spectral Features and Functional Spectral Networks. Spectral Features (SFs) are responses of specific frequency bands at specific anatomic sites that significantly discriminate cognitive tasks. Functional Spectral Networks (FSNs) are patterns of responses across a collection of anatomic sites and frequencies, such that the pattern of response discriminates cognitive tasks.

To make this concrete, we define the voltage measured by electrode *i* as a time series denoted $v_i(t)$. We compute the local frequency transform (method described later 2.2.4), and measure the power spectrum of the response for a set of frequencies. After this pre-processing, the ECoG data has been converted to a set of responses for each electrode *i*, for frequency *f*, at time *t*. These responses are normalized and re-scaled to create the basic input data to most algorithms in this thesis, indexed as *g(i,f,t)*. With this notation, Spectral Features select a particular electrode *i* and a particular frequency *f*, and have responses over time that can be written *g(i,f,:)*, using the matlab convention that (:) allows an index to vary, so that *g(i,f,:)* defines a vector corresponding to the, in this case, time-varying response at frequency *f*, of electrode *i*.

Functional Spectral Networks define patterns that depend on the distribution of responses in all electrodes and all frequencies. To formalize this, we consider *g(:,:,t)*, the set of all responses at a time *t*. For convenience, we stack these responses in a vector ***x(t)***. In this chapter we consider linear weight functions ***w***, which serve to define a pattern whose time response at time *t* is $\boldsymbol{w}^T\boldsymbol{x}(t)$; subsequent chapters will consider alternative functions of ***x(t)*** to define improved Functional Spectral Networks. For both the Spectral Features and the Functional Spectral Networks, we consider them to have functional contrast if the time signal that they define is sufficiently correlated to the tasks that the subjects are performing.

Figure 2.1 illustrates the conceptual difference between Spectral Features and Functional Spectral Networks. The left column depicts the traditional view, measuring spectral responses at each electrode, such as electrode A, and detecting task based variations such as a decrease in the response at low frequencies and an increase in response at high frequencies. The right column illustrates, in a small version, the concept of FSNs: for some tasks there are correlated changes at multiple electrodes. This similarity, in which frequencies increase and decrease in response to a task, we term spectral binding (because the frequency changes seem to be bound together for these electrodes in this task). These bindings may differ for different tasks, as illustrated in Task 2, where electrodes A and B are bound instead of A and C. Functional spectral networks aim to characterize patterns of correlations between multiple electrodes by exploring the graph structure of the spectrally bound electrodes.

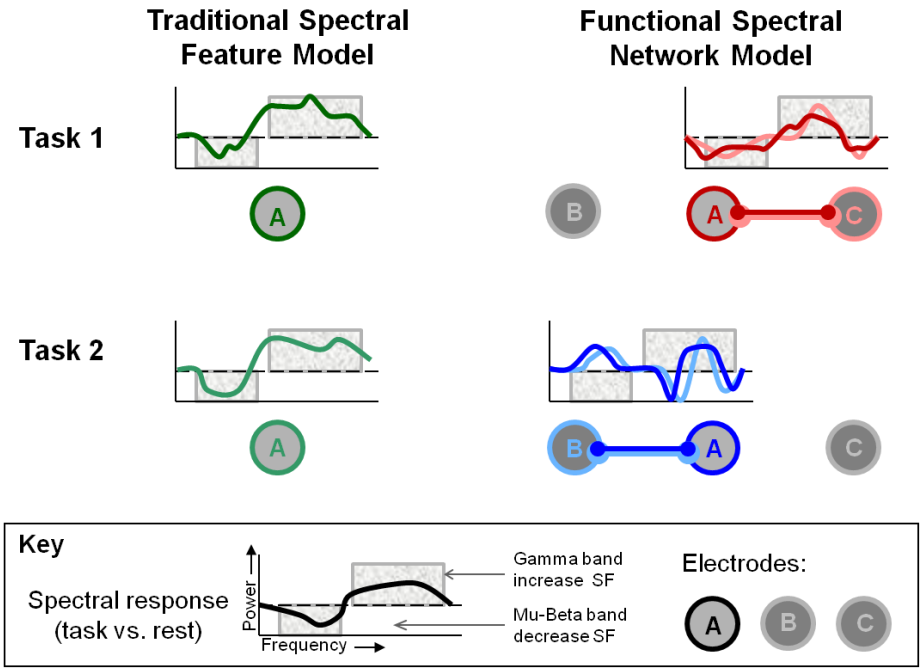

Figure 2.1: Spectral Binding: The plots show the response of one electrode relative to the baseline activity across a collection of frequencies. The key at the bottom highlights the most common reported responses; a decrease in activity in the lower frequencies (e.g. mu and beta rhythms) and an increase in the response in higher frequencies (the Gamma band). Spectral binding captures correlated responses of electrodes, which may respond differently to different tasks, but similarly to each other for the same task. The functional responses to Task 1 (top row) and Task 2 (bottom row) are plotted as amplitude change from their rest level (dotted horizontal line) on the y-axis versus frequency on the x-axis.

To date, work that explores ECoG functional responses has focused on response profiles that are consistent over many tasks. The bottom key of Figure 1 shows this pattern: when a brain region is involved in a task there is often a decrease in the power at low frequencies and an increase at higher frequencies. In this single electrode model (Figure 2.1, left), the cartoon response shown for electrode A in both tasks has similar changes in the response profile shown for Task 1 (in dark green) and Task 2 (in light green). Creating an SF (the single electrode, one frequency band) would suffice to capture the trend in decreased low frequency power, or increased high frequency power and could distinguish between the subject performing some task and being at rest, but often cannot distinguish between tasks.

Spectral binding offers a tool to measure or capture a richer set of modulations seen by electrodes at a particular brain location. Measuring these modulations, and using them to find networks of bound electrodes, gives a new tool to find distinctions in the brain signal patterns measured during different tasks. It captures interactions between anatomic regions during tasks, and allows one to measure the groups or subpopulations of anatomic sites that are formed and dissolve rapidly as tasks change.

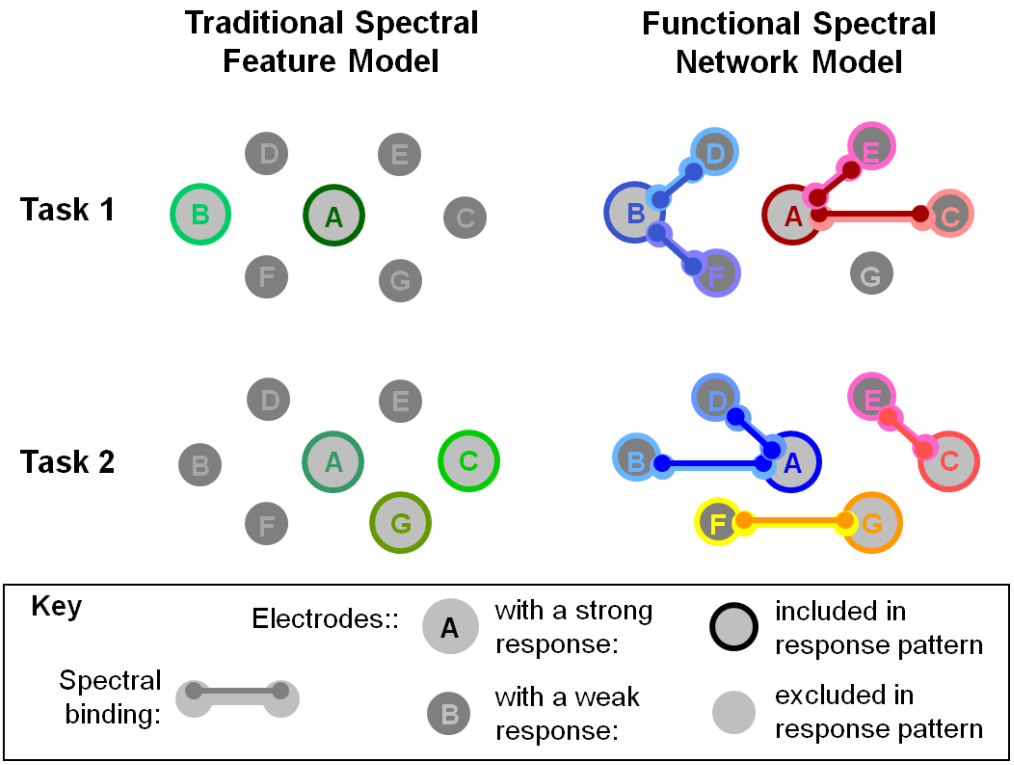

Figure 2.2: Functional Spectral Network Concept. For different tasks, there may be networks of electrodes that are spectrally bound. There may be multiple networks for each task, and networks may be different for different tasks.

Figure 2.2 illustrates a larger scale picture of Functional Spectral Networks, groups of potentially many electrodes (nodes) that are connected because they are spectrally bound during a particular task. These networks may differ between tasks. Classic SF analysis of various tasks may find a few electrodes whose responses distinguish a task, captured in the cartoon Figure 2.2 as electrodes which are colored on the left side. The FSN concept allows for the representations of anatomical and spectral relationships between electrodes to be considered when discriminating Task 1 from Task 2. Exploring how much this improves task discrimination, and what anatomical and spectral relationships are common, is the overall goal of this chapter.

2.1.2 Goals of this chapter

To characterize how FSNs are useful in understanding ECoG electrophysiology, we consider three specific goals. First, we compare the functional contrast of SFs to that of FSNs to measure how much better FSNs are at discrimination tasks. Second we analyze the spatial and spectral patterns defined by the FSNs, and compare them to known anatomical structures. Third, we relate these findings to the ongoing neuroscience debate on whether neural representations are based on diffuse signals across many anatomical regions versus very local, focussed representations.

To address this last question most usefully, we also introduce the idea of core Functional Spectral Networks (Core FSNs). These are defined based on spectral binding for a particular tasks, and choose a small subset of the connected components that give good discrimination performance.

To compare the functional information content of SFs and FSNs, a task was chosen that allowed two levels of granularity in distinguishing mental tasks. Course grained discrimination evaluates the ability to discriminate between speaking versus rest, and fine grained discrimination evaluates the ability to discriminate between the speaking of different categories of words. This tasks allows us to characterize the sensitivity of SF versus FSNs, and to characterize how variable are the FSNs that are generated during different tasks.

2.1.3 Motivation for studying FSNs

The historical view has been to interpret the brain to be a modular structure with distinct areas performing distinct functions. This view has been supported by numerous reports from stroke studies dating back to the 19th century. A large body of neural electrophysiology studies [11, 111-114] and brain imaging studies [115], have supported the view that the brain modules are organized in a hierarchal manner and information is processed serially.

An alternative view is that the function of, and information encoded in, specific brain areas cannot be isolated from the global activity of the whole brain. As early as 1961, Roy John noted, "The fact that an animal can learn or retain the [conditioned] response after a lesion does not of itself warrant the conclusion that the structure normally played no role in the response." [116]. He argued that certain cognitive processes were more likely to be a 'set process' (which would imply cortical distribution) than a 'bit' in a specific brain location and that it is more likely that the lesion of a region alters the processing of that state than it abolishes the state altogether. While historically most work focused on describing the modular processing model of the brain, there is a recent paradigm shift towards explaining cognitive function in terms of the context dependent, transient, coherent behavior of large neuronal populations [117]. This work aims to contribute to this new understanding of brain function.

The key to understanding coherent behaviors of neuronal populations lies in understanding properties such as neuronal synchronization at different spatial and temporal scales. Evidence for distributed coding schemes with transient spectral correlations have been shown in the rat barrel cortex [118], cat primary visual cortex [117, 119], and monkey motor cortex [120], somatosensory cortex [121], and visual cortex [122]. Advanced functional imaging based on fMRI offers growing evidence to support of large-scale inter-regional networks in the organization and encoding of information within the brain [123-126]. However, there is not yet a fundamental description of the transient relations of regional electrophysiological properties and inter-regional cortical networks. How these relations are reflected in spatio-spectral patterns of ECoG response also remains unknown.

A recent set of papers have demonstrated improved ECoG signal cognitive task classification performance when the traditional limited band and anatomically local spectral features are expanded to include larger anatomic areas [127] or

multiple frequency bands [128] or both [93, 102]. While this work motivates our approach, these studies were done using a motor task and single subject data. In this work we present a more comprehensive investigation of the FSN concept.

Near-infrared Spectroscopy has been used to measure spatio-spectral patterns across extended cortical areas in the event-related optical signal (EROS) BOLD response [129]. The EROS was shown to shift in anatomic representation and spectral content over time and between different cognitive tasks. However, the EROS is an electro physiological phenomenon constrained to sub-beta (< 8Hz) frequencies; our work uses the ECoG signal to expand the exploration spatio-spectral pattern analysis to include a much broader range of frequencies.

2.2 Methods

2.2.1 ECoG Patient population

ECoG data is measured from invasively monitored human subjects with intractable epilepsy who underwent temporary placement of intracranial electrode arrays to localize seizure foci. The study was approved by the Human Research Protection Organization of Washington University in St. Louis. Signals were acquired while five patients performed a word repetition task. In conjunction with the speech task, the standard procedure of stimulation mapping [130] was used to locate cortical areas that were essential for speech production or tongue movement for the subjects.

Table 2.1: Chapter 2 Subject Data

Subject	Age	Sex	ECoG implant description	Implant sketch*	Number of task runs
1	58	F	64 clinical-ECoG electrodes; 8x8 grid over the left frontal cortex	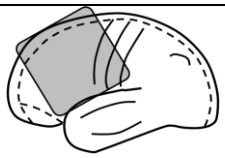	6 runs containing 56, 56, 56, and 56 trials of phoneme categories 'ee', 'eh', 'ah', and 'oo' respectively in total.
2	48	F	64 clinical -ECoG electrodes; 8x8 grid over the left frontal-parieta cortex	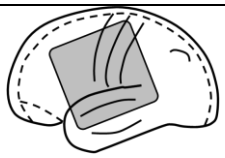	6 runs of 9 trials of each phoneme category.
3	49	F	48 clinical -ECoG electrodes; 4x8 grid over the left temporal cortex	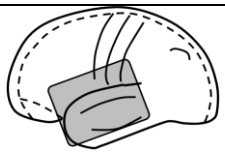	6 runs of 9 trials of each phoneme category.
4	46	F	48 clinical -ECoG electrodes; 4x8 grid over the right frontal-parietal-temporal cortex	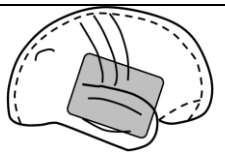	4 runs of 9 trials of each phoneme category.
5	36	M	48 clinical -ECoG electrodes; 4x8 grid over the left frontal-parietal-temporal cortex	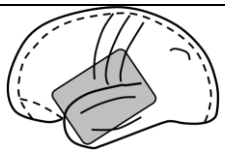	6 runs of 9 trials of each phoneme category.

*grey shaded areas represent the approximate areas of cortical surface covered by the implants

2.2.2 ECoG recording and electrode localization

The recording devices used in this study were 64 or 48 electrode grids with equally spaced rows of eight electrodes each encapsulated in a silastice sheet with a 2.3mm diameter exposed area and 1 cm center-to-center spacing. Bio signal amplifiers were used to record the changing field potentials at a sampling frequency of 1.2 kHz with 24-bit resolution. BCI200 software was used to synchronize task cue stimulus presentation with the recorded ECoG signal and recorded microphone signal. The clinical Cortical Stimulation Mapping (CSM) procedure was also was done performed on each subject to indicated electrode pair locations that elicited either a mouth motor or sensory response or resulted in speech arrest.

2.2.3 Stimuli and task description

Subjects repeated a 36-word list, cued randomly through headphones, (between 6-18 times) into a microphone. The 36 words were consonant-vowel-vowel-consonant words that consisted of 8 words from each of four phonemes classes 'EE', 'EH', 'AH', and 'OO'. Examples of these words include "peek", "bed", "read", and "book". Sufficient pause was given after each word so that a period of non-speech of at least 2 seconds in length could occur before a new audio stimulus was given. We call these periods the Inter-Trial Interval (ITI). The speech task structure is depicted in Figure 2.3.

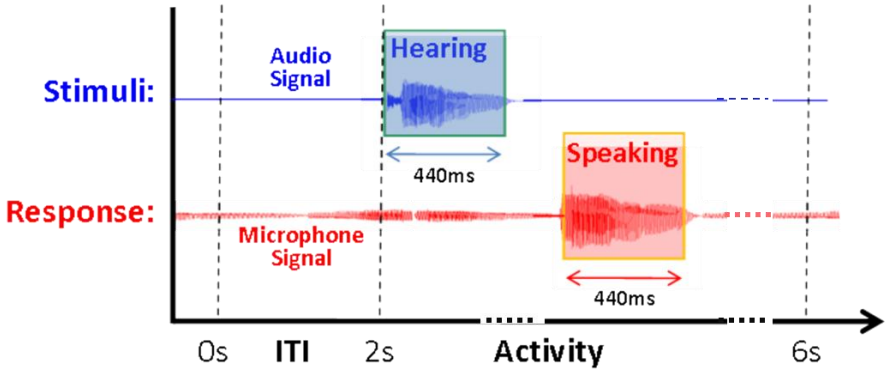

Figure 2.3: The timing structure of speech tasks.

A speech task includes two interesting temporal features, the time when the audio prompt is given, such as when the user hears the word prompt, and the time when the subject responds. In order to best match, from multiple trials, the ECoG signals that correspond to the speech response, our analysis uses the voice onset time (VOT) of the response as an anchor, and all trials are aligned to that time. Then, for functional analysis, each trial of the speech task was broken down into overlapping temporal segments with respect to the onset of the recorded speech response. Each segment or temporal period has a length of 167ms. The three second interval from 1s before to 2s after speech onset is broken up into 37 overlapping temporal periods in steps of 83ms. These are labeled t1, t2, t3… t37 respectively, and depicted in Figure 2.4. Trials for which a clear and distinct VOT time could not be defined, due to either lack of clear overt speech production by the subject or contamination from utterances of speech that were not part of the task, were not considered in the analysis.

The speech task was analyzed with the ECoG signal during each temporal block from all speech trials compared to ECoG signal during ITI periods. We use these temporal blocks to discretize the signal in order to more easily explore when there are parts of the ECoG signal that correlate with different task behaviors, and in order characterize trends across different subjects and tasks about what patterns of ECoG signal response occur at different times.

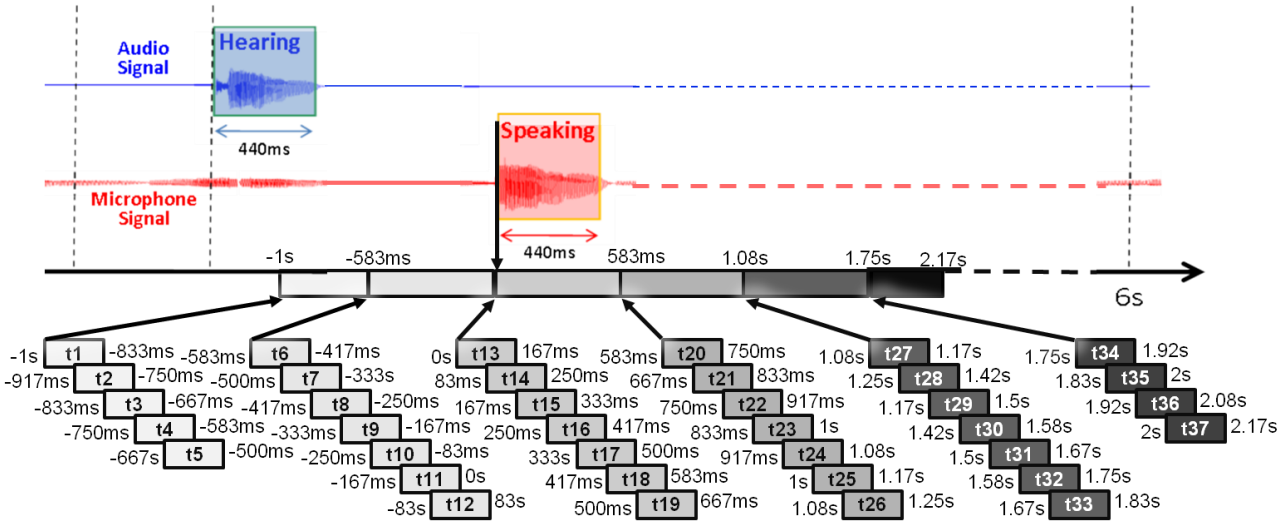

Figure 2.4: Speech task analysis temporal structure.

2.2.4 Defining Spectral Features (SFs) from ECoG spectral response data

In order to define SFs and FSNs that significantly discriminate the speech task conditions we first calculated the spectral response of the ECoG signal using a Gabor Wavelet Dictionary [131]. This is in contrast to the majority of the ECoG work done to date which used either the band pass filter method or the maximum entropy method used by the BCI2000 system (see 1.2.6) to extract spectral features. Using a wavelet dictionary to define ECoG signal feature has recently been shown to be a robust method for extracting spectral features with temporal resolutions well fit to individual frequency ranges [93].

A wavelet with a Gaussian envelope width at half max of 4 wavelengths was used to get the spectral response centered at each sample point of the signal for 88 frequencies sampled exponentially from the range of 1 to 338 Hz. It is common in electro-cortical signals that the power follows a 1/frequency trend. Thus, we follow the standard procedure to use the natural log of the Gabor Wavelet Dictionary amplitude response, and this is defined as the spectral response for each of the 88 frequencies for each recorded ECoG electrode; the variables *g(i,f,t)* discussed earlier..

The spectral responses of each of the 88 frequencies for each ECoG electrode channel were then analyzed for functional significance with respect to the speech condition comparisons described above to determine the SFs. Standard R-squared analysis was used to evaluate how consistently each frequency's spectral responses differed between the test conditions. For one patient at one time interval, Figure 2.5 (left) show the R-squared score, at each frequency and electrode, thresholded so that scores with a p-value worse than 0.05 are grayed out and only the remainders are colored.

The frequency responses in ECoG signal are often not independent from each other, so further analysis was done to determine bands of spectrally adjacent frequencies that are all significant. Clusters of contiguous parts of the spectrum were grouped to include frequencies whose power variations were statistically significant (p-value<0.05) and which had the same direction of change (ie. increase or decrease) during the task condition. These frequency clusters are the Spectral Features (SFs) referred to in this work.

For each task condition (e.g., discriminating "oo" from "ah"), and for each time-period (e.g. t13), we compute a best SF. This best SF is chosen as the SF that maximizes the sum of the R-squared values for all the contiguous frequencies that are component parts of that feature. The response of the best SF is computed by summing the responses of all its component frequencies. This response is what is compared to FSN responses in the remainder of this chapter.

2.2.5 Defining Functional Spectral Networks (FSNs) from ECoG spectral response data

Functional Spectral Networks (FSNs) are defined as patterns ECoG responses that discriminate the brain state of one task performance condition from another. To determine the spectral patterns that best discriminate the task conditions we used Discriminant Function Analysis. The task conditions we consider are the differentiation of the articulation of words from the inter-trial interval (ITI), and the more subtle differentiations between the articulations of four different phonemic classes of words from each other.

Discriminant Function Analysis (DFA) is a method used to find a weighted pattern of time series variables that maximally discriminate the time series into specified groups [132]. Variations of this method have been used in many fMRI studies (such as [133-135]). DFA has been shown to give better results than the more popular method of Logistic regression when the sample sizes are on the order of 50 or less per condition [136], which is the case for this work (see Table 2.1). The manner in which we apply DFA in this work is closely related to Linear Discriminant Analysis (LDA) which has recently been applied to classifying ECoG data based on spectral response [93, 102, 127-128].

DFA finds variables that have maximal F scores (ratio of between-groups variance over the polled average within-group variance) between two groups. Thus, a task variable can be used to group the data into specific task groups and DFA can be used to find the weighted set of variables that maximally discriminate those two groups by linearly solving for a constant a and regression coefficient b_1 through b_m in the equation:

$$label = a + b_1 x_1 + b_2 x_2 + ... + b_m x_m ,$$

the values $x_1,...,x_m$ are the spectral ECoG signal features (or their PCA coefficients) as described below. The *label* vector is integer valued and in this case corresponds to the task label at each time point. We always compare only two

conditions to each other, so the label vector was either a 1 or a 0 for each feature sample point. The conditions and time periods compared are described in section 2.2.3.

On high dimensional data, a PCA decomposition gives a low dimensional representation of the time series data, and it is common to DFA in this low dimensional space. In this low dimensional space, Discriminant Functions define a projection vectors of PCA coefficients that best discriminates the task conditions. We project the Discriminant Functions back onto the frequency/electrode space to determine the FSN pattern representation as patterns across frequency and anatomy. See Figure 2.5 (right column) for an example of a FSN pattern in terms of frequency response across the electrodes.

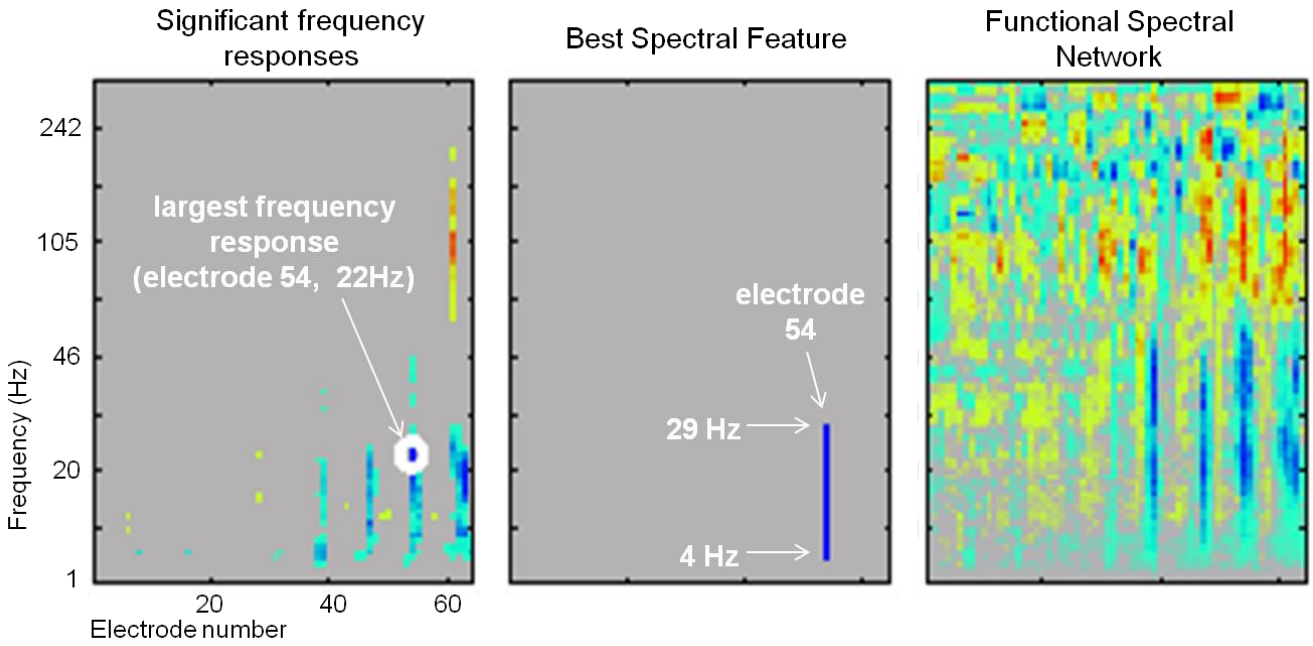

Figure 2.5: Functional features methods figure. Left: Spectral features (SFs) distinguishing rest (ITI) vs. speech for the period of 200-100 ms before speech onset (t10) for Subject 1. Middle: The SFs with the highest cumulative R-squared value for the same comparison as the SFs. Right: The FSN for the same comparisons.

In order to quantify the functional contrast of FSNs compared with SFs, the columns of the FSN pattern can be concatenated to make one long weight vector **v**, the spectral responses *g(:,:,t)* can be concatenated to make one vector **h(:,t)**, then response value *R(t)* of each FSN was calculated for every ECoG sample point as the dot product of these vectors:

$$R(t) = \mathbf{v}^{\mathrm{T}}\mathbf{h}(:,t)$$

2.2.6 Comparing SFs and FSNs using non-parametric statistics.

Spectral Features and the Functional Spectral Networks are compared in terms of their ability to discriminate cognitive tasks using a Monte Carlo p-value statistic. A description of MC p-value method as it relates to neural electrophysiological data is given in [137]. To compute the MC p-value in our case, we consider the features (SF or FSN) computed from data during two task conditions. A *test statistic* value is computed for the difference in the distributions of the data arising during the two task conditions. That same test statistic is then computed for the data for a large number of random partitions of the data into two groups, referred to as the *permutation distribution*. The Monte-Carlo p-value, for the task based partition of the data is computed by calculating the percentage of the test statistic values of the permutation distribution that are greater than the true test partition statistic.

R-squared analysis was performed on the best SF response value and used as the SF test statistic. To calculate the permutation distribution of SF R-squared values, the entire process of first defining SFs based on the R-squared values of the individual spectral frequency responses and then finding the best SF for each comparison and computing its response was done, for each of 1000 random permutations of the trials. This was repeated separately for each speech task time period for each conditional comparison done.

R-squared analysis was also performed on the FSN responses and this value was used as the test statistic for the FSNs. The principal component loading responses for each of the permutation distribution partitions were used to recalculate a DFA pattern in the PCA space for each random partition. Thus a new FSN was created for each permutation partition whose projection onto the SF space was used when calculating the FSN response values for the permutation distribution. It was not necessary to redo PCA on the data for each random partition because PCA was done over the entire data set and not done with respect to any data groupings.

The MC p-value has the advantage that the data does not need to give a Gaussian distribution of the test statistic in order to evaluate the significance of the test condition. A further advantage of this method is that Monte-Carlo p-values are comparable across different test statistics for different measurements because the same null hypothesis is tested.

2.2.7 Definition of Core FSNs

Core FSNs allow for an evaluation of how anatomically diffuse is the discriminant information within the FSN for each task. Core FSNs are defined to represent a (greedily chosen) minimal set of electrodes required to discriminate the functional task conditions. The four step process for defining Core FSNs is depicted in Figure 2.6 (step 1), Figure 2.7 (steps 2 and 3), and Figure 2.8 (step 4). This process, and how the responses of Core FSNs were defined, is discussed below.

2.2.7.1 Step 1: Split FSN into sub-FSNs

First, for each FSN, we cluster electrodes with similar functional spectral response patterns. The clustering uses a similarity measure that forces the groups to correspond to groups of spectrally bound electrodes. As an example, in the far right column of Figure 2.5, each column represents the functional spectral response of an electrode within the FSN, the electrodes are grouped based on the correlation of each column to the other columns. The similarity between electrodes *i,j* is computed as:

$$g(i,:,t)^T g(j,:,t),$$

which is the correlation between the frequency response profiles of these electrodes. This similarity measure is used as input to Affinity Propagation [138], a robust clustering method for which the number of clusters does not need to be predetermined. An exemplar data point (ie. ECoG channel or column in this context) is assign to represent each cluster, and these clusters are referred to as sub-FSNs. Later these are visualized as star-graphs where the exemplar electrode is connected to all the other electrodes in the sub-FSN. Figure 2.6 depicts the subdivision of an example SFN into sub-SFNs.

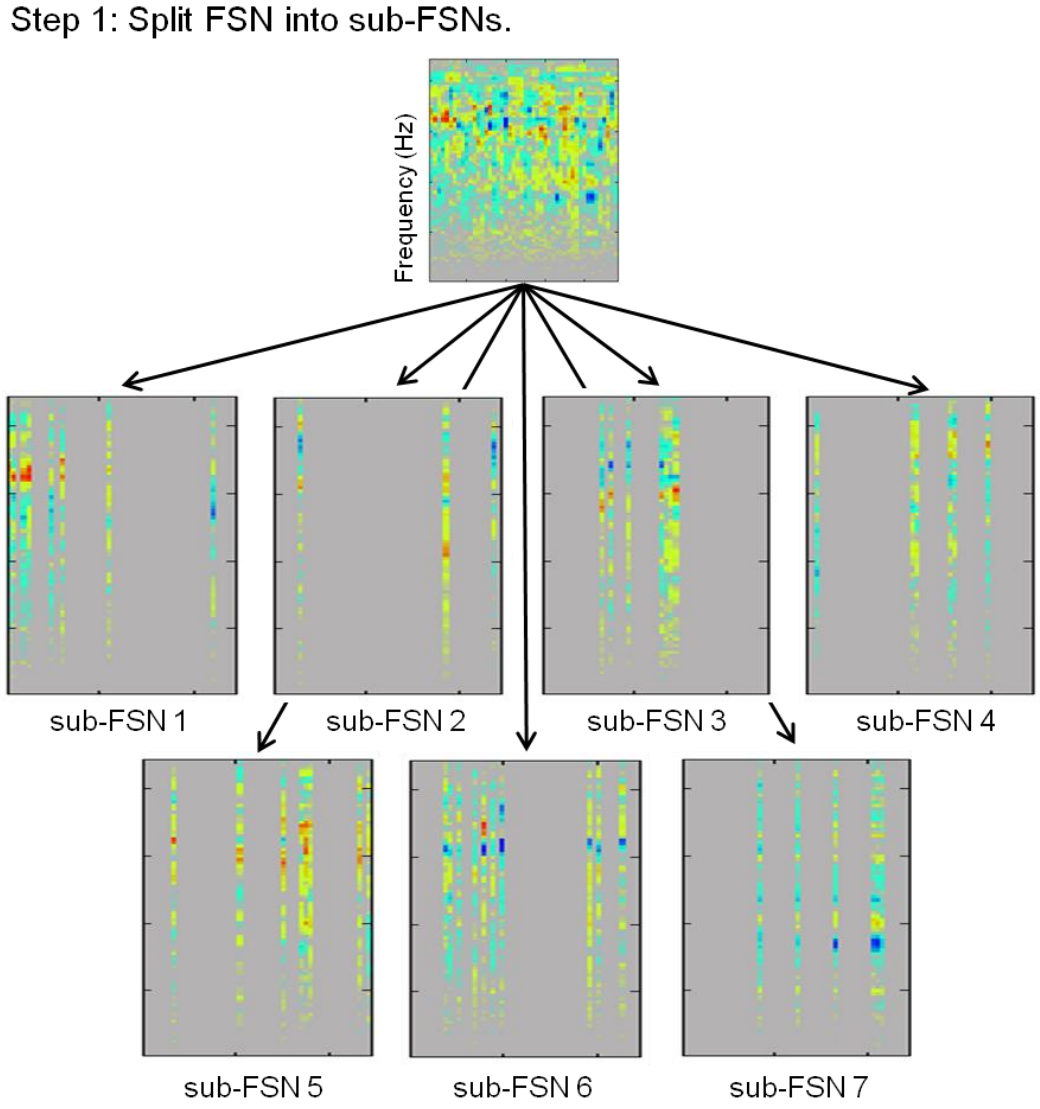

Figure 2.6: Step 1 in the method for defining Core FSNs.

2.2.7.2 Step 2: evaluate the functional contrast of sub-FSNs

The sub-FSNs form component pieces of the overall pattern of signal variation. We evaluate their independent ability to discriminate between task conditions in two ways. First, the response of each sub-FSN was computed in the same way as the full FSN. R-squared analysis was performed using the sub-FSN response values. Second, R-squared analysis was done on the response of the entire FSN when the sub-FSN is excluded. Figure 2.7 'Step 2' plots these values for the example sub-FSNs of the FSN shown in Figure 2.5.

Two orderings of sub-FSNs were then made based on these two values. One with the sub-FSNs ordered from greatest to least R-squared value and one with the sub-FSNs ordered from greatest to least decrease in R-squared value

when the sub-FSN is removed. For both of these orderings cumulative sub-FSNs were then compiled by progressively adding sub-FSN until the complete FSN was again formed.

2.2.7.3 Step 3: define and evaluate cumulative FSNs

For each of these cumulative sub-FSNs the R-squared value was computed. These were tested for significance using the MC p-value test. Random partitions of the trials were used to generate pseudo-sub-SFNs which were used to form partition distributions of at least 1000 samples of pseudo cumulative sub-FSNs with the same number of included channels for each step of the true cumulative FSNs. This allowed for determination of the stage in the cumulative sub-FSNs lists when the cumulative sub-FSN becomes a statistically significant FSN using the MC p-value. The two cumulative sub-FSN orderings for the example FSN are depicted in Figure 2.7 'Step 3'.

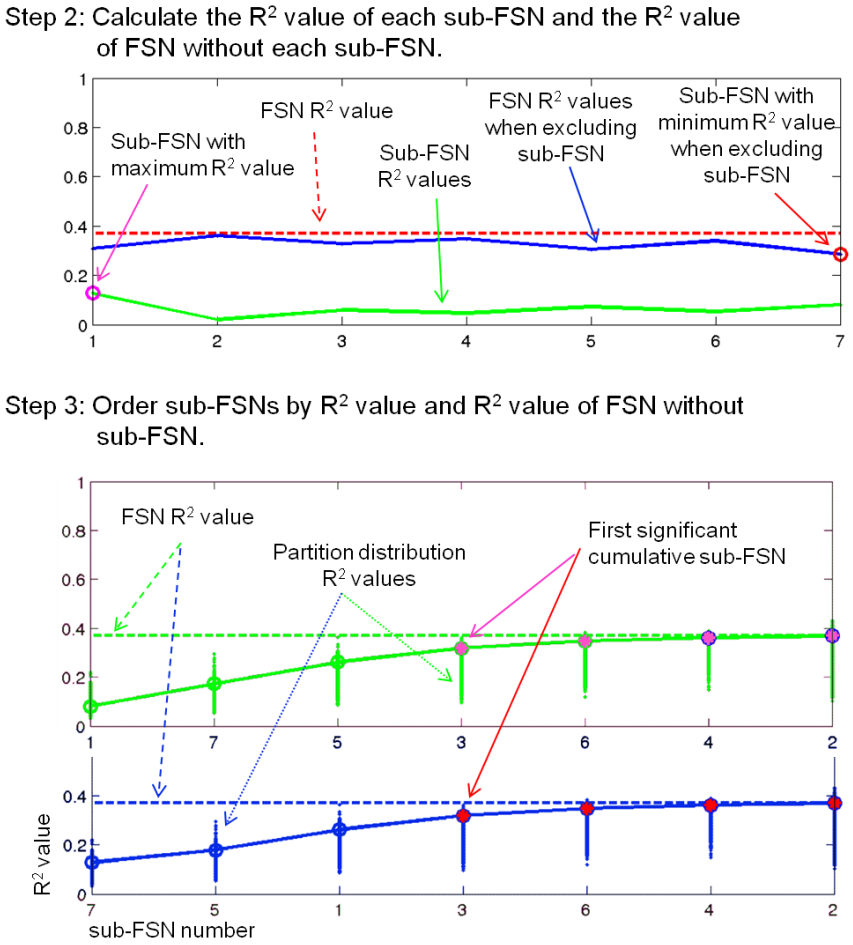

Figure 2.7: Steps 2 and 3 in the method to define Core FSNs.

2.2.7.4 Step 4: define Core FSN as best cumulative SFN

Since the goal of the Core FSN concept is limit the FSN to the populations of spectrally bound anatomic sites that make the largest functional contrast contributions to significant task discrimination, the Core FSNs are defined as the significant cumulative sub-FSN with the fewest sub-FSNs from either orderings that has significance. This greedy approach serves to find limited groups of electrodes that are able to discriminate between task conditions. The 4 sub-FSNs for the Core FSN of the example used here are shown in Figure 2.8 along with representations of the relative positions in the ECoG grid and plots of the individual spectral responses of the electrodes in each of the sub-FSNs in the Core FSN.

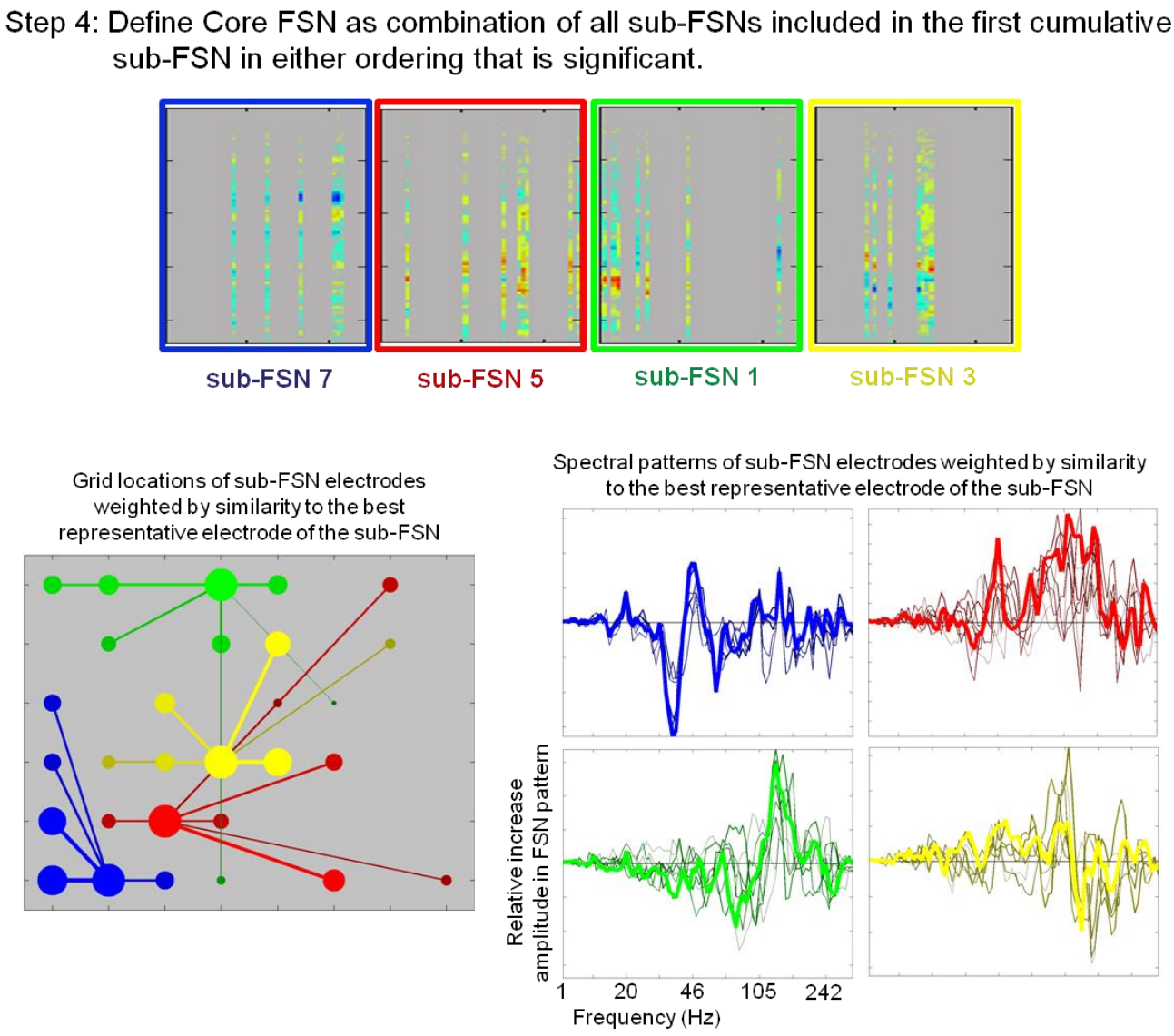

Figure 2.8: Step 4 in the method for defining Core FSNs.

In order to help compare the anatomic and spectral content of the SFs and FSNs, the significant Best SFs and Core FSNs are visually depicted in Figure 2.9.

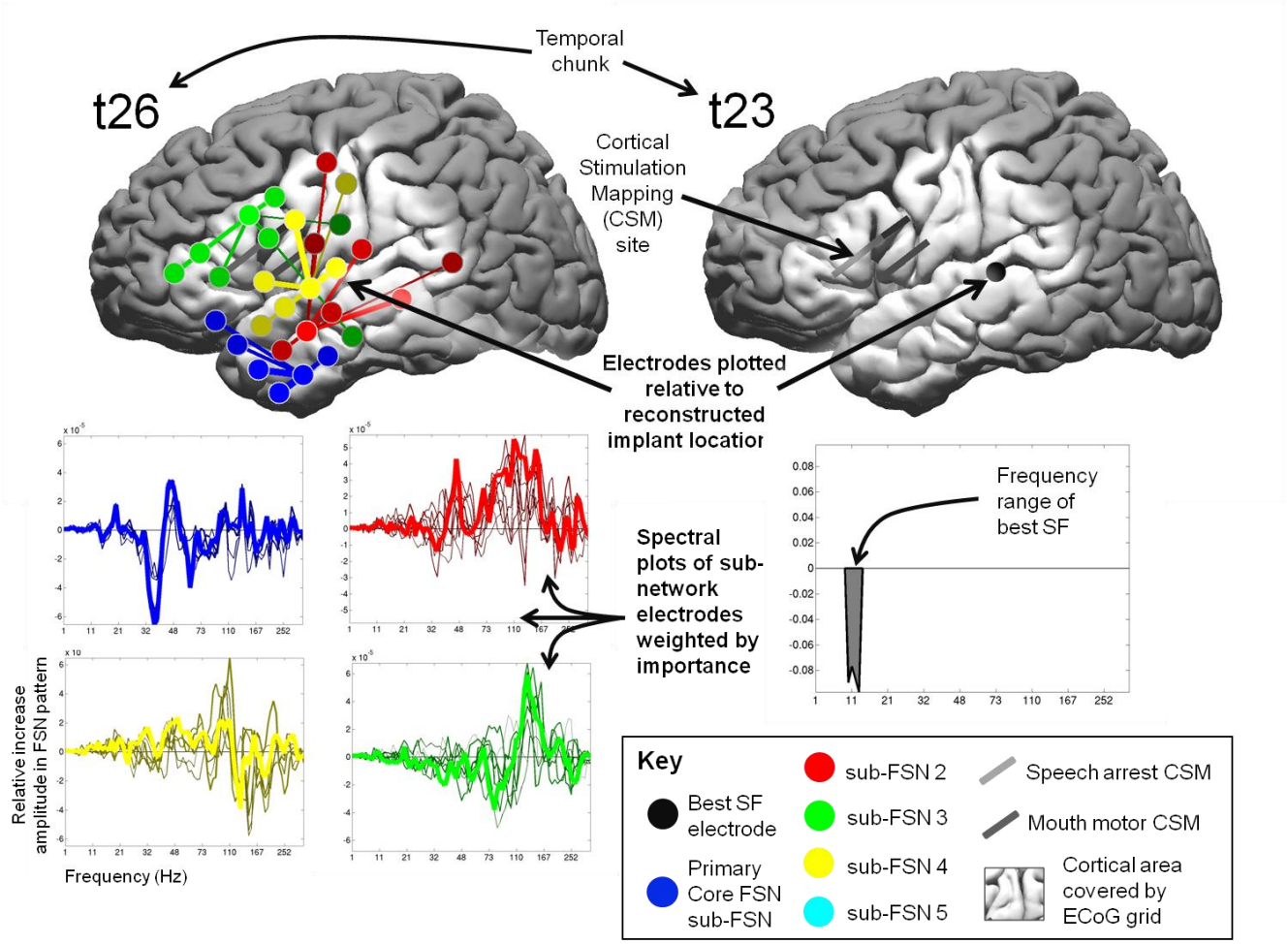

Figure 2.9: Explanation of SF and FSN plots. The left column illustrates the features of the Core FSN visualizations using the Core FSN from time period t26 and condition phoneme 'ee' versus 'eh' for Subject 5 as an example. The right column illustrates the features of the Best SF visualizations using the Best SF from time period t23 and condition phoneme 'speaking' versus 'rest' for Subject 5 as an example.

2.3 Results

There are two main results consistent across all subjects. First, the Core FSNs had earlier and longer significant detection of speech events than the Best SFs. Second, the Core FSNs had higher significance for classifying spoken phonemes. These two results, illustrative examples of the Core FSNs, and general trends in spatio-spectral content of the Core FSNs are presented in the following sections. For completeness, all of the identified Core FSNs for all speech task conditions and subjects are plotted in Appendix A according to the example given in Figure 2.9.

2.3.1 Core FSNs had earlier and longer significant detection of speech events

The fist main result is shown in Figure 2.10. The figure summarizes the discriminative R-squared value results for the 'speaking' verse 'rest' condition for all five subjects. The voice onset times (VOTs) used to align the task trials and define the time periods are indicated by the black vertical lines. The Best SF (red line), complete FSN (green line), and Core FSN (thick blue line) are plotted over all task time periods with the significant results indicated respectively by the red triangles, blue squares, and blue circles. For reference, the R-squared value levels that correspond to significance (a MC p-value of 0.05) are indicated with dashed lines.

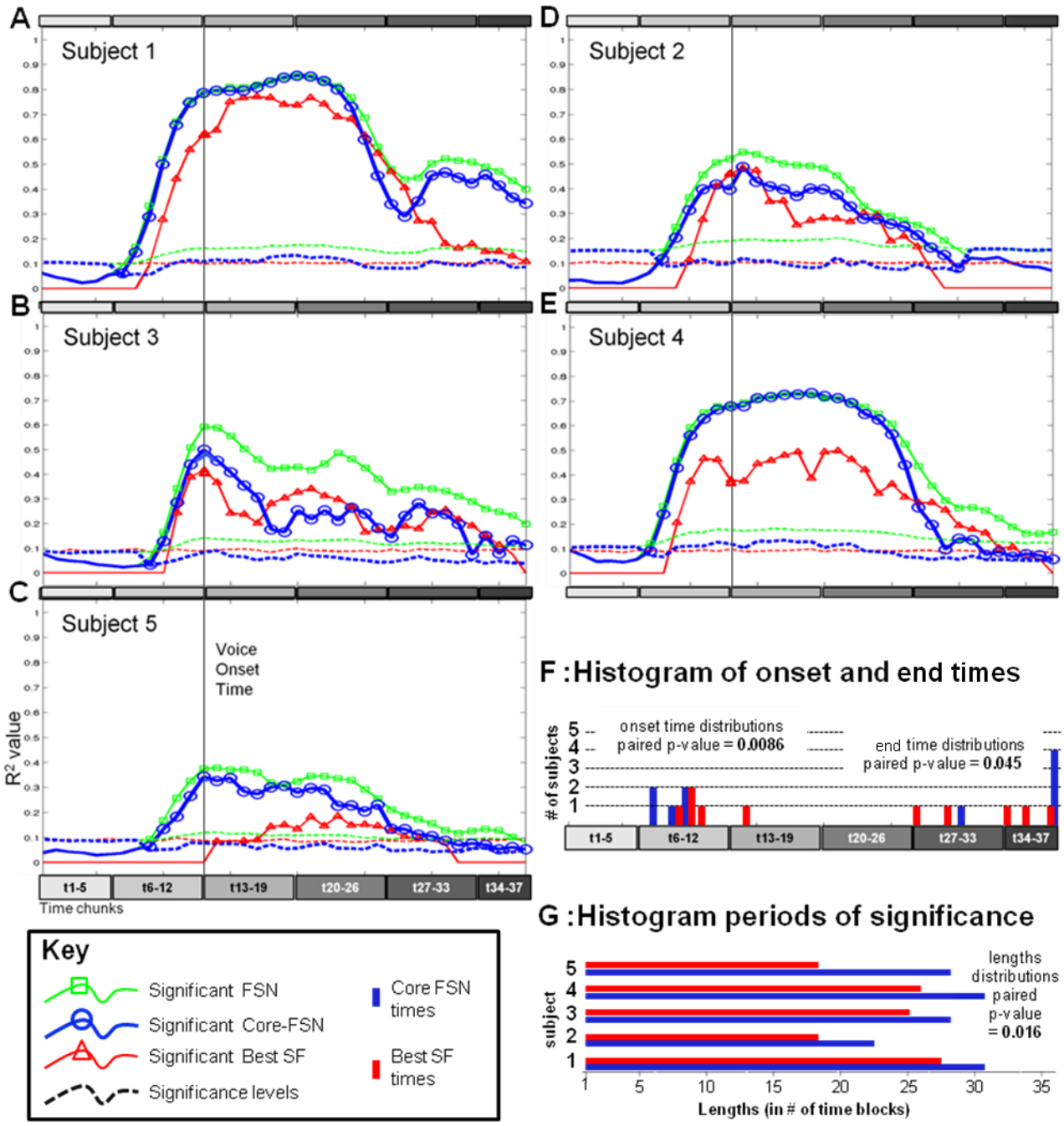

Figure 2.10: Timing of significant responses for speaking versus rest. Plots A-E show the R-squared values for subjects 1-5 respectively. The solid lines indicate the R-squared values of the Best SFs (red), complete FSNs (green), and Core FSNs (blue). The dashed lines indicate the significance levels for the solid line of the same color. Time periods with significant R-squared values for the Best SFs, complete FSNs, and Core FSNs are marked respectively with triangles, squares, and circles. Plot F gives the histograms for time periods marking the onset and end of significance for Best SFs (red) and Core FSNs (blue). A paired student's t-test was used to determine the given p-values of significance between the Best SF and Core FSN distributions.

The data in Figure 2.10 show that the functional contrast of FSNs becomes significant earlier in the task and remains significant longer than that of SFs. In all subjects (plots A-E) there are time periods showing discrimination between

tasks starting approximately half second before the VOT and, surprisingly, lasting up to two seconds after the VOT, which was the limit of the analyzed trial time. However, Figure 2.10 F show that the onset times of significance for the Core FSNs are significantly earlier than the onset times of the SFs (pair p-value < 0.01) and the end times are significantly later (pair p-value < 0.05). This leads to the length of total time periods that are significantly detected as active speech events being significantly (pair p-value < 0.05) longer for FSNs (as seen in Figure 2.10 G).

Figure 2.10 also highlights that the R-squared value required for significance is different for the SFs, core FSNs and FSNs. The FSNs have higher significance thresholds because there are more degrees of freedom in choosing the DFA projection vector. Thus, in the process of computing the MC p-value this approach does better on the randomized partitions. The core FSNs have less flexibility because they are created by composing correlated parts of the FSN, giving them less flexibility and therefore an intermediate threshold for significance.

Considering that the Core FSN threshold levels are roughly equal to those of the SFs, the Core FSNs generally have more functional contrast than the best SFs. The exceptions to this are a period around VOT for subject 2 and later periods after the VOT in subject 3. It can also be said that at the point of VOT the functional contrast values of the Core FSN are as good as or better than the complete FSN while they tend to get comparatively worse at later time points. Thus, in general limiting the FSN to a smaller set of electrodes with spectrally similar responses decreases functional contrast at later time periods. This is an indication that when the initial mouth motor response to the task has attenuated the functional contrast becomes more anatomically and spectrally diffuse.

For some patients and time points, FSNs are able to distinguish tasks when SFs are not. For subject 5, at the VOT, there are no significant SFs. This is evidence that this subject did not have a strong ECoG response to the initial mouth motor movement despite the fact that there were several positive mouth motor CSM sites (electrode sites indicated as essential to speech production, see 1.2.5) for this subject (see Figure 2.14 which uses subject 5 as an example). The R-squared values for this subject are generally low indicates that ECoG response for this subject was relatively weak, possibly due to a low task participation level. However, despite this there is still a broad temporal range of significant FSNs compared to the number of significant SFs showing that the FSNs are better able to capture the more subtle ECoG spectral response then SFs are.

2.3.1.1 The Core FSNs for speaking versus rest display a spatio-spectral pattern that is anatomically focused and spectrally consistent

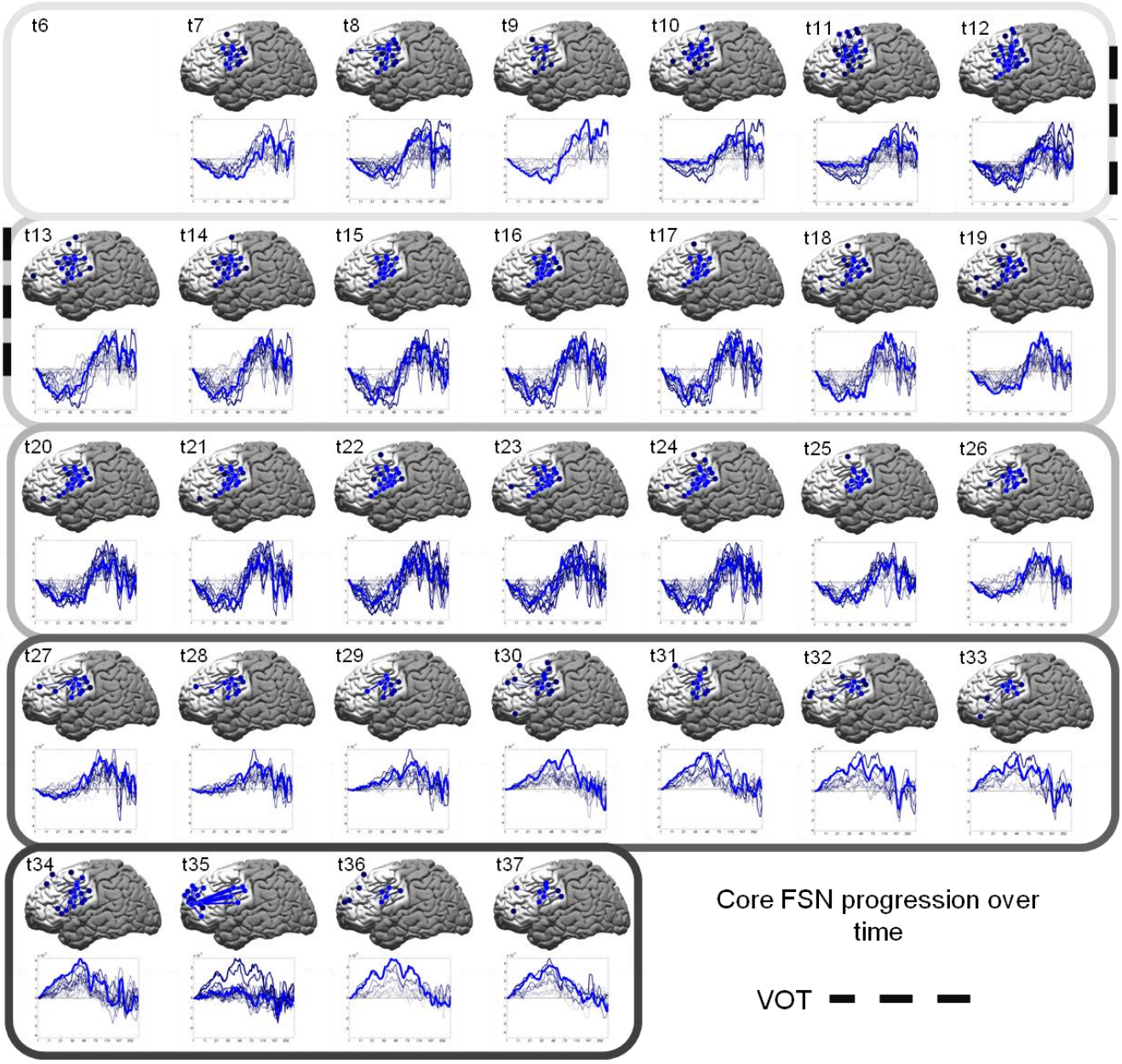

Figure 2.11: Subject 1's Core FSN over time. Each brain plot gives the anatomic locations for each spectrally bound group in each Core FSN, weighted by strength of response. Each spectral response plot (below the each brain plot) gives the spectral response of electrodes in each spectrally bound grouping for each Core FSN, with magnitude of response on the y-axis and frequency on the x-axis.

The Core FSNs for speaking versus rest remain generally focused around the positive CSM sites. They also display a typical initial spectral response to a motor task, but this response profile tends to shift its spectral content over time. These general trends are illustrated using the example of subject 1's Core FSNs in Figure 2.9. The figure shows the Core FSNs for the speaking versus rest condition for the FSNs at every time point from Subject 1. The Core FSNs are visualized according to the convention described in Figure 2.9. The Core FSNs of Subject 1 all consist of a single sub-FSN indicated in blue. This is also true for all significant speaking versus rest Core FSNs of the other four

patients with the single exception of time period t34 for Subject 5. Another result seen in all subjects is that the anatomic coverage of the Core FSNs for the speaking versus rest conditions remains generally focused around the positive CSM sites. Also the typical spectral response that binds the electrodes together shifts its spectral content over time, which is most evident starting from time period t28, with the low frequency no longer have smaller response than baseline, but higher frequency responses remaining larger than the baseline.

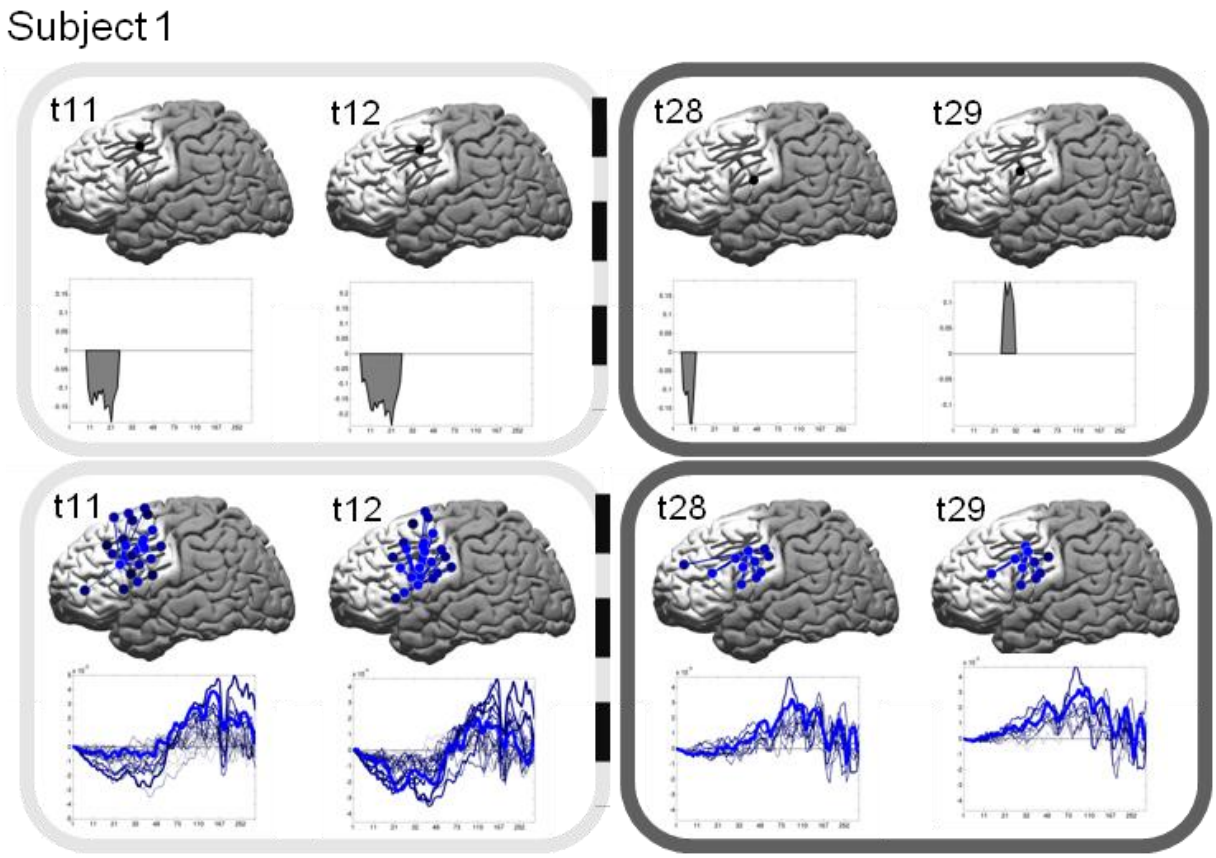

Figure 2.12: Example of Best SFs and Core FSNs for speaking for subject 1.

The Best SF and Core FSN anatomic locations for speaking versus rest match the CSM sites well. Figure 2.12 shows both the Best SFs and Core FSNs for Subject 1 for the two time periods just before the VOT (t11 and t12) and two time periods just over a second after VOT (t28 and t29, see Figure 2.4 for a review of the task time periods). The Best SFs before and after the VOT are located within the positive CSM area. This was true for all significant Best SFs for speaking versus rest for Subject 1 except for those of time periods t34, t35, and t36. For those time periods t34, t35, and t36 of Subject 1 the magnitude of the R-squared values are relatively low (see Figure 2.10 A). This indicates that there is a general good match between Best SFs anatomic locations and CSM sites with the match decreasing when the ECoG spectral response is weaker. The bottom row of Figure 2.12 also highlights the trend, discussed above, that the Core FSN anatomic locations for speaking versus rest match the CSM sites well.

The typical spectral response that binds the electrodes together shifts its spectral content over time, which is most evident starting from time period t28 in Figure 2.11 and illustrated in Figure 2.12. The left column of Figure 2.12 shows that the spectral content of the best SFs and Core FSNs just before the VOT fits the standard profile of a decrease response at the mu band (low frequency) and coupled increase in the response in the higher frequency gamma band. The best SF plots show that the most significant SFs are mu band features in this case. However, the trend across subjects was that they varied between mu band decrease and broad gamma band increase at time periods around the VOT. While the anatomic locations of the best SFs and Core FSNs for the speaking versus rest task remain consistent, their spectral content does change. By looking at the spectral content of the best SFs and Core FSNs at the later time points shown in the right column of Figure 2.12 you can see that the best SF frequency bands become narrower and that the spectral content of the Core FSNs shifts from the expected motor response to very broad band increase that includes the mu band. Changes in spectral content were seen across all five subjects even when the anatomic locations of the best SFs and Core FSNs remained focal to the positive CSM sites as illustrated in Figure 2.12.

There is more anatomic network diversity in Core FSN at later time periods after VOT. Figure 2.13 shows this general trend toward network diversity throughout the task. Time periods t33 – 36 encompass a period when the Core FSN expands to include a group of electrodes in the frontal region. This expansion was only strongly seen for a single time period (t35). Such a transient expansion to include a new group of electrodes in a different area of cortex was also seen at later time points in the other four subjects. Figure 2.14 depicts examples of these expanded Core FSNs (right column) along with the corresponding Core FSNs at the time period just before the VOT (left column).

Another trend that is clear from these two figures is that the spectral content of the Core FSN at these later time periods is more diverse than just before VOT. The spectral patterns later in the task also do match the standard motor response spectral pattern. In fact in the cases of Subjects 2 and 4 a mu band increase coupled with a decrease in the gamma range is seen. The spectral diversity of the Core FSN after the VOT is most extreme at time period t35 for Subject 1 and t34 for Subject 5. While the Core FSN for t35 for Subject 1 remains a single sub-FSN there is a clear split in the spectral patterns of the electrode. This split in response patterns is even clearer for t34 of Subject 5, which is the only example of a Core FSN discriminating speaking versus rest with two sub-FSNs included in its Core FSN.

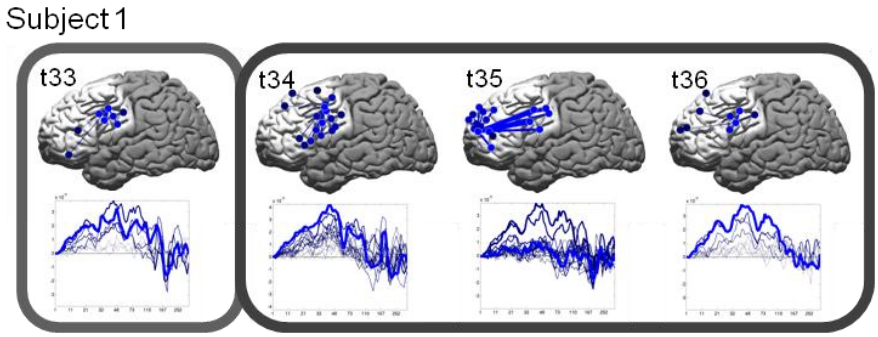

Figure 2.13: Example of broadening of anatomical coverage over time of Core FSNs.

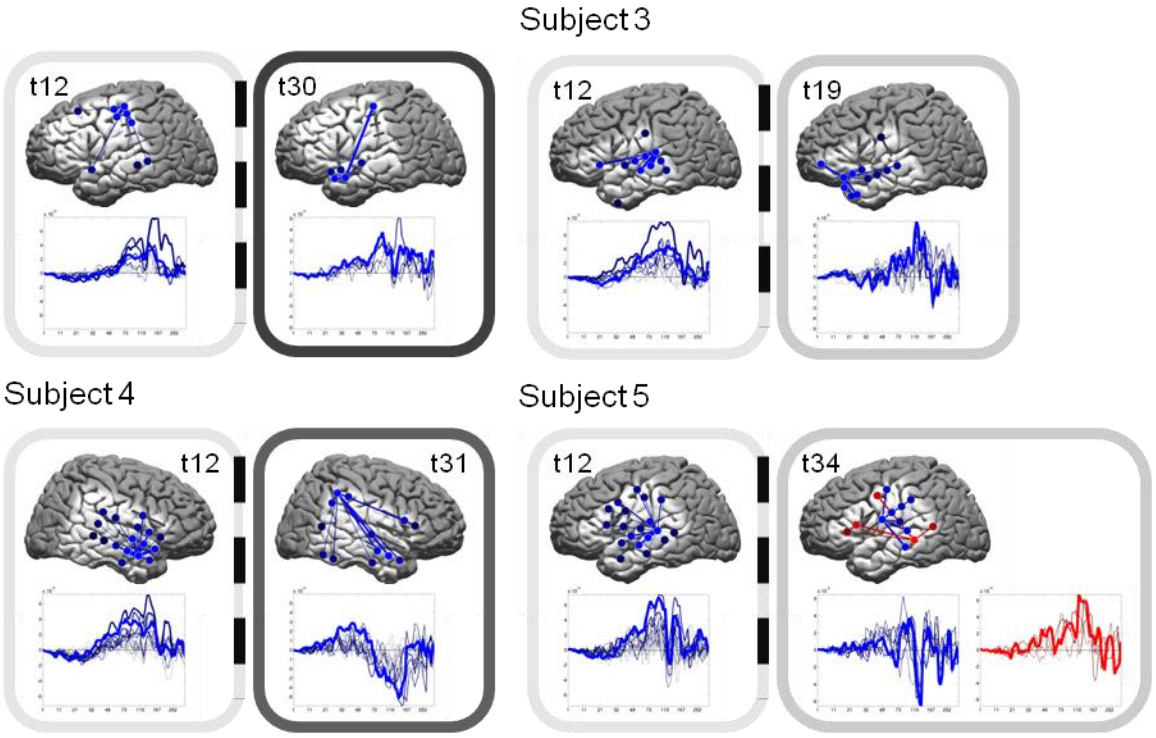

Figure 2.14: Example of characteristics of Core FSNs for speaking versus rest condition.

2.3.2 Discriminating spoken phonemes

2.3.2.1 Core FSNs have higher significance for classifying spoken phonemes

Core FSNs are better at the finer graining discrimination task of classifying spoken phonemes. A summary of the significant SFs and FSNs found in our analysis is given in Figure 2.15 and Figure 2.16. Figure 2.15 shows FSNs discriminate more phonemes than SFs for all of the five subjects. The figure shows a grid of gray lines representing every phoneme discrimination condition for each time period for all 5 subjects. The conditions indicated in the grid are depicted in the figure key. The phoneme conditions with significant SFs are indicated with black bold lines in the top grid and the significant Core FSNs are indicated with a bold blue line in the bottom grid. The total number of significant SFs and FSNs are given in the column of numbers at the far right of the figures. The bar plot in Figure 2.16 B shows that the increase in number of significant time periods is statistically significant (paired p-value < 0.01) upon group analysis. The differences in ECoG spectral response is more subtle for the phoneme conditions than the speaking versus rest conditions. Hence, these findings further support that FSNs are better able to discriminate cognitive task information in spectral response than SFs.

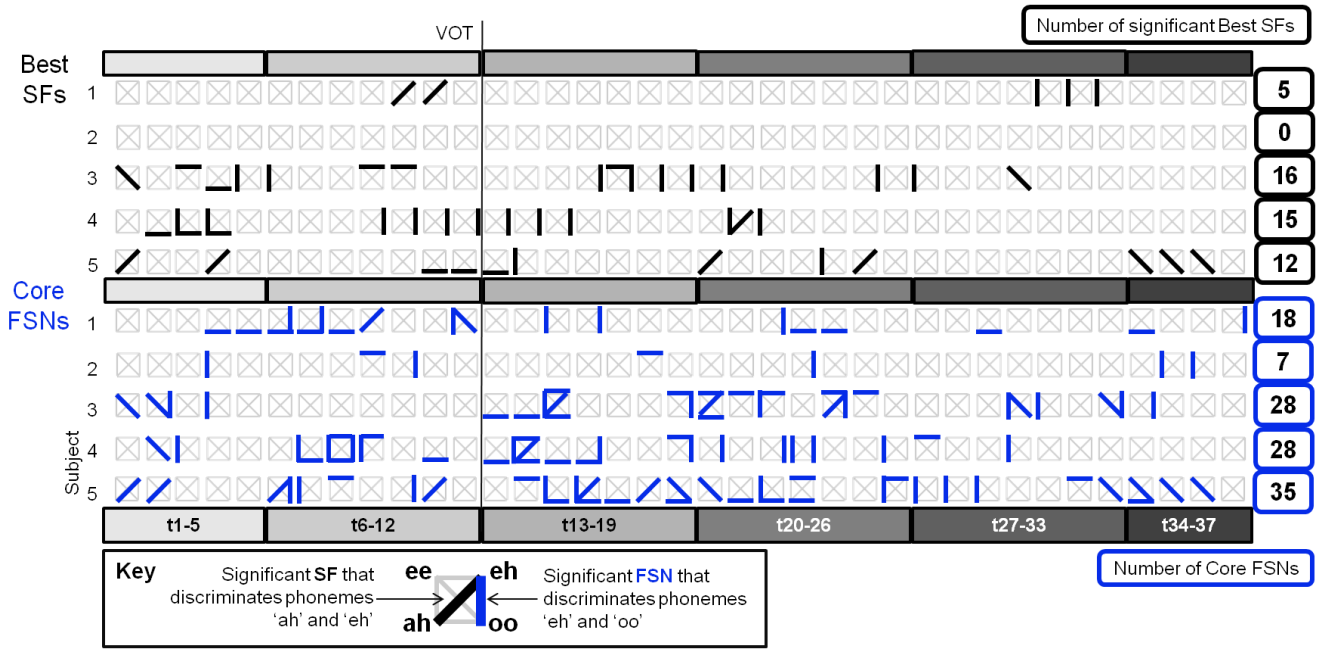

Figure 2.15: Table of FSN phoneme discrimination per subject.

Figure 2.15 also shows that the SFs and FSNs were very transient with different phonemes being distinguishable at different time periods. This is less true for SFs which are seen to more often consistently discriminate a certain phoneme condition over a longer period of time than the FSNs that more rapidly switch from discriminating one phoneme condition to another. It is also notable that the distribution of time periods and phoneme conditions SFs is not a subset of the FSN distribution. There is only moderate overlap in terms of time periods and phoneme conditions that can be discriminated with FSNs and those that can be discriminated with SFs. Only 4% (8/(166+48)) of the total found SFs and FSNs discriminated the same phoneme pair at the same time point.

Figure 2.10 shows the time periods t1-t5 contain no significant SFs or FSNs separating spoken words versus rest, so it is interesting that FSNs and SFs exist that distinguish between different phonemes. It is likely that these are due to brain responses to the auditory cue. Since the data is time-locked to the voice response, not the end of the auditory prompt, phoneme word groups that contain longer words may extend into these first time periods. Also, in this time range, there are more significant SFs than FSNs indicating that these responses are local.

The magnitude of the change in the ECoG spectral response can be independent of how well the FSNs can distinguish the conditions. The subjects with the most FSNs for the phoneme conditions are not the subjects with the most functional contrast in distinguishing the speaking versus rest condition (see Figure 2.10). It is also not true that subjects with fewer significant SFs have fewer significant FSNs.

FSNs can discriminate all phoneme pairs in 3 out 5 subjects. Figure 2.16 summarizes the phoneme conditions that are discriminable with SFs and FSNs per subject. Every significant phoneme condition in depicted in Figure 2.15 is represented with a thin black (SFs) or blue (DFNs) line on the grids in Figure 2.16. The grids have a gray line indicating all possible phoneme conditions just as in Figure 2.15. Subjects for which all phoneme conditions are

successfully separated with at least one significant FSN are encircled in blue. The most noticeable results is that for three Subjects (3, 4, and 5) all phonemes conditions have at least one significant FSN and no subjects have a significant SF for all phoneme conditions. There are in fact no phoneme conditions with significant SFs for Subject 2 despite the fact that this subject has a comparable number of SF to FSNs for the speaking versus rest condition (as shown in Figure 2.10).

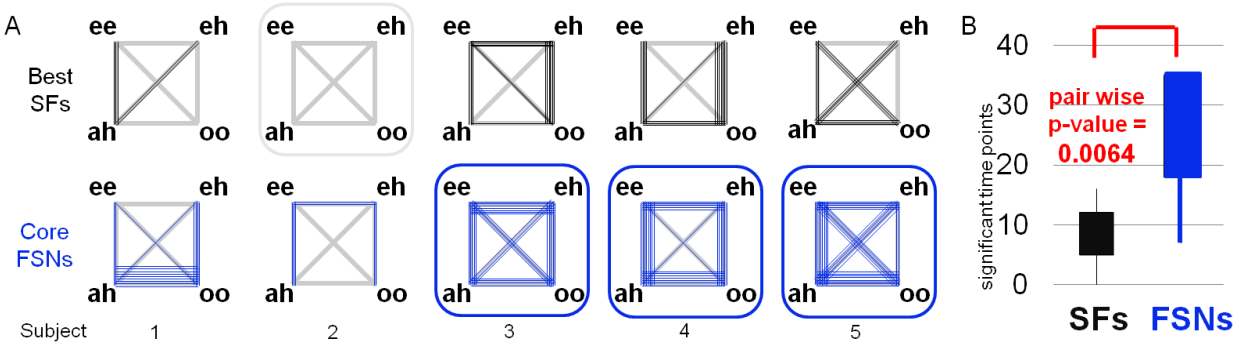

Figure 2.16: Total SF and FSN phoneme pair discrimination. Left: summary phoneme discriminant SFs and FSNs (listed with one column per subject). Right: box plot showing distributions of total number of phoneme discriminant SFs and FSNs over all subjects.

2.3.3 Core FSN diversity as a function of task.

Table 2.2: Phoneme discriminant Core FSN anatomic characteristics

Number of spectrally bound groupings	<25%	25-32%	33-49%	50-65%	66-74%	>75%	Totals per row
1	29	1	0	0	0	0	30
2	9	8	10	2	0	0	29
3	2	1	9	7	2	0	21
4	0	0	0	12	7	2	21
5	0	0	0	4	4	6	14
>5	0	0	0	0	0	3	3
Totals per column	40	10	19	25	13	11	

Phoneme discriminant Core FSNs are much more diverse in their spectral and anatomic scope than speaking versus rest Core FSNs. While it was the case that every Core FSN for the speaking versus rest condition for subject 1 consisted of a single sub-FSN, that is not the case for the phoneme conditions. The number of sub-FSNs in the Core FSNs ranges from one up to five and the anatomical coverage ranges from ~3% (2/64 electrodes) to ~96% (46/48 electrodes). Table 2.2 summarizes the anatomic and spectral scope of the phoneme discriminant Core FSNs in terms of number of different spectrally bound groupings (rows) and number of electrodes included (columns). Each of these measures is divided into 6 levels. The number of phoneme discriminant Core FSNs at each level are given in the table. It can be seen from the table that 66% (77, total from light grey and white cells, out of 116 total) of the Core FSNs consisted of at least 3 groupings with 25% of the electrodes included. 48% (56) of the Core FSNs included at least 1/3 of the electrodes divided into 3 groupings. In fact 1/3 (38) of the phoneme discriminant Core FSNs were made up of 4 or more spectrally bound groups and included at least half of the electrodes. Hence, many of the phoneme conditions have Core FSNs that are anatomically more diffuse and spectrally more diverse. The more specific results quantifying the anatomic coverage and spectral diversity of the phoneme discriminant Core FSNs are given respectively in the following two paragraphs.

In general, for all five subjects the phoneme discriminant Core FSNs were much more anatomically diffuse than the speaking versus rest conditions Core FSNs. Figure 2.17 gives histograms of the numbers of the electrodes includes in the speak versus rest Core FSNs and phoneme discrimination Core FSNs for each of the five subjects. Because the number of electrodes is a measure of how anatomically diffuse the Core FSNs are, the figure shows that in all five subjects there are significantly (p-value < 0.01) more electrodes in the phoneme discriminant Core FSNs than the speaking versus rest Core FSNs.

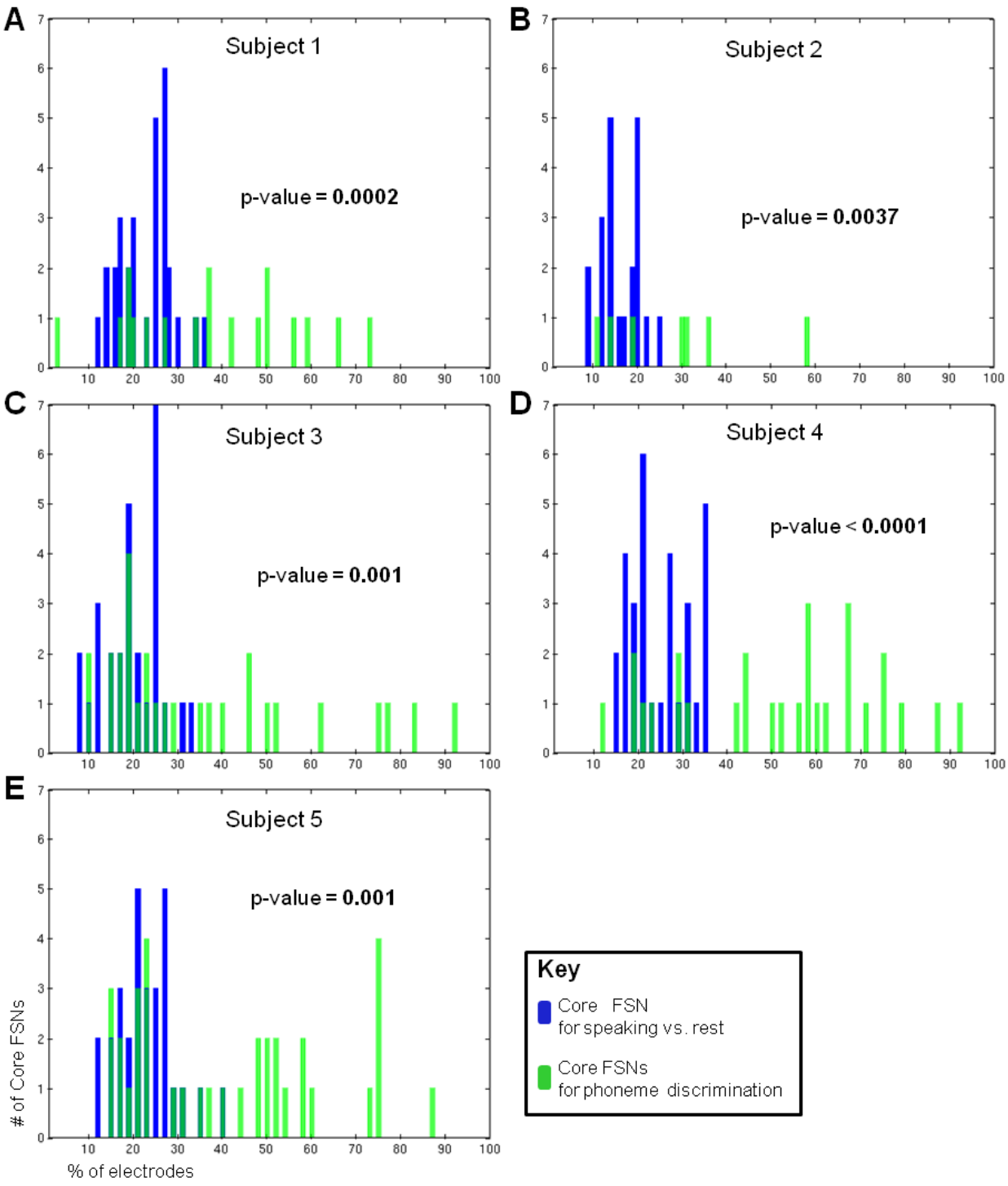

Figure 2.17: Histograms of the percentage of electrodes included in the Core FSNs for speaking versus rest and phoneme discrimination. Plots A-E give the histograms for the speaking vs. rest Core FSNs in blue and the histograms for the phoneme discriminant Core FSNs in green. The p-value testing the null hypothesis that the distributions represented by the two histograms are the same are given in the top right of each plot.

Core FSNs for phonemes are also more diverse in their spectral content. Figure 2.18 depicts all of the significant Core FSNs for Subject 1 according to the method described in Figure 2.9. The figure serves as an exemplar of trends that are seen across the other four subjects. Figures with the complete set of significant Core FSNs for subjects 2 through 5 are given in (Appendix A). Each sub-FSN within each Core FSN is assigned a separate color and has a separate spectral plot. Thus, the more colors and spectral plots that a Core FSN has the more spectral diversity it displays. Closer inspection also reveals that the Core FSNs for the phoneme conditions for Subject 1 are not generally focused at the positive CSM sites. The figure also shows that the phoneme discriminant Core FSNs for subject 1 often contain a group of electrodes in the most frontal region of the ECoG grid similar to the group of electrodes that the Core FSN for speaking versus rest briefly expanded to include during time period t35 (see Figure 2.11). This indicates that more frontal regions, less associated with motor activity, are often important in distinguishing phoneme conditions.

The final trend is that differences in spectral content of sub FSNs from one Core FSN to another tend to relate different groups of electrodes to each other and bind similar groups of electrodes with different spectral content. This is depicted in Figure 2.19. Sub FSNs with similar spectrally binding patterns can be seen to correspond to different groupings of electrodes for different Core FSNs. In addition, sub FSNs with similar electrode groupings can be seen to correspond to different spectrally binding patterns. Both of these trends are highlighted in more detail with specific examples relating to the concepts of spectral diversity and spectral binding in the following section.

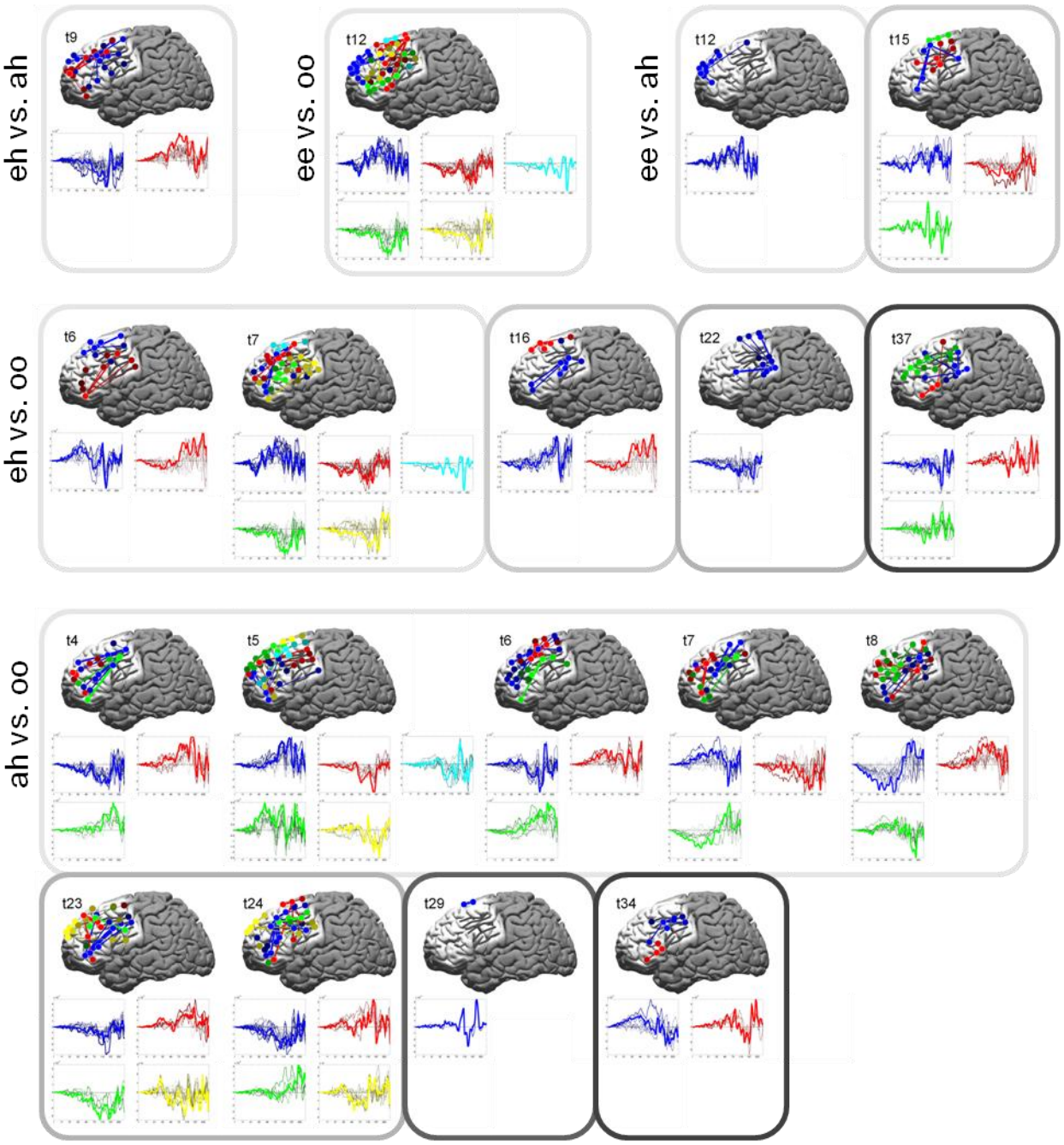

Figure 2.18: Subject 1 FSNs for phoneme discrimination.

2.3.3 Phoneme discriminant Core FSNs clearly illustrate the concepts spectral diversity and spectral binding

We conclude the results with two examples of Core FSNs that clearly demonstrate the FSN concept introduced in section 2.1.1. The two key conceptual components of FSNs are that of spectral diversity and spectral binding. Here

we first present an example of spectral diversity and spectral binding within a single Core FSN in Figure 2.19. We then show an example of spectral diversity from one functional task to another within the same general anatomic locations in Figure 2.20.

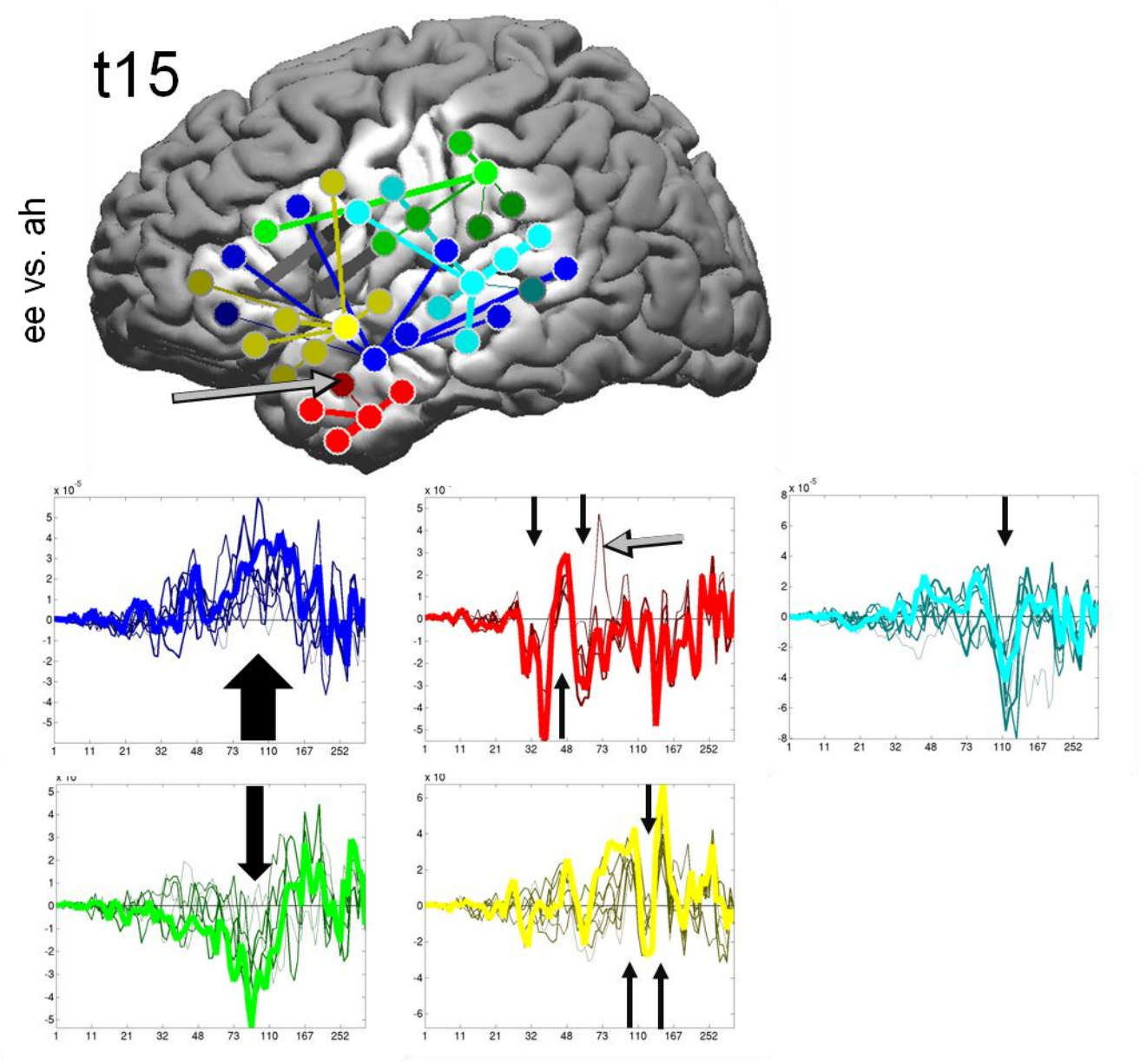

Figure 2.19: Example of spectral binding within a single Core FSN. Figure shows Core FSN for Subject 5 of speaking condition 'ee' vs. 'ah' at time t15. The black arrows indicate the spectral response frequency bands within each spectrally bound group of electrodes that demonstrate a strong response and large in-group consistency. The grey arrows on the brain plot and the top middle spectral response plot indicate an example of an electrode that is only weekly spectrally bound to its group. See Figure 2.9 for further explanation of figure markings.

Figure 2.19 displays an example of specific narrow band spectral patterns that are very consistent within the sub groups of electrodes of a Core FSN. The Core FSN for Subject 5 for the 'ee' vs. 'ah' phoneme condition comparison

at time t15 is shown. The Core FSN contains 5 sub-FSNs representing five subpopulations of anatomic sites that are 'bound' by similar functional response patterns. These populations range from relatively anatomical focal (sub-FSN 2, red) to quite diffuse (sub-FSN 1, blue). These populations are also joined by varied spectral responses. Sub-FSN 1 shows a broad band gamma increase, whereas sub-FSN 3 (green) shows a mid-gamma range decrease. Sub-FSN 5 (cyan) shows a narrow higher gamma band decrease. Sub-FSN 2 shows a lower gamma range alternation between a decrease-increase-decrease while sub-FSN 4 (yellow) shows an increase-decrease-increase pattern at the higher gamma ranges. It can also been seen that each sub-FSN contains multiple anatomic sites with a high degree of correlation at the previously highlighted frequency ranges. This supports the notion that a variety of subpopulations of anatomic sites can be bound together by a variety spectral response patterns. The grey arrows on the brain plot and the top middle spectral response plot of Figure 2.19 indicate an example of an electrode that is only weekly spectrally bound to its group.

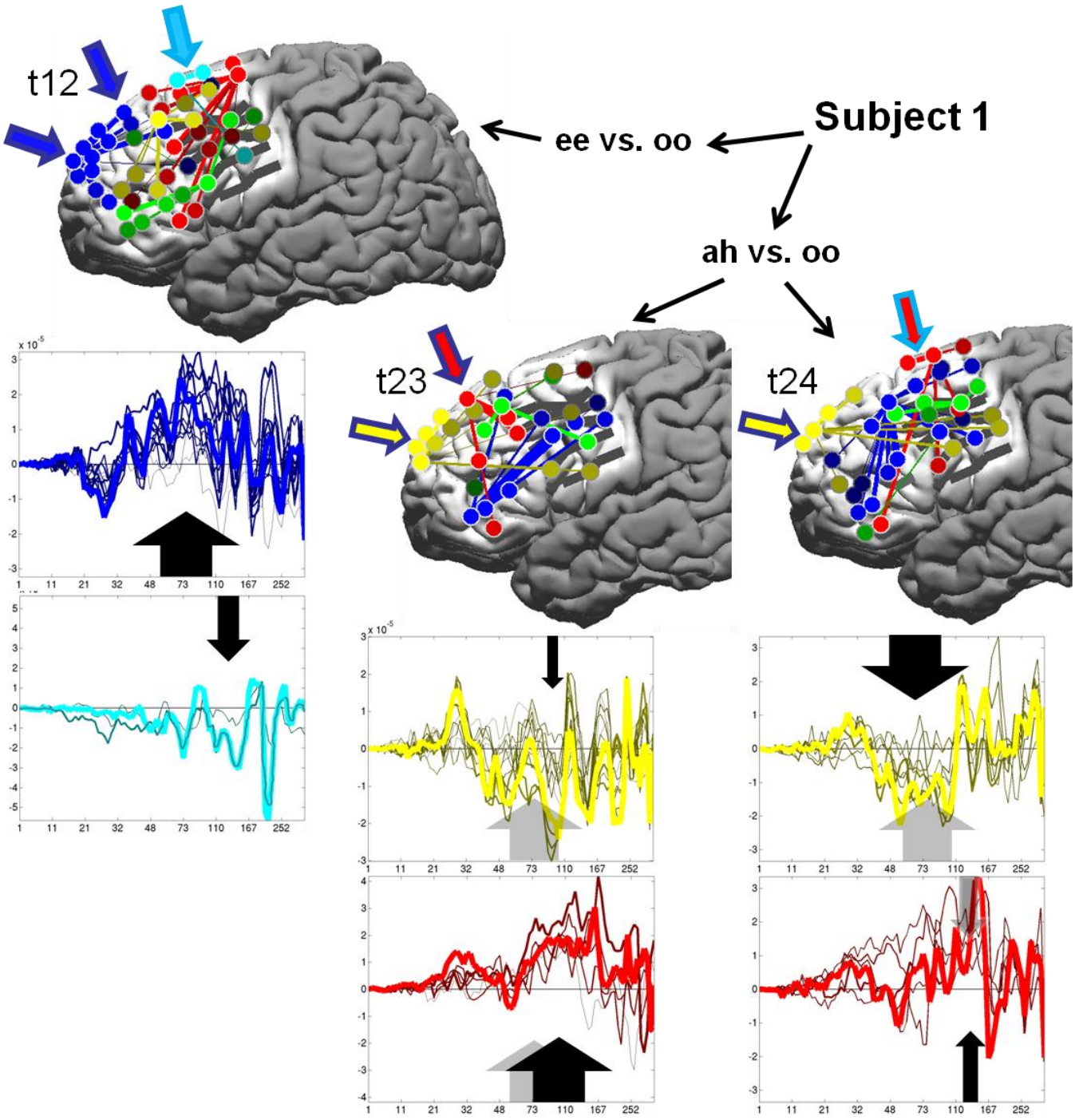

Figure 2.20: Example of spectral diversity of an anatomic area across different functional task contrasts. Figure shows Core FSNs for Subject 1. The top left subfigure depicts the Core FSN of speaking condition 'ee' vs. 'ah' at time t12. The bottom two subfigures display the Core FSNs of speaking condition 'ee' vs. 'oo' at times t23 and t24. Several spectrally bound groups of electrodes within the Core FSNs are indicated with colored arrows. The inside color of the arrows corresponds with that of the group they point to. The outline color corresponds to that of the group in the 'ee' vs. 'ah' at time t12 Core FSN with electrodes at similar anatomic sites. Only the spectral plots for the spectral bound groups highlighted with colored arrows are shown below the corresponding brain plots. The black arrows in the spectral plots highlight the spectral response frequency bands within each spectrally bound group of electrodes that demonstrate a strong response and large in-group consistency. See Figure 2.9 for further explanation of figure markings.

Figure 2.20 gives an example of spectral diversity across different functional task contrasts from electrode from the same general anatomic sites. The top left subfigure depicts the Core FSN of speaking condition 'ee' vs. 'oo' at time t12. The bottom two subfigures display the Core FSNs of speaking condition 'ah' vs. 'oo' at times t23 and t24. The figure shows that the 'ee' vs. 'oo' Core FSN includes a large group of mostly very frontally located electrons (indicated by the blue colored arrows). This group's most spectrally binding feature is a broad band increase in low gamma (marked by the think black arrow in the top left spectral plot). Contrasting this group with the smaller groups of spectrally bound electrodes with overlapping anatomical sites in the Core FSNs of the 'ah' vs. 'oo' condition (indicated by the yellow colored arrows and spectral plots), show that the electrodes at these sites display a narrow band and broad band gamma decrease when contrasting a different task condition at a different time period of the task. Since both task conditions contrast two different active states ('ee' and 'ah') against the same active state ('oo'), the flip in response directions in the spectrally binding feature is not simply due to a flip in the direction of the comparison of the states. It can also been seen that Core FSN of the t23 time period of the 'ah' vs. 'oo' condition contains a small spectrally bound group of electrodes (indicated with the red arrow with a blue outline) that also overlaps anatomically with the large frontal group of the 'ee' vs. 'oo' Core FSN and retain a slightly shifted version of the its spectral binding feature (indicated by the think black arrow in the red bottom middle spectral plot).

A flip in the direction of a spectrally binding feature is also demonstrated for the small group of two strongly bound frontal parietal electrodes in subject 5's 'ee' vs. 'oo' Core FSN at t12 (pointed to by the cyan arrow in the upper left brain plot of Figure 2.20). These two electrodes show a high gamma decrease in this Core FSN (indicated by the think black arrow in the bottom left cyan colored spectral plot) while they show a gamma increase in the same range as part of a spectrally bound group in the t24 'ah' vs. 'oo' Core FSN (pointed to by the red arrow with a cyan outline in the right most brain plot and the black arrow in the right most bottom red colored spectral plot). Electrodes at these sites, along with those in the large frontal group, illustrate the FSN concept that one task ('oo') contrasted with another ('ee') at one temporal period (t12) leads to a different spectral contrast than contrasting that task with another ('ah') at a different time point (t23 and t24).

2.4 Discussion

2.4.1 Functional Spectral Networks have improved functional contrast as compared to limited band single site spectral features

By formally defining the concept of FSNs, we were able to compare the functional contrast of anatomically and spectrally diffuse spectral patterns to that of traditional limited frequency band single anatomical site ECoG signal

features. Our results expand on a recent set of papers that demonstrate improved ECoG signal cognitive task classification performance when the traditional limited band and anatomically local spectral features are expanded to include larder anatomic areas or multiple frequency bands or both [93, 102, 127-128]. Here we highlight two important differences in the functional contrast of the FSN approach and the traditional approach demonstrated with this work.

First we observed that using the FSN method a statistically significant electrophysiological response to a cognitive task verse resting brain state could be observed over a long time span. The onset of the temporal range of significant detection of active state versus resting was earlier for FSNs than SFs and the end of significance was the same or later for all five of the subjects. Hence we conclude that FSNs are more sensitive to the differences between resting and active brain state than SFs.

This property can be leveraged to better investigate the time sequence of brain activity. Many temporal investigations of brain response look at the relative timing of an electrophysiological property between anatomic sites. FSN can be used to stress the temporal differences in an anatomically and spectrally diffuse response to a task.

A second difference between SFs and FSNs highlighted by our results, was that FSNs showed a greater degree of functional contrast when differences in similar active brain states were considered. In contrast to the 'speaking' vs. resting state comparison, comparing spoken words of different phoneme categories will highlight more subtle differences in brain activity due to such differences in mouth motor activations need to produce different phonemes and possible differences in language activations stemming from different words. While significantly discriminant SFs were also found between these subtle brain activity differences, there were more discriminative FSNs found for all five of the subjects. In total there was a highly significant increase in the number of features with discriminant contrast between the phoneme conditions when FSNs were considered as opposed to SFs. In addition significant discriminative contrast was found between all phoneme conditions for a majority (3/5) of the subjects with FSNs, while no subject was found to have significant discriminative SFs for all of the phoneme comparisons. Also of note, several cases demonstrated less functional contrast between the resting state and the combined actives states, but a larger degree of functional contrast between the different active states. This could be due to differences in activation and/or different general levels of activation between the active brains states. However, in either case FSNs were shown to be more sensitive to these differences. Taken together, these results lead to the conclusion that significantly more functional contrast between different active brain states is represented in FSNs than SFs and that these results point to the FSN method as a powerful tool for studying functional electrophysiological brain response with ECoG.

This results warrant further investigation of ECoG spectral response with the FSN method. Here we give two interesting avenues for further investigation. First, would be interesting to explore the functional contrast of spectral networks in the context of more cognitive tasks. The indication from our results is that it is most interesting to use FSNs to explore tasks with subtle differences in mental states. Second, FSN concept could be used to explore an even broader range of electrophysiological interactions in functional brain response. We define the SF and FSN concepts in terms of frequency band amplitude response, but conceptually they could refer to other functional spectral properties

such as task induced phase reset or phase amplitude coupling. It would be interesting to contrast the functional contrast of a task induced phase resetting in a limited frequency bands at a single anatomic sites versus patterns of phase resetting across multiple frequency bands and multiple anatomic sites.

2.4.2 Functional Spectral Networks are varied in their temporal, spectral, and anatomic characteristics

Core FSNs demonstrated a wide variety of spectral, anatomic and temporal characteristics. The refinement of FSNs into Core FSNs provided a way to investigate in detail how the key spectral and anatomic characteristics of FSNs varied over time and functional task. Our analysis showed Core FSN with both broadband and narrow band spectral binding features across many different frequency bands. Our analysis also showed Core FSNs with only a very small percentage of electrodes from a specific cortical area being included up to almost all electrodes being involved. In addition, some Core FSNs were seen to be spectrally and anatomically consistent over several seconds of functional response while others were present for only a single 167 ms period. Within the context of this diversity the Core FSNs for the functionally general 'speaking' active state versus resting state contrast displayed much more consistency than those for the more subtle contrasts between different active speaking states. These general trends are discussed further below.

Core FSNs for speaking vs. resting state were anatomically consistent and often focused around anatomic sites indicated for speech involvement with CSM. The fact that the spectral and anatomic content of the speaking vs. resting state Core FSNs was relatively consistent and focal agrees with a recent study that showed that a maximum classification accuracy of 93% on an imaginary gross motor movement task can be achieved with only three spectral features [93]. On the other hand, phoneme discriminant Core FSNs displayed a wide range of anatomic involvement and spectral diversity. Unlike the Core FSNs for speaking vs. resting state, Core FSNs for the phoneme conditions were not generally focused at the positive CSM sites.

Spectrally bound groupings of electrodes within phoneme discriminant Core FSNs also varied in size and anatomically representation. Many were centered on an area of anatomical focus, but the number of anatomic sites included varied considerably for just one in a single case to almost a third of the electrodes being included. Also, Many Core FSNs included groupings from many different cortical areas. However, groupings that included anatomically sparse and disperse electrode sites were also found. For some examples these anatomically disperse electrodes were none-the-less, strongly spectrally bound by a specific spectral response feature.

Phoneme discriminant Core FSNs featured a high degree of spectral diversity. Spectrally binding features were seen across the range of electrophysiologically relevant frequency bands. While many of the strongest spectrally binding features were in gamma range (>40Hz), spectrally binding features in mu and beta bands were present as well. The

spectrally binding features of the same general group of electrodes were also seen to shift range and direction between active states and across different task times.

While it is hypothesized that the main contribution to the spectral content that determines the spectrally bound groupings within a Core FSN are mainly due to differences in the functional response of different electrophysiological phenomena because they display significant functional contrast by definition, other factors will influences these groupings as well. Some of these factors are due to differences in sensitivity of the electrodes to the underlying electrophysiological phenomena. One example of this is shown in Figure 2.19. The grey arrows on the brain plot and top middle (red) spectral response plot indicate the anatomical locations and spectral response of a weekly spectrally bound electrode. The arrow in the spectral plot indicates the spectral feature most divergent from the rest of the spectrally bound group. It can be seen that while this electrode is near to the rest of the electrodes anatomically, it is positioned over a sulcus while the others are positioned on gyri. This fact will certainly influence its sensitivity to electrophysiological phenomena relative to the electrodes.

Another factor influencing the spectral content of functional response is signal noise. While this noise should not be correlated to task performance, it can introduce shared features in the spectral response of electrodes when it is persistent in the ECoG signal and common among them. Subject 3 served as a good example of this. Many of the divisions among the spectral groupings of the Core FSNs for this subject coincided with the amplifiers they were measured with. This indicates that common line noise among an amplifier had a common influence on the spectral response features of the electrodes native to that amplifier. This would tend to make electrodes that share an amplifier more similar in there functional response, as it limits the shape of that response, and thus more likely to be spectrally bound together in a Core FSN. It should be stressed that while such noise was seen to cause some electrodes with small functional contrast to be included in groups that showed strong fictional contrast based on non-functionally relevant features, the general spectrally bound groupings seen for subject 3 were shaped by the functional spectral response characteristics of the most active electrodes.

Despite the limited complicating factors to the FSN method discussed above, the interesting diversity of spectral and anatomic content of FSNs motivates further exploration of the concept with using different ECoG implants. There are two trends in the clinical implantation of ECoG devices that could be exploited. First, the implants are often not limited to the single grids of electrodes considered in this study. Considering all implanted electrodes would expand the range of anatomic sites that contribute to FSNs. Another trend in ECoG implants is the increased uses of smaller implants with finer grain spacing and smaller electrodes. While these implants limit the anatomic coverage to smaller more functionally specific cortical areas, they also sample the electrophysiological response differences of these areas on a much more fine grain level with electrodes that will reflect the electrophysiological phoneme of the cortex differently. Not only may the spectral content of FSNs differ at these scales, the relationship between SFs and FSNs may be different.

2.4.3 The functional contrast of a combination of multiple spectral response features is greater than its individual parts

The general conclusion that we draw from this study is that the functional contrast of a combination of multiple spectral response features is greater than its individual parts. We were able to illuminate this fact using a formal definition of our concept of FSNs. Here we discuss why this is the case on a conceptual and technical level.

Conceptually SFs are limited in the extent of the functionally induced brain state differences that they are sensitive in two ways. First SFs are anatomically limited and only measure anatomically local differences in brains state. Second SFs are limited to reflecting only the electrophysiological phenomena of a single frequency range. FSNs greatly expand these limitations.

FSN are able to compile information over large cortical areas. The ECoG implants used in this study had electrodes that measured the summed electrophysiological response from an approximately 1 cm area of cortex for a combined 64 or 48 cm^2 combined cortical coverage. 1 cm corresponds roughly to the size of 3-5 functional cortical columns. This means that while each SFs is limited to sensing the cortical response of a handful of functional columns within a single functional area, FSNs are sensitive to the response of many sites spanning several functional areas. As such SFs are limited to cortical scales traditionally thought to be functionally specific while FSNs can compile functional contrast over several functional areas.

The fact that phoneme discriminant Core FSNs are not generally focused at the positive CSM sites contributes to their improved phoneme discrimination over SFs. The lack of focus on CSM sites is likely due to the fact that these sites exhibit a similar spectral response for all phoneme word groups and thus do not contribute to the functional contrast between active states. This shows that the phoneme discrimination of the FSNs is not based on a level of activation difference between phonemes groups but rather a difference in spectral content at lesser active sites. If it was the case that one phoneme group contained words that significantly activate the positive CSM sites more then another then this phoneme condition would be discriminated by a Core FSN that was similar to the speaking versus rest condition Core FSN. The similarity of spectral response at electrodes site most activated by the task is likely a large factor preventing SFs, which will be most concentrated at these electrodes sites, from better discriminating the different active states.

FSNs are able to incorporate information across different electrophysiological phenomena represented by different frequency bands. Different frequency bands of ECoG response represent different electrophysiological phoneme with different functional relevancies (section 1.2.4). As such, FSNs are able to combine the functional contrast reflected in multiple electrophysiological phenomena, while SFs are limited to reflecting single electrophysiological phoneme or phoneme that happen to be expressed as spectrally adjoining frequency bands with the same direction of amplitude change in their functional response.

By referring back to Figure 2.1, which demonstrates the difference between the SF concept and the FSN concept, the conceptual advantage of expressing both spectral and anatomic differences is apparent. In Figure 2.1 the functional

contrast between Task 1 and Task 2 is expressed by the fact that different groups of electrodes (ie: [A,B] and [A,C,G]) are activated by the two tasks. As such the anatomic areas of activation overlap at electrode A. However, in the FSN concept electrode A, which reflects the most active electrode for the tasks, is spectrally bound to two different groups of electrodes. Hence in the FSN concept there is no overlap in functional response to Task 1 and Task 2. While this is only a simple example it illustrates how considering the spectral response relationships between electrodes can add additional functional contrast.

Another way in which FSNs can have added functional contrast is that they can leverage the power of redundancy in spectral response over multiple electrodes. When groups of electrodes with similar functional spectral responses to a task are considered as a whole, their functional contrast becomes more robust to variations in individual functional response from trial to trial. Many factors can obscure the true functional response of an electrode on any given trial. Noise factors or electrophysiological factors related to mental load, fatigue or attention can change from trial to trial. These factors may affect different electrode sites and different spectral frequency bands differently causing electrodes within the active group to reflect the active response to the task more of less from trial to trial. Hence if only one electrophysiological feature of one electrode is considered, its representation in the spectral response will be less consistent over the trials then the representation of a spectral pattern that considers multiple SFs. For example any given SFs may be fully expressed for only two thirds of the times a task is performed. If three SFs are considered then on average 2 of them are expressed for each trial and the combined response of all three is very consistent while individually they are not expressed for a third of the trials. This concept of consistency by redundancy can be particularly important when differences between active states are considered.

2.4.4 FSNs support a diffuse and varied representation of functional contrast in ECoG spectral response

The results discussed above support a view that the electrophysiological properties of the cortex provide a substrate for a flexible, transient, and anatomically diffuse cortical processing. We outline the results and conclusions that support this statement below.

FSNs were shown to both be more sensitive to the differences between resting state and active state brain response and differences between multiple active brain states. The fact that FSNs capture significantly more functional contrast than SFs demonstrate that the functional contrast between brain states is not fully captured by single site and limited frequency band spectral response. FSNs demonstrate the functional contrast between brains state is better represented as patterns of relationships between frequency bands across multiple anatomic sites. We discuss the possible theoretical reasons for this conclusion above. Here discuss its implications for our understanding of how functional contrast is represented by the electrophysiological phenomena of the brain.

While FSNs are more anatomically and spectrally diffuse than SFs by the very nature of the FSN concept, they were also found to be so in practice. FSNs demonstrated spectral diversity within a single spectrally bound group over the time span of the task when considering resting state versus active state. The anatomic representation of these groups was also seen to shift over time. In addition a large percentage of the FSNs discriminating similar active brain states were demonstrated to be very diffuse anatomically and diverse spectrally. Considering different active states also demonstrated that the function spectral response of an area of cortex can change from active state to active state and from one time period to the next. The temporal nature of any given set of spectral relationships captured by a FSN was also seen to be quite transient, often being present for only a signal 167 ms period during the task.

Considering that ECoG is well scaled to capture both local cortical activity and more global electrophysiological phenomena (see 1.1.2), the spectral variety and anatomic diffuse nature of FSNs indicates that that both of these scales of cortical activity are reflected in the spectral patterns they define. Add to this context the growing evidence that different frequency bands reflect different electrophysiological phenomena (see 1.2.4), and FSNs can be said to reflect the functional contrast reflected in the combined state of multiple electrophysiological phenomena.

Putting our results into this context leads to the conclusion that the combined state of multiple electrophysiological phenomena over multiple anatomic locations better reflects the functionally relevant features of brain state than the any one of these phenomena represented at a single location. The temporal properties of FSNs, combined with the high temporal resolution of ECoG, indicate that the functionally relevant features of the combined state of multiple electrophysiological phenomena can also shift rapidly. All-in-all this paints a complex picture of the functional response of the brain.

2.4.5 Implications of FSNs for ECoG-based BCI

To date the vast majority of ECoG based BCI has been done on the basis of amplitude response of limited frequency bands at single ECoG electrode sites. The difference in functional contrast between SFs and FSNs demonstrated in this work indicates considering patterns in spectral response across frequency bands and multiple electrode sites has the potential to give improved BCI control features.

FSNs demonstrated that such features could have earlier onset times and are able to be sustained longer. This could lead to control features that are more responsive and temporally more stable. Both are desired characteristic for most BCI applications. The added temporal stability of FSN like control features could also help reduce false positives, especially when separate control features are designated to indicate a non-active state.

FSNs were also demonstrated to increase the functional contrast between active brain states. This could lead to more variations of control features being defined from an ECoG implant, which would increase the degrees of freedom of possible control. Increasing the degrees of control freedom is one of the major goals of BCI, essential to making BCI feasible for many application domains. Multiple degrees of freedom have been achieved based on anatomic

differences in functional representation, but for reasons discussed above, considering patterns in spectral response across frequency bands could further improve these results and increase the stability of these control features.

Further refinement of different active state BCI control features could also help reduce false positives. Preventing the brain from producing unintended activation of BCI control features is a major challenge for BCI users. For this reason successfully BCI control is usually achieved in a very controlled setting and requires significant subject concentration. In addition refinement of active BCI control features to specific differences between specific active states could go a long way towards reducing also positives. Such refinement may require more concentration to activate the BCI controls, but it would allow for less concentration in suppressing them be reducing the range of activity that they responded to. In the context of practical BCI used unintended activations when the user is not focused on using the BCI system are often more detrimental to system function then unresponsiveness of the system when activation is intended.

Chapter 3

Resting State Spectral Networks

3.1 Introduction

The previous experimental studies with ECoG have focused on capturing the cortical activity induced by specific cognitive tasks. This chapter explores ECoG electrophysiology in terms of patterns of activity when a person is not performing a specific cognitive task. We hypothesize that spectral networks that show functional contrast when a cognitive task is performed can be defined based solely on patterns observed in resting state brain activity. This hypothesis is a novel concept in the field of ECoG research and the methods devolved to test this hypothesis offer a new set of tools for investigating cognitive patterns in ECoG.

We begin by formalizing and definition of Resting State Spectral Networks (RSSNs), in order to more formally state our hypothesis. Then we introduce background and further motivation on resting state brain networks. Section 3.1.2 gives the specific of the ECoG signal acquisition, subject tasks and algorithmic methods that were developed. We report the results of our analysis in section 3.4. Finally, we discuss the implications of our results to ECoG, BCI, and basic functional brain properties in section 3.5.

3.1.1 Concept of Resting State Spectral Networks (RSSNs)

In the experimental sections of the last chapter and this one, ECoG signal is recorded while a subject is being asked to perform some cognitive task such as making a hand movement or performing a mental calculation. We define the brain state in these cases as 'active'. We use the term 'resting state' to refer to signal measurements while the subject is being asked to remain still, quiet and relaxed, although we recognize that they may be daydreaming, worrying or otherwise not mentally quiet. The last chapter characterized functional spectral networks as groups of electrodes with correlated changes that can discriminate task behaviors from rest or from each other. In this chapter we generalize this to consider simply "spectral networks", which are patterns of temporally correlated increases or decreases in frequency band amplitudes across multiple anatomic sites.

The key difference is that spectral networks (as opposed to *functional* spectral networks), are not defined in relation to any particular task, and therefore they can be defined solely in resting state data. The hypothesis of this chapter is these patterns defined only in resting state data are still sufficient to discriminate between task activities.

Thus, our first goal in this chapter is to evaluate if spectral networks defined during resting state data have functional contrast, that is, do the responses of these network distinguish between task behaviors. Those networks that have functional contrast we term Resting State Spectral Networks (RSSNs).

Our second goal is to characterize how much better the performance would be if the spectral networks were defined based on data that included the task activities, not just resting state activity. Although trained on active state data, not all correlated groups of electrodes discriminate task activities; those that do, we term activeSNs.

We address this question of the comparison between RSSNs and activeSNs using data that spans across several physical scales and different types of mental tasks. The signals measured through ECoG depend on the size and placement of the electrodes, and how diverse are the anatomical regions that are covered. We analyze the RSSNs for three different resolutions of ECoG spanning from micro-grids that are placed over just a small brain region to grids that cover most of the motor cortex. We also analyze data from subjects who performed one or more of five different cognitive tasks that are known to have neural activity in different regions. The five tasks and their expected cognitive responses are described in section 3.2.2.

Finally, we explore the computational framework of Deep Belief Networks to create a basis set of spectral networks for the ECoG data sets. DBNets have several other properties that recommend them for this type of data analysis. First, we show how they can be efficiently trained on subject data and automatically define a data driven basis for that subject. Second, they produce a probabilistic measure of how well data (measured later) fits that basis. Third, a basis can conveniently visualize and compared to other bases.

3.1.2 Possible impact of RSSNs

Demonstrating that RSSNs are functionally significant would provide strong evidence that ECoG spectral responses reflect a fundamental coordination of neural activity. This idea has been championed by Wolf Singer [29] and others, however, most work on electrophysiological interactions between cortical populations has focused on either phase-phase relationships [53] or phase-amplitude [64] relationships between frequencies that are induced by a cognitive task.

Our earlier work (chapter 2) demonstrated that the relationships between spectral amplitudes contain more functional contrast than the individual amplitude responses themselves, but very little work has looked at amplitude-amplitude relationships across frequency and anatomy in resting state electrophysiology. Schalk, et al. have used models of resting state amplitude response of a single frequency band to identify active areas of cortex during a cognitive task

[139]. However, their models do not include relationships between frequency bands or cortical populations, and this is the first work analyzing spatio-spectral patterns in resting state ECoG electrophysiology.

RSSNs could also provide a new way to explore cortical organization. Traditionally the cortex has been mapped in terms of anatomical features such as neuronal type and interconnections or in terms of functional active state neuronal responses. The recent fMRI literature defines cortical locations in terms of their inclusion in networks of correlated resting state BOLD activity [140-147], and it has been further shown that these networks remain consistent during active brain states [148]. Mantini et. al. were able to show that some of these networks in BOLD were characterized by specific electrophysiological signatures in EEG signal that involved the combination of different brain rhythms [149]. In turn, He et al. demonstrated the presence of covariant networks present at different frequency scales in ECoG signal [150]. This chapter seeks to expand on these results by evaluating patterns in amplitude relationships between many frequency bands and many anatomic sites that can be learned from resting state ECoG signal.

In addition, RSSNs have implications for the field of electrophysiological based BCI. First, the existence of a basis set of spectral patterns provides a new feature space in which to search for BCI control signals. Second, RSSNs could greatly reduce the time needed to find good BCI control features. Third, RSSNs define a basis from which to generate an informative real-time 'brain activity' feedback signal. The impacts on BCI research are discussed in more detail in section 3.5.4.

3.2 Methods

Three methodological decisions were made in this work. First, in order to get a better understanding of the anatomical scale of RSSNs we analyze three different scales of ECoG electrophysiology. Second, in order to assess the robustness of RSSNs we analysis data from four different subjects with different anatomical coverage and assess the functional relevance of RSSNs relative to five different cognitive tasks. Third, we choose to use Deep Belief Networks as our method for RSSN modeling. The methodological details of each of these choices are described in the following three sections.

3.2.1 ECoG Signal Acquisition

This work is based on ECoG recordings from 4 intractable epilepsy patients. Table 1 gives an overview of patient clinical information. The subject group underwent clinical treatment at the Washington University Medical Center in St. Louis, MO, USA (subjects 1 and 2) and the Utrecht Medical Center in Utrecht, The Netherlands (subjects 3 and 4). This group contained one female and three males and ranged in age from 19 to 58. All subjects willingly participated

in a range of research tasks and signed an informed consent statement to allow analysis and anonymous publication of their data. The recording amplifiers and software used was the same as that described in chapter 2 (section 2.2.2). However, the recording conditions at the St. Louis and Utrecht recording sites different in several significant ways. First, in St. Louis a sampling frequency of 1.2 kHz was used while 512 Hz was used in Utrecht. Also, in St. Louis a single skull facing separate electrode was used as the signal reference while a common average reference of all recording electrodes was used in Utrecht. In addition, it is noteworthy that the major source of recorded line noise in the USA is at 60 Hz while 50 Hz in the dominant source of line noise in Europe. While these noise bands were corrected for with software band pass filtering, significant loss of physiological signal around these bands is unavoidable. All of these factors affect the spectral content of the recorded signal and hence influence the spectral patterns that are observable.

Table 3.1: Chapter3 Subject Data.

Subject	Age	Sex	ECoG implant description	Implant sketch*	Tasks performed
1	58	F	63 macro-ECoG electrodes; 8x8 grid with electrode 13 dropped due to bad contact with the cortical surface over the left frontal cortex	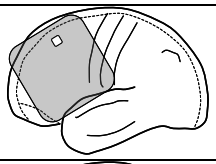	1 run of baseline before HS 6 runs of the HS 2 runs of baseline before HT(c,i) 3 runs of the HTc task 3 runs of the HTi task
2	40	M	12 micro-ECoG electrodes; 4x4 grid with 12 recording electrodes over the left hand motor area	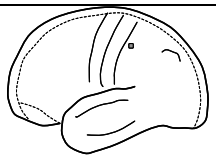	2 runs of baseline before FineM(c,i) 2 runs of FineMc 2 runs of FineMi
3	19	M	32 high-density ECoG electrodes; 4x8 grid over the right mouth motor and pre-motor area	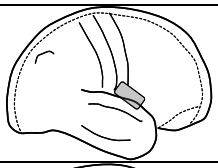	2 runs of baseline before FineSp 2 runs of FineSp
4	26	M	96 macro-ECoG electrodes; 6x8 parietal temporal grid, 4x4 frontal lateral grid, 2x4 frontal basal grid, 2x4 parietal grid, 2x4 subtemporal grid, 2x8 grid over sensory motor area	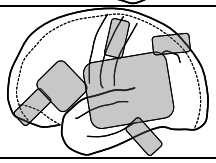	2 runs of baseline before WM 1 run of WM

*grey shaded areas represent the approximate areas of cortical surface covered by the implants from which the data in this chapter comes.

The major methodological source of variation in the electrophysiological signal among the subjects is the specific ECoG implant specifications and locations. All subjects were implanted with an assortment of the general clinical scale implants, referred to as macro-ECoG. For subjects 1 and 4 the macro-ECoG implants were used as the sources for the research data. The research data discussed here for Subject 2 is from a 'high-density' ECoG implant that was developed for research purposes in conjunction with Ad-Tech Medical Instrument Corporation. Research data from subject 3 was recorded a micro-EGoG implant developed with Ad-Tech Medical Instrument Corporation as part of

the 'Leuthardt' ECoG grid design. The number of electrodes, layout, and general locations for each subject's implants are given in Table 3.1.

The three scales of ECoG implants are interesting because they measure the cortical activity at different functional and anatomical scales. Clinical macro-ECoG implants have electrodes of 2.3mm diameter exposed contact surface and 1cm inter-electrode spacing (center-to-center). Due to the electrical conductance of the cortical tissue, each electrode will be sensitive to changes in local field potentials from a slightly larger area of cortex. As such, each macro-ECoG electrode records the activity of a population of neurons covering 3-5 cortical columns. Also, the 1cm inter-electrode spacing means that macro-ECoG electrodes do not overlap in terms of cortical columns and the total cortical coverage of a typical implant will span several functional areas.

High-density ECoG electrodes have a more dense 3mm spacing and a 1.3mm exposed surface. Hence the activity of each high-density electrode reflects a smaller number of cortical columns and is more likely to overlap in terms of cortical columns. The total cortical coverage of the high-density implant was only a little over 1cm by 2cm, and was limited to cover only the mouth pre-motor and motor functional areas.

The micro-ECoG implant had 12 cortical facing recording electrodes (the 4 corner electrodes were skull facing and not used) with 75 micron exposed surfaces and 1mm inter-electrode spacing. The total cortical coverage was just over 3mm in diameter and thus only slightly larger than a normal clinical electrode. Coverage was fully within the hand motor area and the entire implant likely measures only several cortical columns.

3.2.2 Subject Tasks

Data was recorded from four different patients who performed six different tasks. All subjects participated one or more times in a 'rest' task and performed one or more 'active' tasks. An overview of task performance for each subject is given in Table 3.1.

The rest task requires the subjects to rest and remain still with their eyes open while ECoG data was recorded for 3 or 5 minutes. One or two instances of the rest task were always recorded in the same research session just before performance of each active task. Multiple instances (see Table 3.1) of each active task were then performed in succession to minimize environmental differences between them.

The active tasks asked for different behaviors from each subject. There are three important aspects of each task; first, the design of the task and why it targets particular functional areas, second, how the repetitions of the task are organized, third, how the data recorded during the task support labeling the subject behavior at a given time.

3.2.2.1 The hear and repeat phonemes task (HS)

Subject 1 participated in the hear-and-repeat task (referred to as 'HS' in the rest of the text) described in chapter 2 (section 2.2.3). A 'speaking' trial was defined as the period from 300 ms before voice onset time to 500 ms after voice onset time. It is expected that this task will lead to a passive auditory and an active speech production cognitive response. While language may play a role in the task, the simple nature of the task means that the primary expected response will be in the mouth motor area.

3.2.2.2 The overt hand and tongue movement task (HTc and HTi)

Subject 1 also performed an overt hand and tongue movement motor task. The subject was visually cued to repeat movements in a period of 4s. In this time the subject consistently performed 3 movements for both the hand and tongue conditions. The timing of the visual cue was used to mark onset times for the HT task. The trial time period was defined to be 100ms to 2.9s after the visual cue for both movements. Separate instances of the HT task were performed using Subject 1's contralateral (HTc) and ipsilateral (HTi) hand. It is expected that this task will lead to an active hand motor and mouth motor cognitive response.

3.2.2.3 The fine hand movement task (FineMc and FineMi)

Subject 2 performed a task involving three fine hand motor activities; moving a finger, a thumb, or both in a pinching motion (FineM). A 5DT hand glove recorded finger movements to use to mark movement onset times. The trial time period was defined to be 800ms before movement onset to 800ms after movement onset. Separate instances of the HT task were performed using Subject 2's contralateral (FineMc) and ipsilateral (FineMi) hand. It is expected that this task will lead primarily to hand motor response for the finger and thumb movements and an added sensory motor response to the pinch movement.

3.2.2.4 The fine mouth movement task (FineSp)

Subject 3 participated in a read-and-repeat phonemes task (FineSp) consisting of two categories of spoken phonemes (voiced and unvoiced) that involve distinct mouth movements. This task was designed to elicit two different categories of mouth motor responses. The recorded microphone signal was used to define voice onset times and the period of 800ms before and 1s after was included in the trial time.

3.2.2.5 The working memory task (WM)

Subject 4 participated in a working memory task (WM) which required mental calculation of easy and hard mathematical sums. The subject used a button press to indicate the correctness of a visually displayed answer. The periods of 100ms to 1.1s after visual presentation of the sum and 500ms before to 500ms after the button press were used to define the mental calculation and motor response trials respectively. This task is the most complex of the five tasks in terms of its expected cognitive response. The easy and hard mental calculations may lead to two different types of cognitive responses corresponding to fact retrieval and active working memory respectively. The button press is expected to elicit a motor response. Feedback indicating the correctness of the selected answer was also given and may lead to its own unique cognitive response.

All tasks included periods of rest (Inter-trial-intervals (ITI)) between successive task activities. All ITI periods were visually cued and the subjects were asked to relax and remain still and silent, but continue to focus on the screen. Trials of resting activity were defined based on the middle of the ITI period and matched the duration of the corresponding task activity trials.

3.3.3 Deep Belief Network global spectral pattern analysis

The ECoG data from the above patients performing various tasks measures electrophysiological processes with complex interactions across many locations and frequencies. We chose to analyze this data using Deep Belief Networks [151-152], a relatively recent algorithm that learns non-linear patterns in high-dimensional data. This section describes the basics of the algorithm and how we adapt it to our analysis task.

3.3.3.1 Training Deep Belief Networks

Deep Belief Networks (DBNets) are a multilayer neural network structure used to transform high-dimensional data to low-dimensional codes. Their key advantage over prior neural network approaches is their much faster training algorithm, and natural approaches to visualizing their intermediate and final results.

In lieu of (the slower) back-propagation training approach, the algorithm for training a DBNet treats each layer as a Restricted Boltzmann Machine. This takes as input a set of logistic visible units V and these are connected to a set of stochastic binary hidden units H with a full set of symmetrically weighted connections W. Given the activation states $v_i \in V$, $h_j \in H$, and $w_{ij} \in W$ the energy of the RBM is given by:

$$E(V,H) = -\sum_{i \in V} b_i v_i - \sum_{j \in H} b_j h_j - \sum_{i \in V, j \in H} v_j h_j w_{ij} ,$$

where b_i and b_j are the biases of the visible and hidden units respectively [152]. The weight matrix W and biases b that minimizes this energy for a given set of observed input activations of the visible units can be efficiently approximated using the contrastive divergence algorithm [151].

A Deep Belief Network is a stack of these Restricted Boltzmann Machines, where the overall input serves as the input data to the visible units in the bottom layer. For each other layer, and the hidden units of each proceeding layer serve as the input data. Given set of observations, the weights and biases that minimize the energy of the entire network are found by treating each Restricted Boltzmann Machine layer separately. Once trained, each layer is used to general input for the next highest layer. Because each layer can be learned independently of others, it is possible to learn a network with more layers than standard neural networks. The codes at each layer are based on the 'beliefs' or codes learned by the previous layer. In this way each deeper layer represents a higher level of abstraction of the data. Thus, the term 'deep belief' comes from this combination of much deeper networks than standard neural networks, where each layer is based on the beliefs of the previous layer.

We have found the ability of the DBNet model to encode a dataset is fairly robust to changes in network size parameters. In this work we chose for each DBNet to have five layers, including the input layer and the top layer. Five layers were chosen based on the precedent set by the original DBNet results presented by Hinton et. al [152]. The top layer was chosen to have 50 hidden units, and each of these 50 units encodes a spectral network that forms a basis for a data set. The choice to use fifty patterns is intended to be large enough to encompass a variety of ECoG responses and limited enough to provide insight into which spectral interactions are most prominent in resting state and active state electrophysiology. The first two hidden layers were chosen to be of equal size with the number of units being approximately .88 of the number of input features. The size of these layers was chosen to be a fixed ratio of the number of input features so that the complexity of the basis sets encoded were as consistent as possible given the disparity in the number of recording electrodes. The ratio of .88 was chosen so that the number of units was relatively large while remaining reasonable to deal with computationally. The third hidden layer was chosen to be geometric mean of hidden layer and the size of the top layer (50), so that the compression ratio was the same between both layers. The numbers of units for the input layer and four hidden layers for subject 1 though subject 4 are given in Table 3.2.

Table 3.2: DBNet networks dimensions per subject.

	Subject 1	Subject 2	Subject 3	Subject 4
Top layer	50	50	50	50
Layer 4	496	98	306	568
Layer 3	4922	937	1875	5625
Layer 2	4922	937	1875	5625
Input Layer	5544	1056	2112	6336

A separate instantiation of a DBNet was trained for each baseline and active task data set for 500 training cycles (epochs). In our implementation, the input is g(:,:,t), capturing all frequency responses for all electrodes concatenated to make a single vector. The frequency response was calculated with Gabor filters and normalized using the method described in chapter 2, section 2.2.4.

3.3.3.2 Using Deep Belief Networks to get spectral network activation levels over time

A DBNet represents an input vector by activations of units in all layers. These activations can be calculated for a given input vector by projecting the input vector up through each layer of the network. This is done by calculating the hidden unit activations of each RBM layer of the DBNet given the visible unit activations (ie: hidden layer activations of the previous layer) according to:

$$p(h_j = 1) = \exp\left(\frac{1}{b_j + \sum_{i \in V} v_j w_{ij}}\right),$$

where, as in the previous equation, w_{ij} is the weight on the connection between visible unit v_i, and hidden unit h_j, and b_j is the biases of the hidden units [152].

Given an input vector, we term the activations of a top layer hidden unit of a trained DBNet as the 'response' of the DBNet spectral network encoded by that unit. Thus, the response of each of the spectral networks encoded in a DBNet over time can be calculated for a given data set. These responses can be calculated for any data from the ECoG signal that used the same set of implanted grid electrodes and frequency responses.

3.3.3.3 Defining spectral networks from trained Deep Belief Networks

One feature of DBNets that make them particularly suitable for the analysis of signal patterns is that they are generative models. Each unit in the network can be interpreted as encoding for a pattern of values on the input level. Thus, given a trained DBNet, it is possible to visualize the input patterns to which each hidden node in the DBN is responding. This is done by setting the activation level of the hidden node to 1 and that of all other hidden units in the corresponding network layer to 0 and projecting this pattern of activation back down the network to get a pattern of activations of visible units on the input layer. The activations of visible units of a RBM layer in a DBNet can be calculated as:

$$p(v_j = 1) = \exp(\frac{1}{b_i + \sum_{j \in H} h_j w_{ij}}),$$

where, w_{ij} is the weight on the connection between visible unit v_i and hidden unit h_j and b_i is the biases of the visible units [152].

Due to the fact that the DBNet algorithm is probabilistic, the activation of a hidden unit is only the probability that that unit will be active given an input pattern and not a deterministic response to the input data. Thus, the best way to understand the input pattern represented by a hidden unit is to represent the distribution of patterns to which it responds. We visualize this pattern, by setting a node to 1 and generating a distribution of patterns across the visible units of the input layer. We repeat the process many times and take the mean of the projected input layer as a pattern to visualize.

3.3.4 Basic analysis procedures

3.3.4.1 Identifying spectral networks with functional contrast

Spectral networks are defined by training a DBNet on a set of ECoG data. The activation level of spectral networks can be calculated on the training data set or additional data sets. When the data set includes ECoG recordings during a task, some of the spectral networks have an activation level that is correlated with the timing of that task. If the correlation is strong enough that there is significant functional contrast in the response when considering that task compared to rest we consider the spectral network to have functional contrast for that task (the method for determining significant functional contrast is described below). RSSNs are spectral networks encoded in DBNets that were trained solely on resting state brain activity that have functional contrast to at least one task. Likewise, activeSNs are spectral networks with functional contrast encoded in DBNets that were trained the on data that includes the subject performing a task.

The number of RSSNs and activeSNs captures information about the fraction of the variance in the training data sets that is correlated with the functional changes in the task data sets. DBNets are trained to reduce data reconstruction error. Thus a node represents a unique feature of variance in the data.

In this section we describe how we determine whether a spectral network is significantly correlated to a task behavior. Then we expand that method to assess the ability of a spectral network to discriminate among different types of task behavior.

We want to find out what spectral networks of a given subject respond to task behaviors performed by that subject. To do this we first align our spectral network responses to the timing of those tasks. We then average the activation level profile of each spectral network across all instances or trials when a specific task behavior, such as hand

movements in the HT task, is performed. We call these the time-locked-responses (TLRs). If there is a significant decrease or increase in the TLR then that spectral network is added to the set of spectral networks with functional contrast for that behavior.

We determined the magnitude of dip or bump that constitutes a significant TLR through the use of a non-parametric statistical measure called the Monte-Carlo p-value. We chose to use the Monte-Carlo p-value because of its ability to determine a significance level of a conditional effect on a measured quantity when the null-hypothesis distribution of that quantity is hard to determine (see 2.2.6 for a more detailed discussion of the use of Monte-Carlo p-value). We determined the level of significance of the TLR values for each task activity as follows:

1. we form 100 pseudo-TLR by randomly choosing N temporal points in the task data to time lock to (N was set to the number of trials for each of the task activities)
2. the top 1000 values out of the absolute values of the pseudo-TLR values were chosen to form the null-hypothesis distribution.
3. the value at position 50 in the ordered (in descending order) distribution was taken as the level of significance value such that any value greater than this value were greater than 95% of the null-hypothesis distribution

Any spectral network that had significant TLR values to at least one of the activities of an task was included in the set of spectral networks with functional contrast for that task.

One goal of understanding spectral network responses is to use them to distinguish different cognitive states. One spectral network may relate to many different activities, and we must separately answer if it can discriminate between them. A spectral network that has functional contrast to some but not all task activities discriminates among task activities by definition, but a spectral network that has functional contrast to multiple task activities may still discriminate those activities. The direction, magnitude and timing of the significant TLR values can all distinguish one activity from another. To formally define which spectral networks discriminate task activities we consider each spectral network TLR for each task activity separately according to the three step scheme described below.

First, a weighted sum of the significant time points in the TLR is calculated for each trial of each activity. We will refer to this weighed sum as the 'per trial activation' of the spectral network.

Second, the sum of squared means value (r-squared value) between the distributions of per trial activations for each pair of task activities is computed.

Third, the Monte-Carlo p-value method was used to determine the threshold for significance for the r-squared values. The trials for each activity in the pair being compared were randomly reassigned to one of the two activities a 1000 times and the r-squared value of the distributions of weighted sums were calculated for each redistribution of trials. R-squared values > 95% of these random redistribution values were considered to be significant.

A spectral network was counted as being functionally discriminative if it discriminated at least one pair of task activities. Spectral networks that do not have functional contrast to a task activity have no significant time points in

the TLR that are significantly different between that activity and rest and will have a per trial activation of zero for every trial. Thus, the R-squared value will be 0 if a spectral network has no functional contrast to neither activity in a pair and 1 if it has functional contrast for one activity and not the other. For activity pairs for which a spectral network has functional contrast to both activities the Monte-Carlo p-value is used.

3.3.4.2 Analysis of a basis set of spectral networks ability to discriminate task activities

A basis set of spectral networks encoded by a DBNet can be used as input to a classifier. A common approach to training a classifier in combination with a DBNet is to add an auto-associative layer to the top of the DBNet. The auto-associative layer is a fully connected set of weights between input units that represent the top layer DBNet activation patterns and label units that represent a class label pattern for each data sample. A gradient decent algorithm is then used to train the weights, following the method of Hinton, Osindero, and Teh [151], such that each DBNet top level activity pattern produces the correct corresponding label pattern.

In our implementation there is one label unit for each task activity and an auto-associative layer was trained for each DBNet and corresponding task. The label patterns for each data sample were formed by setting the unit corresponding to the activity for a given task trial to 1 and setting all the other label units to 0. For each trial the DBNet top level activations for all of the data samples within the trial time window (see for time windows of each task) were ordered into a single vector. These vectors were then used as the set of input vectors to the auto-associative layer. Classifiers were trained only on trials of active cognitive task execution (ie: there is no 'rest' class), so there is one input vector (representing the DBNet response over the trial time) and one label vector for each performance of a cognitive activity during a task.

The auto-associative classifier was trained and evaluated using the leave-one-out method on the set of training vectors. Training was performed for 30 epochs on all task activity trials except one. The classifier was then used to predict the label of the one trial not included in the training by projecting the DBNet top layer activity pattern through the auto-associative layer and using a winner take all strategy on the resulting label unit pattern to get the predicted task activity class In this way a task activity prediction was acquired for every trial and compared to the actual task activity labels. Since the classifiers are trained on DBNet output and the DBNets themselves are not changed, the results are one way to measure how the collection of spectral networks encoded in a given can discriminating between cognitive tasks.

3.4 Results

In total, 12 DBNets were trained and evaluated with respect to 7 different cognitive task data sets. Five DBNets were trained on the five different resting state data sets. Seven DBNets were trained on the seven different active state data

sets (see Table 3.1). These DBNets will be referred to as rest DBNets and active DBNets respectively. The rest DBNets with significant functional contrast (such as discriminating task behavior from resting state) are called RSSNs. The active DBNets provide a means of comparing the electrophysiology of resting state and active state brain activity in terms of spectral networks. We evaluate these DBNets in four ways to show that there are RSSNs that can discriminate *between* different tasks and compare them to activeSNs.

First, we evaluate the dynamics of spectral networks encoded in the rest DBNets during active state data in order to define RSSNs. The five rest DBNets were assessed in terms of their activation levels during the seven corresponding active task data sets shown in Table 3.1 (7 experiments). To explore how the resting state changes over time, the responses for the rest DBNet of the HS task were evaluated for the HT active task data and vice versa (3 experiments).

Second, we directly compare the RSSNs to activeSNs in terms of task activity discrimination. The seven active DBNets were assessed in terms of their activation levels during the corresponding active task data sets (7 experiments).

Third, performance of the auto associative layer classifiers was evaluated when they were trained on the responses of the rest and active DBNets and tested on the corresponding active task data sets (14 experiments).

Several figures and tables summarize the most important results of this section. The results comparing RSSNs to activeSNs are summarized in Table 3.2. The first, third, and fifth columns highlight the relevance of RSSNs to active brain state dynamics. The second, forth, and sixth columns highlight the comparison of RSSNs to activeSNs. Figure 3.1 and Figure 3.2 show the number of significant TLR points summed over all RSSNs and active spectral networks for each task.

Table 3.3 summarizes the classification results of the auto-associative classifiers trained on the resting state and active state DBNets.

The main results of our analysis are:

1. Spectral networks that have functional contrast for active brain states (ie: RSSNs) can be defined based solely on resting brain activity.
2. RSSN dynamics can discriminate active state brain function at a level that is comparable to that of activeSNs.
3. The electrophysiology expressed in spectral networks during resting state and active state ECoG data are not fundamentally different.
4. We observe that RSSNs are consistent across days.

The specifics of these results are given in the following four sections.

3.4.1 RSSNs can be defined by naive learning of spectral response patterns in resting brain activity

The first result of this work is that resting state ECoG spectral response contains spectral networks (RSSNs) that represent functionally significant signal variation. Using DBNets with 50 top level nodes creates 50 encoded spectral networks. One metric of how relevant these networks are to task activity is simply to count how many networks have functional contrast for some task. Column two of Table 3.3 gives the number of RSSNs and activeSNs for each activity of each cognitive task. The total number of RSSNs that were found to also have the more subtle discrimination *between* the different activities of each cognitive task (using the methods described in 3.3.4.2 Analysis of a basis set of spectral networks ability to discriminate task activities) is given in column four.

There are two main results summarized by column 1 of Table 3.3:

1. RSSNs were found for every tested cognitive task.
2. RSSNs were found for every tested ECoG signal scale.

These results data are detailed below.

Table 3.3: Spectral Network Functional Contrast Results.

Active task	(1) Number of RSSN per activity (50 possible)	(2) Number of activeSNs per activity	(3) Number of RSSNs that discriminate activities	(4) Number of activeSNs that discriminate activities	(5) Number of RSSNs that are activity selective	(6) Number of activeSNs that are activity selective	(7) Best R-squared value for single RSSN	(8) Best R-squared value for single activeSN
HS	**24** Hear [**26** HT] **32** Speak [**26** HT]	**30** Hr. **23** Sp.	41 [**41** HT]	35	**2** Hr.[**5** HT] **17** Sp.[**15** HT]	**7** Hr. **6** Sp.	**.48** Hr.[**.48** HT] **.67** Sp.[**.66** HT]	**.47** Hr. **.87** Sp.
HTc	**10** Hand [**20** HS] **6** Tongue [**11**HS]	**24** Hd. **16** Tg.	11 [**27** HS]	22	**16** Hd.[**6** HS] **7** Tg.[**2**HS]	**16** Hd. **7** Tg.	**.48** Hd.[**.55** HS] **.28** Tg.[**.28** HS]	**.94** Hd. **.47** Tg.
HTi	**8** Hand [**13** HS] **12** Tongue [**13** HS]	**16** Hd. **15** Tg.	15 [**21** HS]	23	**8** Hd.[**4** HS] **8** Tg.[**4** HS]	**8** Hd. **7** Tg.	**.50** Hd.[**.49** HS] **.28** Tg.[**.36** HS]	**.86** Hd. **.45** Tg.
WM	**15** Recall **19** Working Mem. **17** Button Press	**17** Rl. **17** WM. **16** BP.	30	31	**2** Rl. **2** WM. **11** BP.	**6** Rl. **2** WM. **11** BP.	**.28** Rl. **.43** WM. **.57** BP.	**.46** Rl. **.40** WM. **.85** BP.
FineSp	**22** Voiced **21** Unvoiced	**29** Vd. **27** Un.	26	33	**2** Vd. **6** Un.	**5** Vd. **1** Un.	**.74** Vd. **.40** Un.	**.72** Vd. **.26** Un.
FineMc	**21** Fingers **20** Thumb **21** Both	**22** Fr. **22** Tb. **23** B.	27	34	**1** Fr. **4** Tb. **2** B.	**7** Fr. **4** Tb. **2** B.	**.67** Fr. **.18** Tb. .72 B.	**.59** Fr. **.24** Tb. .79 B.
FineMi	**17** Fingers **15** Thumb **18** Both	**17** Fr. **16** Tb. **17** B.	22	22	**0** Fr. **3** Tb. **3** B.	**2** Fr. **3** Tb. **0** B.	**.33** Fr. **.39** Tb. .55 B.	**.45** Fr. **.32** Tb. .49 B.

The results in the first column of Table 3.3 show that there are RSSNs found for all of the diverse cognitive tasks, highlighting that patterns in resting state data can detect active states on which it was not trained. In general, more complex, mentally engaging, activities lead to a greater number of RSSNs.

RSSNs were also found for every tested ECoG signal scale. The top four rows (highlighted in dark grey) of Table 3.3 give the results of the four cognitive tasks data sets that were recorded using the clinical macro-scale ECoG implants (see Table 3.1 for individual implant details). Row five (light grey highlight) and rows six and seven (lighter grey highlight) respectively give the results for the data sets recorded with the high-density and micro-scale ECoG implants. Column 2 shows that for each of the three ECoG measurement scales there is at least one task for which at least 20% of the DBNet encoded spectral networks are RSSNs.

3.4.2 RSSN dynamics can discriminate active state brain function at a level that is comparable to that of activeSNs

The results in Table 3.3 confirm two more important aspects of RSSNs. First, not only can RSSNs discriminate task behavior from rest, they can also discriminate between cognitive tasks. Second, the task discrimination of activeSNs was not significantly better than that of RSSNs. Columns 3, 5 and 7 of Table 3.3 show the total number of RSSNs found to discriminate among the different activities performed during one task, the number of RSSNs found to respond only to a single mental activity within each task, and the R-squared value of the most discriminative RSSN for each of the activities within the task. Columns 4, 6, and 8 contain these values for the activeSNs. The R-squared values reported are those of a cognitive task activity versus time periods of rest combined with all other activities within that task.

3.4.2.1 RSSN dynamics can discriminate active state brain function

While the above results show that RSSNs are relevant to the spectral response dynamics of active cognitive tasks, the fact that an RSSN is responsive to a particular task does not mean it will be able to discriminate amongst different tasks. However, RSSNs that significantly discriminate between cognitive task activities (column 3 of Table 3.3) were found for all of the tasks and because these tasks were measured with different size ECoG grids, all three resolutions of ECoG signal measurement.

The results demonstrate that the task discrimination is not based solely on a level of response. Column 5 of Table 3.3 shows that for every cognitive task activity (with the exception of ipsilateral finger movements, see row 8) RSSNs that were only responsive to that cognitive activity were found.

The RSSNs reported in column 5 have non-significant TLRs for all of the activities except the one indicated and have statistically significant R-squared values for that activity versus ITI and versus all other activities.

The number of RSSNs per activity is not always correlated with the activities with the best discriminant RSSNs, as indicated by comparing columns 3 and 7 of Table 3.3. In the case of the WM, fineSP, FineMc, and FineMi tasks, the number of RSSNs are very similar per activity while there are considerable differences in the R-squared values of the best discriminant RSSNs per activity. For the HS and HTc tasks it is the case that the activities with the most RSSNs also have the highest R-squared value. However, for the HTi task the tongue movement activity has the most RSSNs while the hand movement activity clearly has the discriminant RSSN with the highest R-squared value. A larger number of RSSNs indicates a greater diversity in the form of spectral relationships that are relevant to cognitive task performance. However, the above results show that greater spectral diversity does not necessarily mean that the spectral networks are more relevant to distinguishing between cognitive tasks.

3.4.2.2 The functional contrast of RSSNs is largely similar to that of activeSNs

By design, active DBNets encode for spectral networks that reflect brain states that were induced to contain electrophysiological responses relevant to task performance. Thus, it can be expected that activeSNs should be more relevant to task performance (have greater functional contrast) than RSSNs. But, in fact only the HTc and HTi tasks have a number of activeSNs that is considerably greater than the number of RSSNs. The rest of this section focuses on the more interesting question of the discriminating amongst different activities.

It is not always the case that activeSNs are more task specific than RSSNs. Columns 3 and 4 of Table 3.3 show the number of RSSNs and activeSNs that distinguish between activities. These columns are largely similar except that the HTc and Hti tasks still have more activeSNs and individual activity selecting activeSNs. Columns 5 and 6 shows no clear tend about whether RSSNs or activeSNs have more specific activity selections.

Aside from the number of RSSNs and activeSNs, we evaluated several possible ways that RSSNs and activeSNs may have different performance characteristics. First, each RSSN and activeSN has an R-squared value describing its ability to discriminate task activities. A students t-test on the distributions of the best R-squared values indicates a trend but with the current data this is not a significant difference (p-value 0.16) ActiveSNs and RSSNs performed better on some tasks than others, and there was a relatively high correlation (Pearson Correlation Coefficient 0.68) about which tasks they did better on. This mandates the use of a paired student's t-test which finds a significant difference (p-value of 0.027).

When the strictly motor activities from the tasks recorded with Macro-scale ECoG are excluded there is no significant difference between RSSNs and activeSNs in terms of best R-squared values. The better performance for activeSNs is mostly due to very high activeSN R-squared values for the hand movement activity of the HTc and HTi tasks (rows 2 and 3) and the button press activity of the WM task (row 4). The RSSNs also perform poorly relative to the activeSNs for the tongue movements of for the HTc and HTi tasks. These activities are all examples of motor movement

activities measured on the macro ECoG scale. When these motor activities are not considered the paired student's t-test p-value becomes 0.56. Additionally, motor activities do not have this affect the small scale. The FineMc and FineMi tasks involve motor movements measured on the micro ECoG scale and the best R-squared values for the RSSNs and activeSNs are very similar (paired student's t-test p-value 0.86). The electrophysiological significance of these results is highlighted in the discussion section below.

RSSNs are also largely similar to activeSNs in terms of the temporal characteristics of their responses to task activities. This trend can be seen in Figure 3.1 and Figure 3.2 which compare RSSNs and activeSNs in terms of the numbers of spectral networks with significant TLR time points over the trial timing. Red lines indicate the number of activeSNs that had a significant TLR at each sample time point in the task trial time range. Blue lines indicate the number of RSSNs. These figures show that both RSSNs and activeSNs have temporal responses. The general timing of the spectral network responses relative to the task performance (green vertical lines) and temporal patterns of expected brain responses (dotted green line) can be seen.

The temporal trends in the spectral network responses between task activities for these tasks are clearly shown by both activeSNs and RSSNs. Two interesting trends highlight this result (highlighted with the green text). First, the response onset for the thumb movements is earlier than the finger movements in the FineMc task and vice-versa for the FineMi task. Second, the pinch movements (which involve both thumb and fingers) for both FineM tasks show both thumb and finger movement response dynamics.

The FineSp task (Figure 3.2 H) shows a temporal trend between task activities, where the response onset times are earlier for the voiced than unvoiced activities. This is seen in both the RSSNs and activeSNs, but RSSNs have a delayed response onset relative to the activeSNs.

Another interesting temporal trend that is seen in activeSNs and RSSNs is shown in the top two plots of Figure 3.2 G. These plots demonstrate that the distinction between the short and fast response of the memory recall activity and the sustained response of the working memory activity of the WM task is present for both types of spectral networks. Figure 3.2 G also demonstrates that there is a reduced response to the button press activity for RSSNs compared to activeSNs (bottom plot). The second peak that shows up in the ActiveSN response is likely caused by the button press response for this condition. Hence, the lack of a second peak in the RSSN response to the memory recall activity indicates a reduced response to this motor activity.

Just as with the best R-squared values, the relatively poor response to the motor movement condition of the WM task for RSSNs compared to activeSNs is also seen for the other motor movement activities for Macro scale tasks (ie: the hand and tongue movements of the HTc and HTi tasks, shown in Figure 3.1 E and F). The maximum number of RSSNs with a significant response (given in blue squares to the right of each plot) was approximately half that of the maximum number of activeSNs (red squares) for each of these task activities.

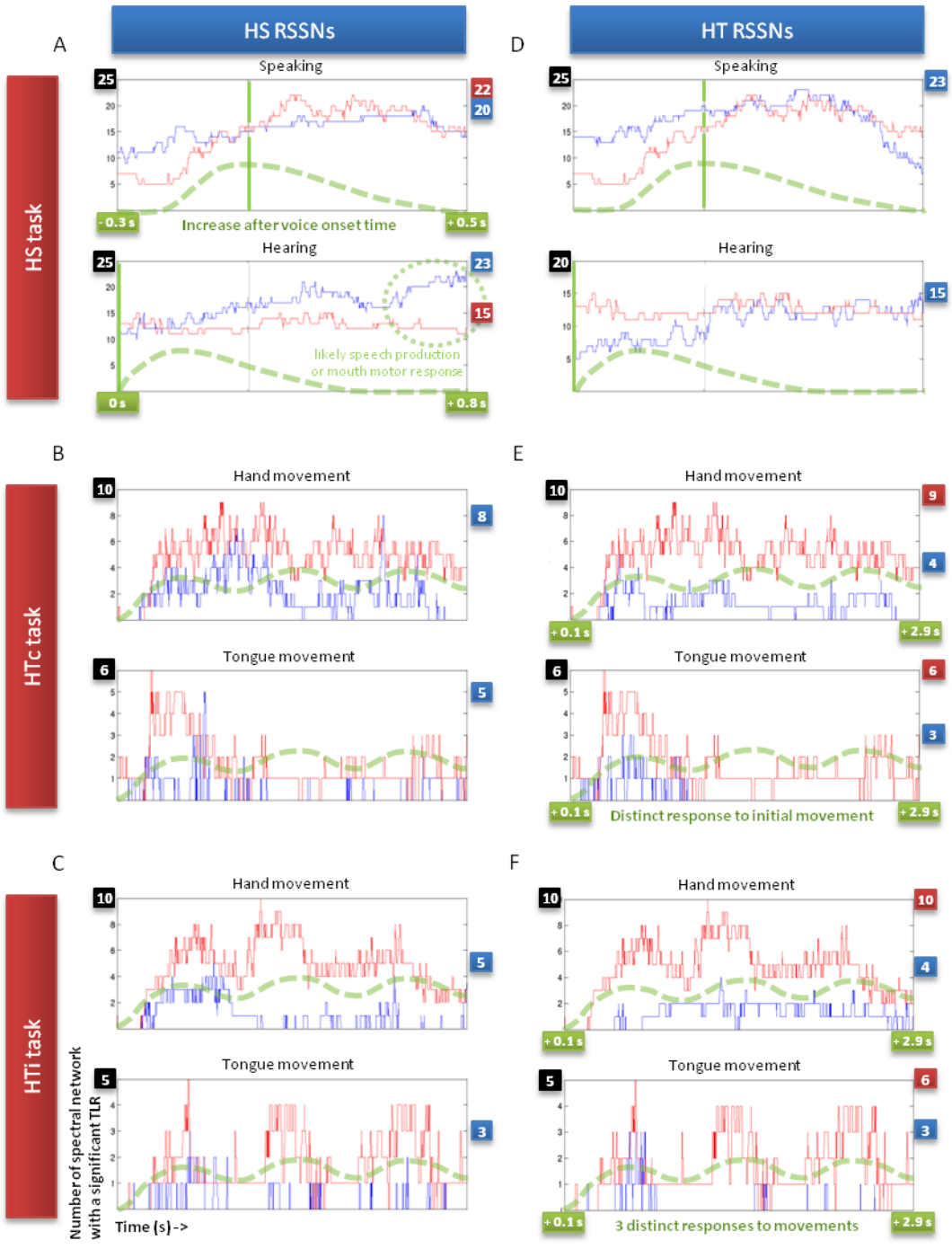

Figure 3.1: Left column: These plots show the number of TLR patterns that are significant at each trial time, for RSSNs trained on the HS task (blue line) and activeSNs also trained on the HS task (red line), when applied to HS (A), HTc (B), and HTi (C) task data. Right column: Summed TLR for HT RSSNs and acitveSNs applied to HS (D), HTc (E), and HTi (F) task data. The number of spectral networks with significant responses (y-axis) is given for each temporal sample point (x-axis) of the task. The black square to the left of each plot gives the upper limit of the y-axis scale. The number of RSSNs for the time point with the most RSSNs with a significant response is given in the blue square on the right of each plot. The red square shows the same for activeSNs. The task timing relative to the time lock points (vertical bars in some plots) is summarized with the green markings (see section 4.2.1 for further description of timing for each task). The dotted lines give a reference point for expected brain response and are not actual recorded performance measurements. Temporal features of interest are highlighted in the green text.

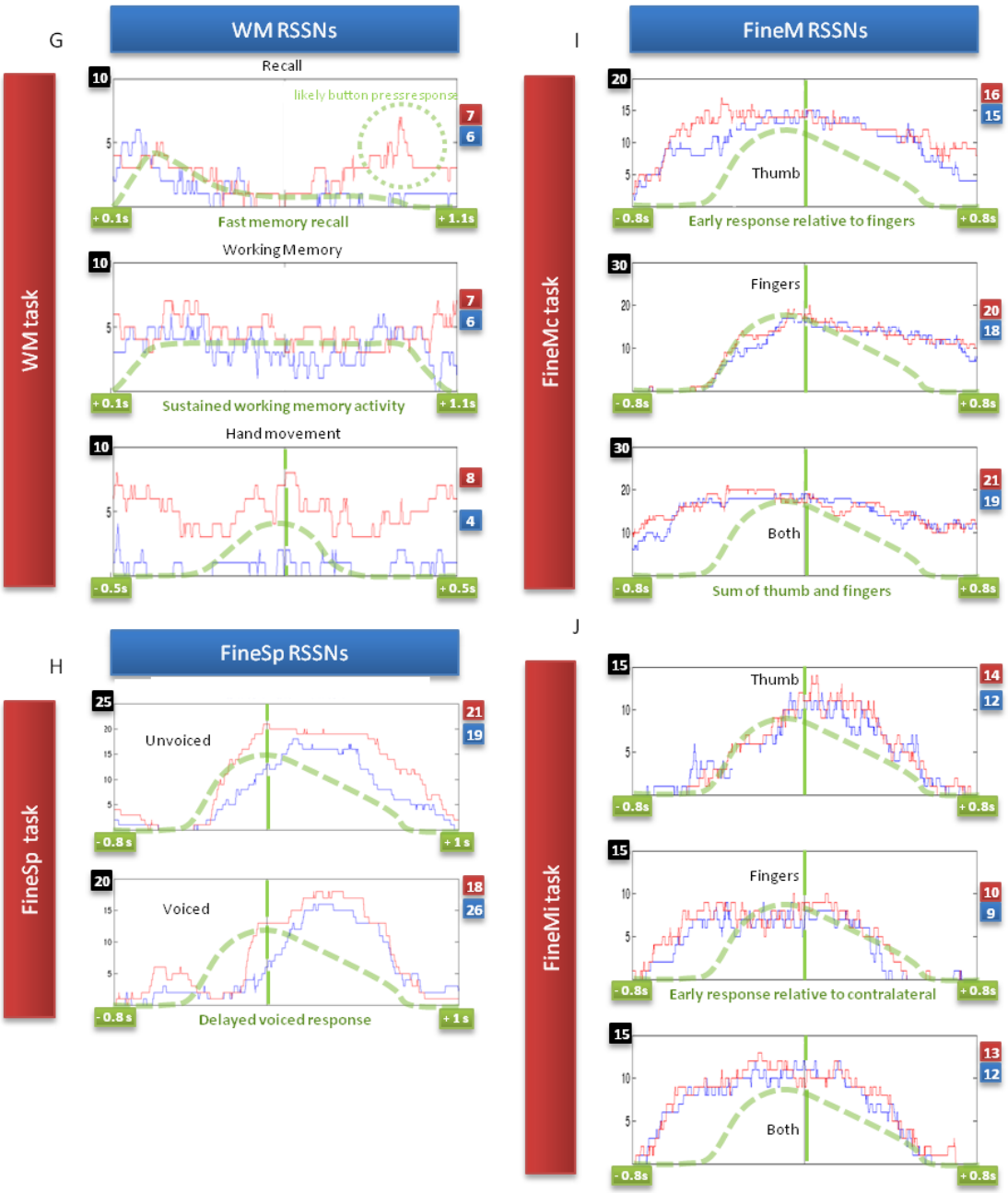

Figure 3.2: A comparison of summed TLR patterns showing RSSNs (in blue) and activeSNs (in red) over the time course of a trial. The left column shows patterns for the WM (G) and FineSp (H) task data. The right column shows patterns for the FineMc (I) and FineMi (J) task data.

3.4.3 Patterns learned from resting state ECoG spectral response data can be used as a basis for classification for multiple tasks at multiple ECoG scales

We compared the performance of classifiers trained on the activation levels of rest state trained DBNets to those of classifiers trained on active state trained DBNets. The classification results demonstrate that patterns learned from resting state ECoG spectral response data can be used as a basis for classification for multiple tasks at multiple ECoG scales when the tasks induced a sufficient brain response. Above chance classification scores are achieved with resting state trained DBNets for all cognitive tasks except the FineMi task, and in this case the DBNet trained with active task data also shows near chance level results. In fact, the classification values per cognitive task activity (columns 1 and 3) are very highly correlated between RSSNs and activeSNs (Pearson Correlation Coefficient 0.92). In general, the performance on the macro ECoG scale was higher, but on smaller ECoG scale implants the resting state trained DBNet classification results are better when compared active state trained DBNets.

Table 3.4: DBNet Cognitive task Classification Results.

Active task	(1) Per activity classification % of resting state DBNets	(2) Total classification % of resting state DBNets	(3) Per activity classification % of active state DBNets	(4) Total classification % of active state DBNets	(5) Chance level classification %*
HS	**85** Hear [**80** from HT] **95** Speak [**91** HT]	89.1 [85 HT]	**92** Hear **100** Speak	98.4	50.4
HTc	**73** Hand [**79** HS] **69** Tongue [**76** HS]	70.8 [77.5 HS]	**90** Hand **90** Tongue	90	50
HTi	**82** Hand [**77** HS] **66** Tongue [**66** HS]	74.1 [71.6 HS]	**94** Hand **94** Tongue	94	50
WM	**68** Recall **64** Working Mem. **63** Button Press	63.7	**82** Recall **83** Working Mem. **71** Button Press	75	38.3
FineSp	**76** Voiced **75** Unvoiced	75.7	**85** Voiced **79** Unvoiced	81.8	50
FineMc	**73** Fingers **55** Thumb **62** Both	61.9	**79** Fingers **53** Thumb **64** Both	63.4	33.5
FineMi	**38** Fingers **47** Thumb **28** Both	35.7	**32** Fingers **54** Thumb **31** Both	36.6	33.8

***chance levels are determined based on the number of trials in each class**

3.4.4 RSSNs can be consistent across multiple days

To evaluate the consistency of resting state spectral networks over the period of several days, we trained two DBNets on resting state data, and then evaluated their performance on active state data captured on another day. The performance was largely the same as that of DBNets trained on resting state data from only several minutes before task performance. Subject 1 performed the HTc and HTi tasks a day before the HS task and resting task recordings we were made just before task performance on both days. This allowed us to compare the performance of these resting state DBNets on tasks that were performed on separate days. Specifically, the HS resting state trained DBNet was evaluated on the HTc and HTi cognitive tasks and the HT resting state trained DBNet was evaluated on the HS task. The results are given between square brackets in Table 3.3 and Table 3.4 and plots B, C and D of Figure 3.1 and Figure 3.2. Key results are further discussed here.

RSSNs from resting state data sets on separate days perform similar to RSSNs from data just before task performance. Table 3.3 shows that the DBNet trained on the rest HS task encodes for more RSSNs for both the HTc and HTi tasks than that of the rest HT trained DBNet, while the DBNet trained on the rest HT task encodes for only slightly fewer RSSNs for the HS task then that of the rest HS task trained DBNet. This pattern is repeated for the number of RSSNs that discriminate between the R-squared values of the best RSSNs. The activity classification results in Table 3.4 also show this trend. These results indicate the resting state spectral network dynamics can be relevant to discriminating active state brain function a day later or earlier.

3.5 Discussion

In this work we have developed a new method for exploring the electrophysiological relationships between cortical ensembles during resting state. This was based on a novel combination of electrocorticography (ECoG) and Deep Belief Networks (DBNets). Ours is the first work analyzing patterns of amplitude response relationships in resting state electrophysiology in this way. The RSSNs provide a basis set of spectral response patterns whose dynamics are highly correlated to cognitive task performance both as a whole and as individual units. We further show that RSSNs can be defined at different ECoG scales and can be consistent over days. Based on these results we conclude that RSSNs capture electrophysiological phenomena representing the functional organization of the brain.

This section discusses the details of the results that lead to this conclusion, then highlights the significance of this work to electrophysiology, and finally discusses the implications of RSSNs for ECoG based BCI.

3.5.1 RSSNs represent spatio-spectral patterns present in resting state electrophysiology that are relevant to functional brain dynamics

By demonstrating the existence of RSSNs we show that resting state electrophysiology contains temporal associations between frequency bands and across cortical sites that are relevant to brain dynamics during task performance. We show that the performance of a cognitive task significantly affects these spatio-spectral patterns, and we demonstrate that the dynamics of RSSNs are able to discriminate different mental activities from each other.

That fact that RSSNs can be used to discriminate separate task activities from each other provides strong support of our conclusion that they reflect the functional organization of the brain. The alternative is that signal patterns measured by ECoG in resting are unrelated to cognitive task signals, and that training on active task data is mandatory. If this is the case then it is not expected that RSSNs responses could be used to discriminate separate task activities from each other. Our analysis shows the contrary. The results demonstrate that there are RSSNs that discriminate task activities for every cognitive task tested.

In addition it was shown that RSSN task discrimination is not based solely on a level of response because RSSNs specific to a single cognitive task activity were found for every activity except one. This fact proves that there are spatio-spectral patterns in resting state ECoG data that have specific relevance to changes induced by a specific mental activity.

The most interesting result is that RSSNs were stable over the span of days. The dynamics of RSSNs defined on resting state data a day earlier or later than the cognitive task as to the functional dynamics of the task as RSSNs recorded just minutes before the task.

Measured by their performance relative to activeSNs, RSSNs perform much better on task activities that are complex than task activities that are simple. Examples of complex activities are the 'hearing' activity of the HS task, the 'working memory' activity of the WM task and the less distinct activities of the fineSp, fineMC, and FineMi tasks. Examples of simpler activities are the general 'speaking' activity of the HS task and large motor activities of the HTc, HTi and WM tasks. Both in terms of the best R-squared values of individual spectral networks and the overall temporal response of the spectral networks, RSSNs were seen to be surprisingly similar to activeSNs for the group of more complex activities while the activeSNs showed a considerable larger response for the group of simple activities. In fact the RSSNs had higher best R-squared values for 6 out of the 10 more complex activities (see Table 3.3 columns 7 and 8).

One explanation for this is that complex activities induce weaker responses overall, so all activities are more difficult to distinguish from noise. A second explanation is that the brain response for more complex activities is more anatomically and spectrally varied than that of simple activities and these patterns are better reflected in resting state brain activity. This explanation is supported by the fact that the classification scores for tasks involving simple activities are similar to scores for complex activities. One good example of this is the WM task for which the 'recall' and 'working memory' activities perform better than the 'button press' activity for both the active and resting state trained DBNets.

3.5.2 RSSNs encode for electrophysiological phenomena at three fundamentally different scales

The RSSNs can encode for functionally relevant spatio-spectral patterns at three different scales of functional organization in the brain. RSSNs were found for all three ECoG recording scale investigated in this work. There is both a functional basis and an anatomic basis to believe that different ECoG scales will differ in functional and spectral content.

RSSNs demonstrate that the electrophysiological phenomena of different functional anatomic scales are also expressed in resting state data. The micro ECoG scale is constrained to a single functional area and measures the interactions of cortical sites that correspond to separate cortical columns within this area. The meso ECoG scale measures cortical sites that encompass multiple columns but still measure interaction within a single general functional area. The macro ECoG scale reflects the interactions over diffuse functional areas between cortical sites that cover multiple cortical columns. Functional areas and cortical columns are also related different electrophysiological phenomena. Synchronous activity in lower frequency ranges that encompass much larger cortical populations can be seen as interactions among cortical columns and even functional areas (see chapter 2 1.3 for further discussion on the meaning of frequency bands in ECoG). Hence, given the above context, the RSSNs of each ECoG scale can be expected to originate from different electrophysiological phenomena. RSSNs were shown to be functionally relevant to the electrophysiological phenomena at each of the three scales. Below we discuss the differences between the results for these different scales.

Relative to the macro-scale, the micro and meso ECoG scales have more resting state spectral patterns that are more similar to the active state patterns. This result is demonstrated in terms of match between RSSN and activeSNs best R-squared values and response timing, although this result is drawn from only one data set each from the micro and meso scales and two data sets from the macro scale. At the large scale, the fact that RSSNs and activeSNs are less similar suggests that the spectral relationships between functional areas are likely to vary more than those within functional areas. This may allow for more flexibility in functional organization from a limited set of functional areas. This could also be due to differences in coverage among the data sets because the micro and meso ECoG implants were placed in areas that were more specifically targeted by the tasks. This indicates that functionally defined anatomic areas are functionally specific even in resting state ECoG response.

One of the results that stand out the most in our analysis is that RSSNs are the least task specific for motor movements recorded at the macro scale. At the macro-scale, few of the electrodes cover the motor cortex where motor movements are known to produce localized signals. RSSNs did indeed perform well in the FineMc task, when more of the electrodes are focused in that region.

3.5.3 Spectral Networks, provide a new way of analyzing electrophysiological responses in non-active states

Spectral Networks provide a new way of analyzing electrophysiological brain patterns. This work is the first to combine the advantages of the ECoG platform with the advantages of the DBNet algorithm to explore patterns in electrophysiological dynamics. Due to the complex framework of connections between cortical areas, their electrophysiological interactions are likely to be expressed as non-linear relationships. DBNets have been shown to be a powerful unsupervised method for finding non-linear patterns in high dimensional data. As such, they are well suited to explore the significance of patterns in the resting state spectral response of ECoG signal.

We use this method to demonstrate that patterns of DBNet responses, learned during rest, correlate with cognitive tasks, and therefore define the existence of RSSNs. This is the first work to show that spatio-spectral patterns in resting state ECoG response have functional contrast as opposed to defining spectral features based on their functional contrast. As such the RSSN method is akin to the Resting State Networks found in BOLD brain response, which are also shown to persist during active state activity. Where RSSNs and BOLD Resting State Networks differ is that RSSNs demonstrate considerable more variety in consistent resting state activity then is observable with fMRI. BOLD Resting State Networks only represent a spatial pattern of areas with fluctuations in a single manifestation of cortical activity. Each RSSN reflects a spatial pattern in resting state activity with a specific spectral content. This allows RSSNs capture different spatial patterns associated with the different the forms of cortical activity manifestations recorded with ECoG.

than the active task, performed as well then RSSNs defined on data just before the active task data was recorded.

Because each top level unit of a DBNet encodes for a distribution of possible non-linear spatio-spectral patterns in the data, they can be used to compare spatio-spectral patterns from possible non-linear interactions between neural ensembles in active state and resting state data to the known linear spatio-spectral relationships defined with functional contrast. Each top level unit of a DBNet encodes for a distribution of spatio-spectral patterns that represent linear and non-linear associations between spectral bands and anatomic sites. These distributions can be represented in the spatio-spectral domain. Once represented in the spatio-spectral domain, a clustering method, similar to that used in chapter 2 to define spectrally bound groups within FSNs (section 2.2.7), can be used to group anatomical sites that often share similar spectral content in activeSNs or RSSNs. These groups and there spectral content can then be related to known spectral phenomena. Some groups are likely to show spectral response patterns and anatomic groupings that do not show up as significant functional responses features and are only noticed because they are consistent across many SNs. One interesting question is how the anatomic locations of spectral groupings of RSSNs relate to Resting State Networks found in BOLD. This could help illuminate the resting state spectral characteristics that are most correlated to resting state correlations in BOLD signal.

3.5.4 Implications for Brain Computer Interface applications

The traditional method of first screening for spectral features that discriminate a specific cognitive task from resting state is time consuming and laborious for the subject. This can present a major challenge for patients with compromised health conditions. An extreme example is using BCI to restore the ability to communicate in locked in patients. The best target cognitive task for these patients is unclear and they are extremely limited in the screening tasks they can perform.

RSSNs can help to greatly reduce the time needed to find good BCI control features. The fact that RSSNs are defined by resting state electrophysiology means that they can be determined without the use of a functional screening task. If a relatively small set of RSSNs contain spectral patterns that are good control features, then the search space for control features would be reduced. In fact, control features may even be able to be selected based on the spectral and anatomical characteristics of the RSSNs alone, which would require no function specific screening process at all. This may make BCI easier for target groups such as locked in patients for which active response tasks are not possible. In addition, resting state trained DBNets define a basis from which to generate an informative real-time 'brain activity' feedback signal without any functional screening. We demonstrate the use of a DBNet defined basis to do just this in the next chapter.

Chapter 4

The Brain Mirror

4.1 Introduction

This chapter explores methods to support online, real time data summary and analysis tools, to rapidly identify multiple user controllable brain patterns. The previous chapter showed that DBNets provide a computational framework to capture representations that support discriminating between cognitive tasks. Here we explore the use of online training protocols, so that the DBNet can automatically adapt over time. We compare this approach to a baseline of using incremental PCA for adaptive signal representation, and we characterize how well these methods correlate with cued behaviors, which serve as proxies for controllable brain states. In addition we implement the online DBNet approach in the form of the 'Brain Mirror' software system, which is capable of recording, adapting to, and generating visual feedback from ECoG signal in real-time in the clinical setting.

We begin by formalizing the problem of learning of learning control features online and highlighting the algorithmic contributions. We then introduce the data evaluated in this chapter, the online DBNet training scheme, and Brain Mirror system. We conclude by evaluating the performance of the algorithms and discuss the significance of the results.

4.1.1 Formalization of the online control feature selection problem

The three main requirements of an interactive system for BCI control feature selection are:

1. The system adaptively defines a set of brain signal features that are responsive to changes in the user's thoughts without pre-screening of the brain signal.
2. The system generates continuous feedback that conveys the dynamics of the brain signal features so that the user can detect features they can control.
3. The system supports the user's ability to select and practice with the specific controllable features, and map those control features to interface elements in a BCI application.

Based on these requirements we formalize the online control feature learning problem as follows:

1. A set of patterns is learned naively (without task labels) and incrementally on a small window of data moving through a cognitive task data set.
2. Response values of encoded patterns are generated incrementally for each data sample.
3. The set of encoded patterns can be selected so that their responses discriminate individual cognitive activities.

4.1.2 Algorithmic and Experimental Contributions

The best linear basis for reconstructing a signal drawn from a given distribution (measured as sum of squared reconstruction error) is given through Principal Component Analysis. But patterns of neural signals at the scale measured by ECoG arise from non-linear interactions of large groups of neurons, and in chapter 3 we established that DBNets are well suited to learning a non-linear basis for distributed patterns in ECoG data. Thus, we explore here the potential to incrementally train DBnets.

We evaluate the effectiveness of these DBNets within the Brain Mirror system on 4 subjects who performed a range of tasks. We quantify the relationship between the task a subject was performing and the signal patterns learned by the DBNets-based Brain Mirror system, and show that it is more effective than a linear signal decomposition approach based on PCA. This holds across a wide variety of experimental conditions and for neural signals corresponding to many tasks.

All attempts to define distributed spatio-spectral patterns in ECoG made so far have used mental state labels on active task data sets to define a distributed set of spectral features [93, 102, 127-128]. A method for defining adaptive spatio-spectral features has also been described in the literature [93]. This method uses a PCA basis and DFA to find discriminative patterns, which is very similar to an adaptive version of our method for defining FSNs. With our Brain Mirror implementation of online DBNet training we showed the DBNet method to be better suited for adaptively defining spatio-spectral patterns than this online PCA basis representation when no labels are used.

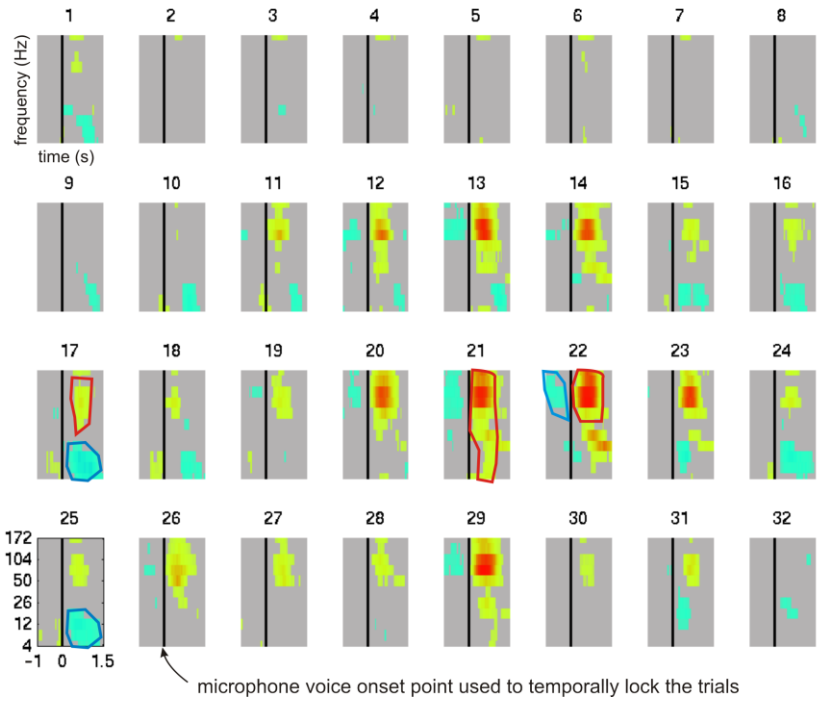

Figure 4.1: Example of Time-locked Response (TLR) based Spectral Control Features (SCFs) for the 'oe'-'ah' activity in the FineSp task. Each plot represents the TLR for 1 of the 32 electrode channels for each frequency (y-axis) across time (x-axis). The non-parametrically statistic TLR points are in grey, the positive response. E values and in red, and the negative response value are in blue. Three positive SCFs are circled in red and three negative SCFs are circled in blue.

4.2 Methods

4.2.1 Human Subjects and Data Recording

This work considers the data recorded from subjects 1-3 for the HS, HTc, FineM, and FineSp tasks considered in chapter 3. In addition data recorded from a subject (Subject 4) implanted with a 6x8 clinical macro ECoG grid over left tempero-parietal region was analyzed. Subject 4 participated in a task (Multi) using the SIGFRIED cortical mapping system (see section 1.4), in which the subject was visually cued to repeat overt hand movements, tongue movements or speak for long periods of 15 seconds for a total of 4 times. The activity cue time points were used as labels. Like the other tasks periods of rest (ITIs) were also included.

4.2.2 The standard spectral control feature selection method used for comparison

As a basis for comparison, we implement a standard method for choosing control features for BCI control. There are multiple variations of the same basic approach used in choosing control features from spectral ECoG data, in this chapter we define spectral features using the method to define the Best SFs in chapter 2, and refer to these features as Spectral Control Features (SCFs).

An example of the significant components of the TLRs for all SFs of all electrode channels for the 'oe-aa' activity of subject 3 performing the FineSp task is given in Figure 4.1. Six groups of significant TLR components, which define six SCFs, are circled in Figure 4.1. For example the SCF chosen for the red circle in plot 17 (electrode 17) of Figure 4.1 would be the frequency band 50 to 148 Hz with a positive weight. Likewise, the band 4 to 18 H with a negative weight could also be chosen from electrode 17. Generally, the functional importance of the SCF is based on both the frequency and temporal span of their significant TLR components, and the best SCFs are chosen as BCI control features. In this work, the SCFs were ordered according to the absolute value of the total weight in frequency and time and the top 20 SCFs of each task were chosen from the sets of SCFs from each task activity. These SCFs serve as that set of brain features against which the Brain Mirror features (defined later) are compared.

4.2.3 Online Deep Belief Network training

Because of the online nature of the Brain Mirror system the traditional training paradigm for DBNets had to be modified. The traditional method of DBNet training is to exhaustively train the DBNet on a representative sampling of the entire data set. Each layer of the DBNet is trained to convergence before it is used to generate input to the higher layers. In the Brain Mirror system the DBNet layers are updated as the live data is streaming through, in order to allow the representation to adapt to changes in the signal patterns.

This forces two fundamental changes to the traditional paradigm. First, the DBNet layers are trained on samples from a small sliding window rather than random samples from the entire data. Secondly, each layer of the DBNet is trained based on the current state of the layers below, even though those layers have not converged to a stable representation. In this context the learning rates and the learning momentum are key factors in determining not only the convergence properties of the DBNet (as they are in the traditional training method) but also the form of the data patterns they encode. The consequences of the online training scheme are further discussed at the end of this chapter in section 4.6.3.

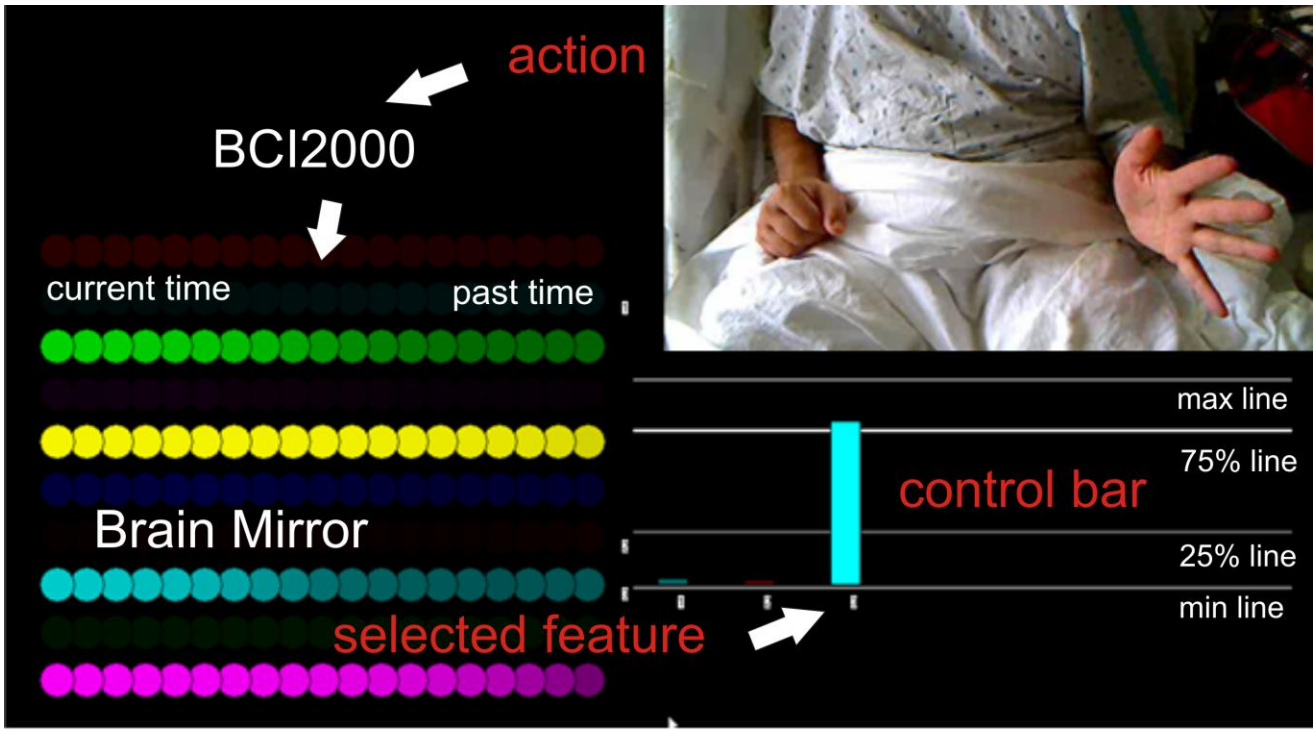

Figure 4.2: Brain Mirror Screen Shot. Three control features have been selected as control features to drive the control bars. The third feature is currently activated by the subjects hand movement.

4.3 The Brain Mirror System

The Brain Mirror system is built on top of the BCI2000 [74] system, a common platform for clinical recording and analysis of brain signals. BCI2000 can perform real-time signal pre-processing, computing the frequency response for many frequencies, for many electrodes, and normalizing this response, so that it has zero-mean and unit variance. In current use, a linear combination of a few of these features to serve as control features in simple closed loop control tasks.

The Brain Mirror system (see Figure 4.2) replaces this simple linear combination of frequency responses, and instead considers the responses of the top layer units of the DBNet as potential features. The Brain Mirror summarizes the recent time history by showing these features (the response to each top-layer DBNet unit) as either active "colorful", or inactive "dark", with the current time step on the left and the recent history going to the right. If the patient finds they have good conscious control over the brightness of one of the features, they, or the experimenter, can select that feature at which point it will drive a control bar on the right on the screen. When the control feature can reliably be moved above 75% of maximum strength or below 25% of maximum strength the subject is deemed to have demonstrated control, and the chosen feature would be considered suitable for controlling an external device.

4.3.1 The Brain Mirror User Experience

Here we describe the user experience of using the Brain Mirror system to self-select a set of BCI control features. The self-control feature selection process consists of four stages, which are listed below.

1. The initialization phase: the feedback is initialized and started.
2. The Exploration phase: the user views the brain signal generated feedback and looks for feedback features that response to their cognitive actions.
3. The practice phase: the user indicates a feedback feature that they perceive to be able to intentionally modulate through cognitive activities and the experimenter selects it as a control feature. The user then practices modulating the chosen control feature until they can consistently control its magnitude through the performance of a cognitive task.
4. The building phase: the user iteratively returns to the exploration phase and works through the control feature selection and practice phase to find additional control features that can be controlled independently from the previously selected control features.

Each of these phases is describe in terms of the specific experience of a Brain Mirror user in the following subsections.

4.3.1.1 The Brain Mirror Initialization Phase

When the user first sees the Brain Mirror there is a black screen with the green words 'Waiting to start' in the center. When the Brain Mirror is started an initialization countdown appears in the form of decrementing blue numbers that turn green when the countdown is within 3 seconds of completion. After this initialization countdown has finished the Brain Mirror begins to generate feedback causing the colored rows of feedback features to appear. In the first moments all rows appear bright and constant in intensity. After a brief period the rows grow dark and then subsets of rows begin to brighten and darken. The user is instructed that the changing intensities represent different brain activity patterns and that they can begin to explore cognitive activates as a means to change these patterns.

4.3.1.2 The Brain Mirror Exploration Phase

Once the colored feedback rows begin to change independently the user can begin to explore to responses to various cognitive tasks. This process can be completely self-paced or guided by verbal instructions from the researcher. In either case the user performs several repetitions of a task and watches the Brain Mirror feedback features change intensities. As the users explores different cognitive activities it becomes clear that a certain cognitive activity, for example a hand movement (as in Figure 4.3), causes a colored row to brighten each time it is preformed. The user then indicates to the researcher that they think they can control that row, for example the aqua blue row third from the bottom in Figure 4.4. The researcher then selects this row as a control feature by clicking on it.

4.3.1.3 The Brain Mirror Practice Phase

Once a feedback feature has been selected as a control feature the Brain Mirror system creates a control bar which is the same color as the selected row and whose height is controlled by the intensity of the color of the left most circle in the selected row. The user then begins to practice holding the control bar above the 75% line by performing the cognitive task and preventing the bar from going above the 25% line by relaxing and avoiding performing the cognitive task. In this phase the user can explore variations on the cognitive task to increase the reliability of control over reaching the 75% line and cognitive strategies for preventing the bar from reaching the 25% line.

4.3.1.4 The Brain Mirror Building Phase

After some practice the user may decide that they can consistently control the height of the bar with the cognitive strategy they have developed. They can then return their attention to the colored rows on the left half of the screen and begin to explore new cognitive activities. During this time the user monitors how both the colored rows and selected control bar are affected by cognitive activities. The user is alert for cognitive activities that cause a row to respond while not affecting the height of the chosen control bar. When such an activity is found a new row is selected as a control feature and the user practices increasing the new control bar while holding the first control bar below the 25% line and vice-versa. Once the user learns to control the two bars independently the process is iterated until no new independently controllable features can be found.

4.3.2 Implementation details

Because the Brain Mirror system is designed to give direct feedback from patterns over all recorded channels and a broad spectral range, 11 frequency bands of 2 Hz width are defined for each channel. Because of the limitations in the BCI 2000 system, and the need to run in real-time, the results in this chapter use a smaller subset of frequencies for each electrode (4, 8, 12, 18, 26, 38, 50, 82, 104, 148, and 172 Hz based on the range of common ECoG features and noise bands). In the initialization phase the BCI2000 system is configured to run for 10s to calculate the mean and standard deviation for each frequency band and then output the normalized amplitude response for each band for all future time points. The normalized amplitude responses are analogous to the responses of spectral features SFs discussed in chapter 2 (section 2.2.4). After the initial 10s, the Brain Mirror system feeds these responses into the DBNet implementation.

The Brain Mirror system is based on a 3 layer DBNet. We found the system to be robust to a range of parameter choices, and in the remainder of this chapter considers DBNets of the same size. The first layer has inputs from each frequency feature in each channel, and 100 hidden units. The second layer is also of size 100, and each node gets input from each of the 100 first layer nodes. The third layer takes input from those 100 nodes and has 20 output units. Each of these 20 output units defines an FSN whose response is visualized for the subject.

The online update of the DBNet is based on grouping the measurements from the patients (captured at 1200 Hz for all patients except Subject 3, whose measurements were sampled at 512 Hz). A sample block is defined to include 32 time points and normalized amplitude responses are calculated for each sample block. The online training window includes the previous 20 sample blocks, so that each sample block is included in 20 epochs of training. This data is fed to the first DBNet layer for one epoch of training, and each high layer is trained on the outputs of the preceding layer. Hence, the DBNet layers are trained on a small sliding window through the spectral feature data.

Each epoch of the DBNet training updates the weights and biases of the DBNet model based on a learning rate and a momentum. Using the notation in paper [152], the parameters s_lr, which constrains how quickly the input weights change were set to 0.001, the parameter b_lr (which affect the weights on the binary hidden units) were set to 0.01, and the momentum m was set to 0.5.

Collectively, these parameters define a relatively small DBNet, with relatively slow learning parameters that adapts to changes over the course of tens of seconds. This proves to be able to robustly encode interesting patterns in a diverse sampling of ECoG data.

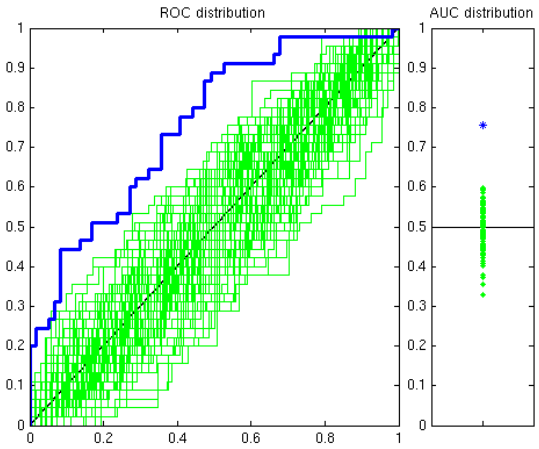

Figure 4.5: An example of Receiver-Operator Curve (ROC) Non-parametric statistics. Left: ROC for the 'oe'–'ah' condition vs. ITI for the FineSp task(blue line) shown with 100 ROCs(green lines) calculated from the response of the 'oe'–'ah' control feature using and equal number of random time-locked trials as there were actual 'oe'–'ah' trials. Right: the corresponding Area Under the ROC partition distribution (green points) and 'oe'–'ah' control feature value (blue point).

4.4 Analysis

4.4.1 Evaluating Brain Mirror FSNs

We now present a systematic comparison that attempts to capture how well the DBNet is able to discover features that correlate with conscious activities of the subject. For testing, we replay each of the five research task data sets as input to the Brain Mirror system and perform the following analysis:

1. Compute the spectral features from the ECoG data stream and incrementally train the DBNet.
2. Log the current responses of the DBNet output nodes, and the state of the DBNet (all of the internal weights and biases that define its current behavior) every 37.5 ms.
3. Evaluate each DBNet output node as a potential Functional Spectral Network (see section 4.4.4.1).
4. Consider the set of FSNs and evaluate their performance as classifiers of activity of the subject (see section 4.4.1.2).

We compare these results of the live Brain Mirror system (BM), with 4 alternatives to the DBNet representation.

1. The final state of the DBNet (finalBM) to capture its performance if trained over a longer time period.
2. Online PCA [153] (onlinePCA), because it is the natural alternative representation to DBNets.
3. Final state PCA (finalPCA), to capture online PCA performance when trained over long time periods.
4. Batch PCA (batchPCA), similar to final state PCA, but is independent of the order of the ECoG signals.

These 4 alternatives, along with the top SCFs and the BM features, give 6 methods to find feature representations that are FSNs and distinguish user activities. For all six methods 20 features were considered.

4.4.4.1 Defining FSNs

To compare the six representations, we use the same analysis procedure as in previous chapters. Based on data time-locked to the beginning of the task, we use non-parametric statistics to find FSNs that were significantly and positively modulated by the task. FSNs are considered to be features with a significant positive time-locked response with regard to at least one of the task activities.

4.4.1.2 Defining independent control features

We then consider how well each feature with functional contrast serves as a classifier of that activity vs. the inter-trial interval, that activity vs. other activities, and that activity vs. all other time points. Different thresholds of the feature give different classifiers, and the receiver-operator curve summarizes the performance for all thresholds. We use the standard "area under the receiver-operator-curve" (AUROC), as a summary statistic for classifier performance.

We first compute the response value for each significant feature for each activity trial. For each trial the dot product of the feature response over the trial with the TLR pattern for that feature is taken as the response of that feature for that trail. Then we compute the AUROC for the responses over all trials. We again use non-parametric statistics to define AUROC values that are significant. To do this, the per trial feature response values were randomly partitioned 100 times and 100 pseudo-AUROC values were computed based on these partitions. An example of the receiver-operator curves for the 100 random partitions and their corresponding pseudo-AUROC values, along with the actual receiver-operator curve and AUROC value for the 'oe'-'ah' activity of the FineSp task, is given in Figure 4.5.

4.4.1.3 Temporal Evolution of Control Features

In addition to evaluating the performance over the entire data set, a third evaluation of the online representations (BM, onlinePCA) was done to characterize the amount of time they needed to find useful control features in the data. To make a fair comparison, we specify the final segment of the ECoG data stream as test data. We use the fact that we logged that weights and biases of the DBNet and the components of the online PCA during the training --- giving us the state of the DBNet and online principal components for different amounts of training time.

For each logged state, we evaluate the testing data and choose the single best control that best discriminates the best activity from the other activities and from the inter-trial intervals for each task. The best activity for each task was chosen as the one with the most significant control features for the Brain Mirror and onlinePCA methods in the above analysis. For this control feature we again use the same two step method as above and use the AUROC to characterize the effectiveness of the best control feature available after a given amount of training time.

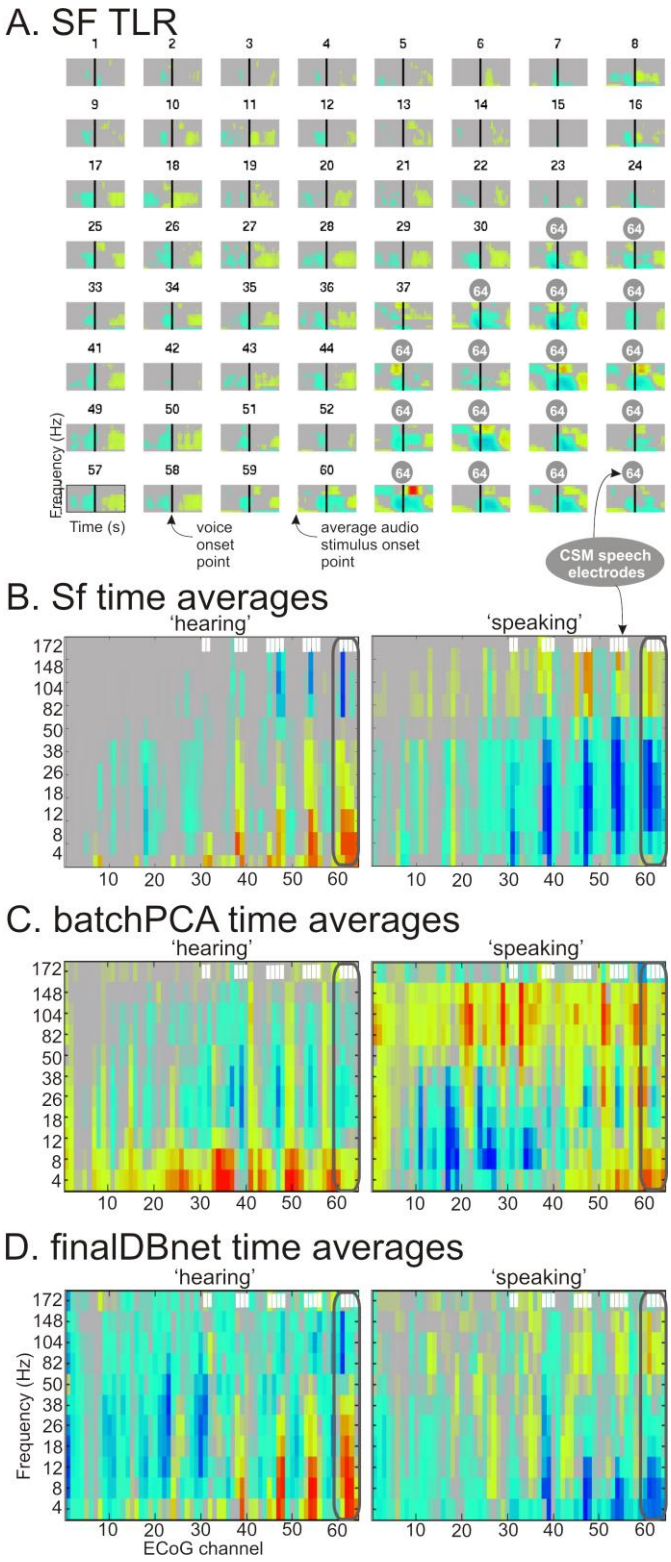

Figure 4.6: Comparison of batchPCA and finalBM control feature spectral patterns. A. SF TLRs including the 'hearing' and 'speaking' activities of the HS task. B. The results of averaging the TRLs of each SF over the time period in A. C. The temporally averaged batchPCA control features. D. The temporally average finalBM control features. The electrodes indicated by CSM as speech arrest electrodes (see section 1.2.5) are indicated with white numbers in A and white boxes in B-D.

4.5 Results

The Brain Mirror system was demonstrated in the clinical setting with an ECoG subject implanted with a 64 electrode grid. A still frame from a video of this test session is shown in Figure 4.2. This figure shows a visualization of the activation of 20 BM features; during this frame 4 are strongly active and two more are very weakly active (in very faint dark blue and dark red). This patient has noticed that the "light-blue" feature correlates to his hand motion, and in this frame is demonstrating control in forcing that feature to achieves 75% of its maximum value. This highlights that the overall system design has potential, and the specific representations created through the incremental DBNet captures features that can be used. Trials on one other patient failed with the very late discovery that the patient was color blind, and otherwise, limitations of the patient population in this study prevented further live experimentation.
Testing the Brain Mirror System by replaying the ECoG data captured in non-interactive settings allows more extensive quantitative testing of how well the system captures features that can be used to define control. The main result of this testing is that the DBNet representation used in the Brain Mirror outperformed several natural alternative, incremental representations. This is especially impressive considering that the SCF (single control feature) representation used labels during training and the batchPCA was trained on more data. The results of the three analysis methods defined in sections 4.4.1.1– 4.4.1.3 are discussed in more detail below.

4.5.1 Naive learning of features with functional contrast

For all tasks the BM system naively learned patterns in the ECoG spectral data that reflected functionally meaningful neurophysiologic phenomenon induced by brain activity. In fact, the DBNet-based representations were the only ones to have at least one significant feature for every activity performed by the subjects in all five tasks (see Figure 4.7).
Figure 4.6 A shows the TLRs of the SFs to voice onset time (indicated by the black vertical line in each subplot) of the HS task. The electrodes at locations indicated as essential to speech production through cortical stimulation mapping (white numbers) show the strongest TLRs to the voice onset times. However, the significant TLRs are not limited to these electrodes. In Figure 4.6 B, the TLR for each electrode (x-axis) and frequency (y-axis) for both the hearing and speaking activities are averaged over the hearing and speaking time periods respectively. In Figure 4.6 C and D the finalPCA and finalBM control features are shown without the temporal component of their TLRs. It can be seen that both the batchPCA and finalBM representations are matches to the patterns of significant SF responses to the hearing and speaking activities. Remarkably, the finalBM control feature patterns match the SF patterns remarkable well considering that no labels were used in the learning process. The following section demonstrates that the features found by the DBNet representations were better control features.

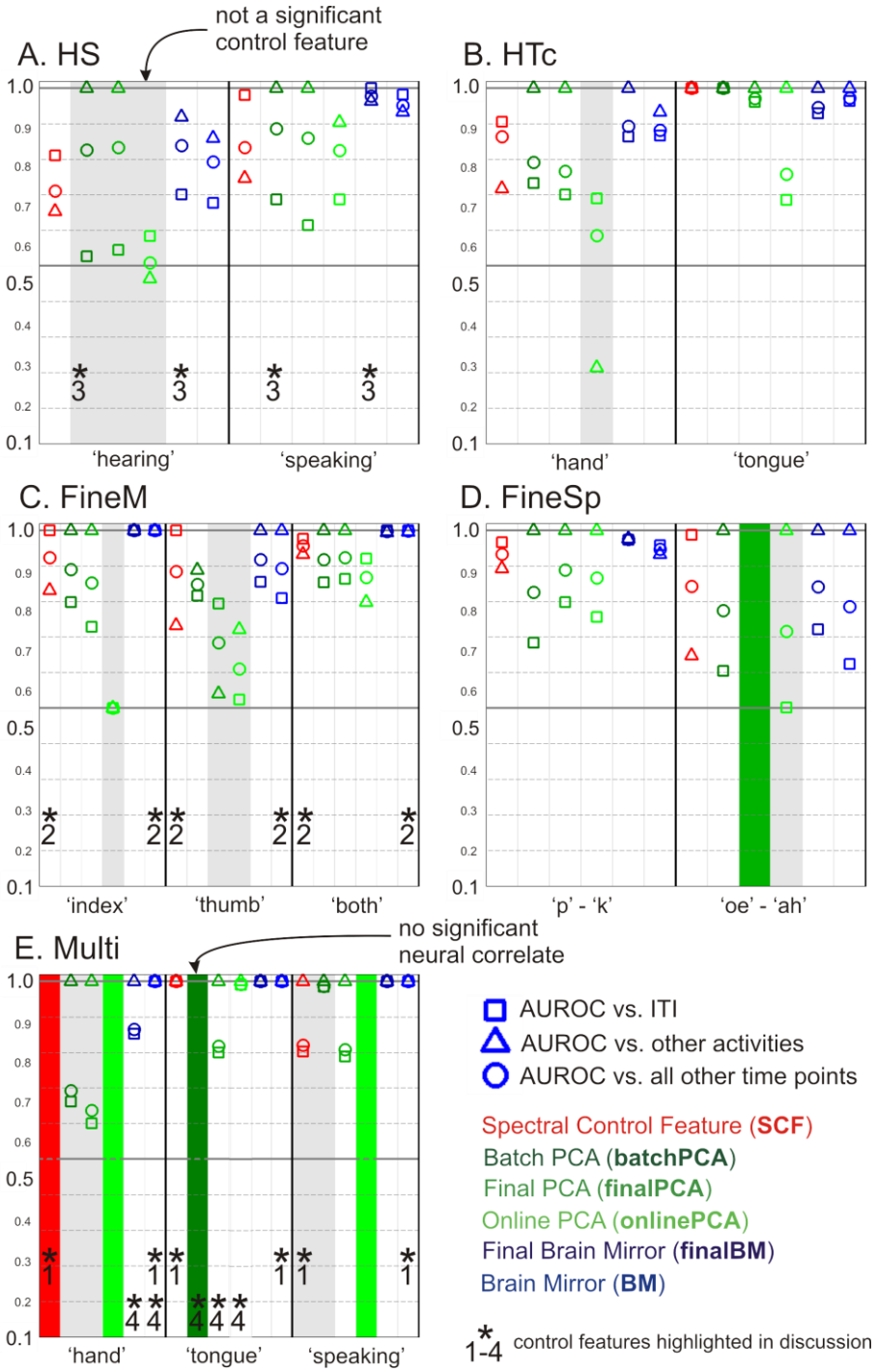

Figure 4.7: Area under the Receiver-operator Curve (AUROC) for the selected control features for each activity in each task.

4.5.2 Finding Control Features

Figure 4.7 summarizes the AUROC scores (squares, triangles, and circles) for all alternative representations and all different tasks and task activities. Task activities that could not be distinguished from other activities by any control

feature are indicated with light grey bars in the corresponding column. If a representation could not distinguish the activity from rest, then the column is marked with a solid colored bar.

Figure 4.7A focuses on the HS task. From left to right, we show the AUROC values for control features that arise from the hearing activity, based on single spectral features (in red), batch PCA (dark green), the final PCA basis (green), the online PCA, (light green), the Final Brain Mirror (dark blue), and the online Brain Mirror (blue). The right side of 3A shows the same evaluation of the control features for the speaking activity. In each case, squares represent the AUROC for classifying the task versus the ITI (a resting state), the triangle is the classifier of one activity versus other activities, and the circle is the AUROC for distinguishing the activity from all other activities and ITI.

The most interesting parts of the result in 3A are that, (a) all representations encode for at least one significant feature for each activity, (b) all representations led to statistically significant control features for the 'speaking' activity, (c) the BM does very well, with the highest total AUROC values (indicated with the circles) for both hearing and speaking, and finally, (d) while PCA based representations produce a control feature for the speaking activity, those features are not independent control features for the hearing condition. These representations are marked in gray. A discussion of the fundamental differences in representations leading to the AUROC results in the columns highlighted with a '*3' in Figure 4.7 A is given in section 4.6.2.

Figure 4.7 B shows results for the HTc task. These results show similar features to those of the HS task. In particular; (a) the BM representations give consistently good results, (b) the onlinePCA representation performs well on the tongue task, and poorly in creating a classifier to capture the hand motion. The fact that the AUROC value for the hand activity control feature verses the tongue activity is considerable below 0.5 (which indicates equal response value to both activities) arises due to the fact that there is an increase in response value for both activities but the response to the hand activity is consistently less the that of the tongue activity.

Figure 4.7 C shows results for the FineM task. For this task, it was again the case that not all representations created statistically significant control features. The most significant result here is that the (BM and finalBM) representations perform very well, and in general, outperform the SCF representation. These results, highlighted by the columns marked with a '*2,' are discussed further in section 4.6.1.2.

Figure 4.7 D shows results for the FineSp task. Again, the online PCA based representations perform poorly and the online DBNet based representation perform as good as or better than the SCF representation.

Figure 4.7 E shows results from a subject doing a task that involves a simple motor activity (hand movement), and mouth motor activity (tongue movement), and a 'speaking' activity. Again, BM features perform well across all categories and the online PCA approaches do particularly poorly. Also, in this task the set of the top 20 SCFs did not include a significant correlation to the hand movement activity while the BM representations did. The columns displaying this result are highlighted with a '*1' and discussed in section 4.6.1.1. An additional result ('*4'), discussed in section 4.6.3, is that the BM representation outperforms the finalBM representation for the hand activity and onlinePCA out performs finalPCA for the tongue activity.

4.5.3 Temporal Evolution of Control Features

The second set of experiments explores how much background signal is necessary for incremental approaches to build a good representational basis. In real use cases, this would bound the time required for the Brain Mirror or Online PCA to compute useful features. To evaluate the timeline we compute the Brain Mirror and Online PCA representation incrementally, and record that representation at each time step. Then we evaluate the performance of the representation for classification tasks, and show how that performance changes as the system uses more and more data.

Figure 4.8 A considers the HS task. The green area corresponds to the best control features defined by online PCA. The dark green line shows the AUROC of the classifier for speaking vs. all other conditions (ITI and other activitie), and the bottom of the green region shows the AUROC of the classifier for speaking vs. hearing, and the top is the AUROC for speaking vs. ITI. The blue regions show the same plot for the BM features. The most relevant part of this plot is the indication that the BM features become good at the classification tasks within 45 seconds. This is dramatically shorter than current BCI training protocols, and also earlier than the online PCA control features. While we do not show these plots for all tasks, the AUROC for the best control feature from each task converges within a minute.

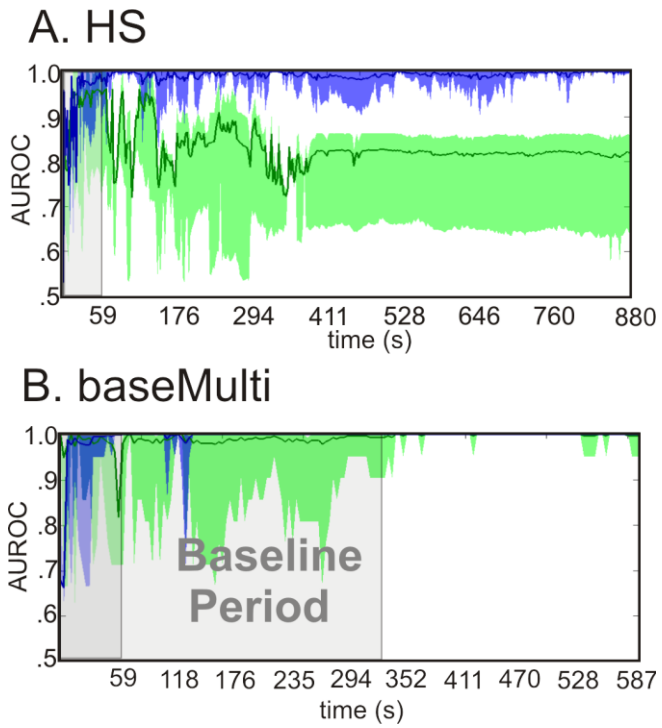

Figure 4.8: Temporal evolution of the performance of the BM (blue) and onlinePCA (green) features. A. The AUROC scores given by the best feature responses of the onlinePCA and BM encoded at each time point of the first 9/10^{ths} of the HS task data to the last 1/10th of the data. B. The AUROC scores for the first 3/5^{ths} of the baseMulti task data to the last 2/5^{ths} of the data. The dark solid color lines show the AUROC of the classifier for the best activity vs. the ITI times and the other activities (corresponding to the circles in Figure 4.6), and the bottom of the light shaded regions show the span between the AUROC of the classifier for the best activity vs. other activities and the top of the light shaded region is the best activity vs. ITI (corresponding to the triangles and squares in Figure 4.6 respectively).

For many of the tasks, there is more than a minute of rest time before the task starts, so the patterns encoded at the beginning of the task reflect patterns in resting brain activity. However, DBNets trained on that data capture variability during the tasks, and classify subject task activity with performance comparable to patterns defined using both rest and all task data. The Multi task highlights this: a 5 minute period of 'resting' activity was recorded before the subject started to perform the task activities. Figure 4.8 B shows that after a short initialization period, the AUROC is high during the entire length of this 'resting' period and does not significantly increase once the subject starts to perform activities.

4.6 Discussion

The main result is that the Brain Mirror approach, based on incrementally trained DBNets quickly converged to control features that were better at discriminating task activities than any natural alternative. This highlights the potential for Deep Belief Networks to offer efficient, real-time representations of ECoG activity patterns. We demonstrated this across a range of patients and tasks, highlight the broad potential for subjects to find controllable

brain signal features for BCI. Real time feedback allows the subject to explore which brain activity patterns they can control and how they can control them.

Particularly interesting are the FineM and FineSp task experiments (Figure 4.7 C-D). In these cases, the ECoG data is from smaller grids covering much less cortex. The Brain Mirror system found patterns that could distinguish between 3 different fine motor tasks from a micro electrode grid and two different classes of mouth motor movements from a high-density grid. These results are on par with the best functional detection results reported to date, even though the Brain Mirror does not require pre-screening for control features. This is important because Microgrids and high-density grids are very new and promising technologies for BCI. The remainder of this section details four key reasons the Brain Mirror system achieves such good results .

4.6.1 BM features verses SCF

The BM based representation has an advantage over the standard SCF representation when there is significant overlap among the SCF from separate activities. Two specific problems arising from overlapping SCF and why the BM representation avoids these pitfalls are discussed below.

4.6.1.1 The most significant SCFs for different activities often overlap.

Multi task results serve as a good illustration of the case when the major SCF is shared by several activities. When the best single features are shared by many different activities, it is not possible to use them as control features to detect each one. Figure 4.9 A shows the TLRs of the three activities. For each subplot, frequency is given on the y-axis and time relative to the time locking point is give on the x-axis. Figure 4.9 B shows the temporal spectral patterns of the BM control features formed by multiplying the DBNet encoded spectral patterns by the TLR for each activity.

In Figure 4.7A, electrodes 19 and 22 contain the control features found from the set of SCFs for the tongue movement and speaking activities respectively, marked with white numbers. The wideband spectral amplitude increase seen in Electrode 19 is the dominant SCF for all three of the task activities.

The lower frequency decrease in electrode 22 is a feature for detecting the tongue movement activity, but there is no good alternative for the hand movement activity. In contrast, neither electrode 19 nor 22 are prominent components of any of the three BM control feature patterns. Because the BM features are anatomically much broader, collective small spectral changes outside these two electrodes can be used to distinguish the task activities. Interesting this is the case even though the DBNet is not trained using activity labels.

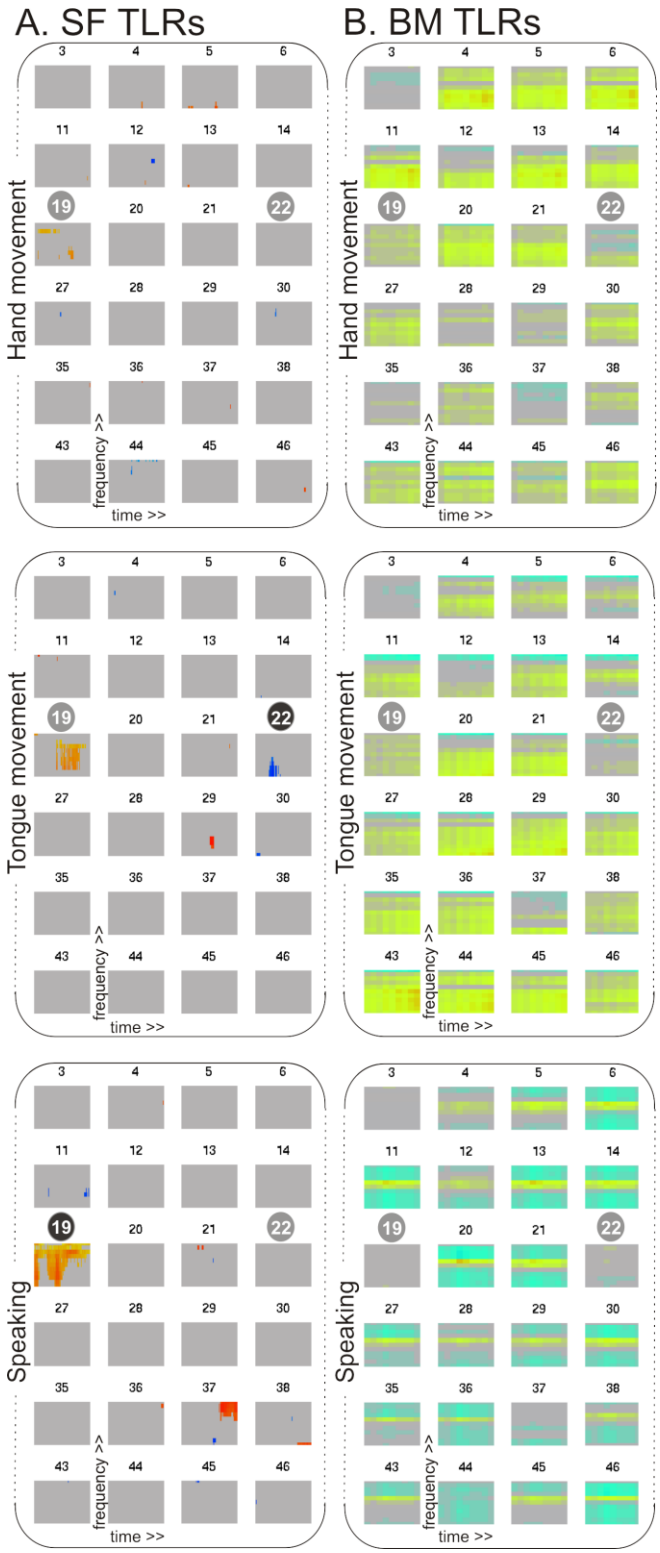

Figure 4.9: SCF vs. BM control feature. A. TLR patterns for a subset of electrodes 48 electrodes from the Multi task for the 'hand movement', 'tongue movement', and 'speaking' activities that include the electrode with the largest TLR for all three activities (electrode 19). B. TLR patterns of the chosen BM control features for the 'hand movement', 'tongue movement', and 'speaking' activities over the same subset of electrodes.

4.6.1.2 When a single activity has SCFs with opposite signs from the same channel that overlap in frequency range.

The FineM task results serve as an example of when a SCF is modulated both positively and negatively by the same activity. Figure 4.10 A shows the TLRs to the index finger, thumb, and pinch movement activities of the FineM task. Figure 4.10 B shows the TLRs of the SCF chosen as the control features for this task. The TLR for the index finger SCF control feature decrease before the onset of index figure movement (indicated by the black vertical line). Figure 4.10 A shows that the chosen index finger control feature is also positively modulated by the pinch activity. The decrease in response value preceding the index finger movement discriminates the response values of this SCF to index finger and pinching movements when the TLR patterns are considered by the classifier. However, the decrease makes this feature less suited as a control feature since each activity driven increase is first preceded by a decrease.

On the other hand, the index finger activity BM control feature focuses in on this decrease, which is repeated across many of the electrodes, as a separate pattern that can itself be a control feature (Figure 4.10 C). The pattern of increases across the same electrodes in the same frequency ranges after movement onset can then be used as the pinch control feature. Such a pattern of coupled increases and decrease is also not an uncommon characteristic of SFs (see Figure 4.1 for additional examples in the FineSp task).

4.6.2 Comparison of BM features and PCA based features

The BM representation also has an advantage over the PCA based methods when the global control feature patterns share significant spectral components. PCA finds the best linear basis for representing consistent variations across the data set. This offers feature responses over many electrodes and provides robustness to noise, but these large variations may not be best suited for classification tasks. The fundamental difference in the two types of pattern encoded with DBNet and PCA representations are well illustrated by the results of the HS task illustrated in Figure 4.6.

The main spectral feature for distinguishing the speaking activity is both the increase in the 100-150 Hz and the decrease in the 4-25 Hz bands, as highlighted by the dark grey ovals in the left columns of Figure 4.6 B. The dark grey ovals in the left columns of Figure 4.6 B point to the fact that the hearing activity demonstrates the opposite pattern. Figure 4.6 C and D show that both the batchPCA and finalBM encode for this opposite hearing pattern in their respective hearing control features. However, since PCA creates an orthogonal basis, the opposite of this pattern cannot be encoded as a separate component. This is illustrated by the fact that the increase in the 100-150 Hz bands in the batchPCA speaking control feature is not coupled with a decrease in the 4-25 Hz bands. In contrast, the non-linear finalBM representation is able represent the opposite patterns as two separate features.

4.6.3 Comparison of online feature adaptation and static features

There was very little difference between the performance of online BM and finalBM control features. The tongue movement activity for the Multi task shows that the fact that the DBNet in the Brain Mirror system continues to adapt to changes in the ECoG signal characteristics as the task is performed can lead to more consistent control features. The advantage of continued adaptation is also seen in the results of the onlinePCA and finalPCA for tongue movement activity of this task. Continued adaptation to the spectral features in the ECoG signal can be expected to be more important in tasks such as the Multi task where activities are performed for longer periods of time and are spaced further apart due to the known phenomena of habituation and resting signal drift in ECoG. However, the generally poor results of the onlinePCA representation and the better results of the DBNet representation indicate that the DBNet algorithm is much better suited for online training.

The online DBNet training scheme used in the Brain Mirror system converges quickly to create robust features, and was successful across several tasks and subjects. This is important because the theoretical basis of the DBNet training algorithm is based on training each layer of the network until it converges. The experiments in this chapter offer experimental evidence that the algorithm remains stable even if the training data is drawn from a changing underlying distribution.

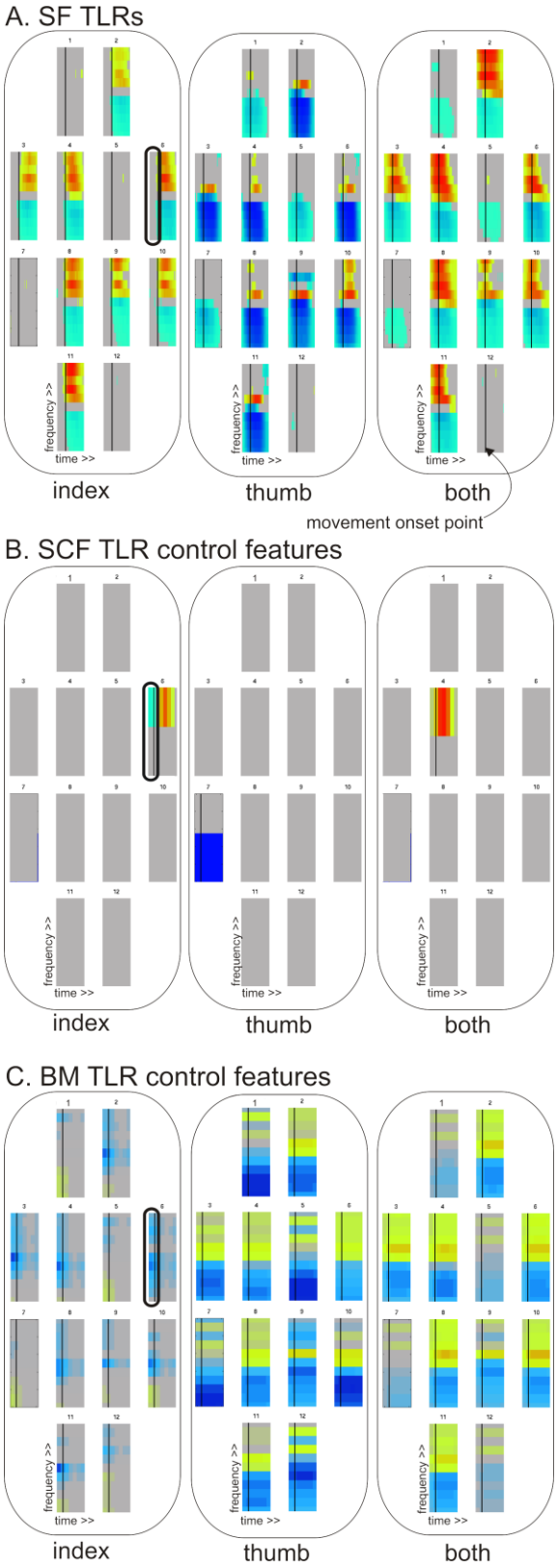

Figure 4.10: FineM control feature patterns. A. SF TLRs for the activities of index movement, thumb movement, and pinching movement from left to right respectively. B. SCF control features for each activity weighted over time by their TLRs. C. BM control features for each activity weighted over time by their TLRs.

Chapter 5

Discussion

This thesis explored a framework to define new, discriminative features based on ECoG data. We discuss how the Brain Mirror system can be used to improve the BCI control feature selection paradigm, then opportunities to use Brain Mirror system as an additional tool for clinical mapping of functional cortex. Finally, we highlight the importance of the use of SNs brain features to the Brian Mirror system.

5.1 Making the most of BCI research opportunities

This thesis demonstrates the feasibility of a user finding and selecting control features. This marks a novel approach BCI control feature selection. It is especially important in the standard clinical context for ECoG based BCI where experimental time with a subject is often limited. Hence making the most of that time is utmost importance to advancing the state of successful BCI control. Here we discuss properties of the interactive Brain Mirror training paradigm that can improve the results that are achievable in a short time.

The first key characteristic of the Brain Mirror system is that it is ready to generate feedback as soon as the patient is ready to participate in research tasks. No screening is needed before the patient can see feedback correlated to mental activities. Our anecdotal experience with BCI testing teaches that motivation is a key factor, and providing feedback in a closed loop fashion is often very motivating for the patient.

Second, the Brain Mirror system provides a faster path to BCI control than traditional screening by leveraging the power of interactive feedback. The Brain Mirror system allows a subject to perceive direct correlations between their intentions and the dynamics of the feedback features. This allows the user to find features that are correlated with their intentions with fewer cognitive task repetitions than are needed to detect statistically significant correlations with screening tasks. Additionally, subjects often require extensive practice and need to adapt their mental strategy to gain good BCI control based on their actions, especially if these are imagined actions rather than physical ones. Feedback is a crucial part of this process. If the features found with screening do not produce feedback that is sufficiently correlated to the user's intentions while doing the control task then successful control is rarely achieved. The Brain Mirror system provides feedback so subjects can see the effects of adjusting their mental strategy

A third key characteristic of the Brain Mirror system is that the feature space and feedback is less constrained than existing screening protocols. The Brain Mirror system feedback features reflect electrophysiological phenomena over a

broader frequency and anatomic range than the spectral features that can be identified with screening tasks. Our experimental exploration shows that the features defined with DBNets are responsive to a broad range of cognitive tasks.

Hence, the Brain Mirror system allows the user and experimenter to interactively explore new cognitive tasks or variations of a task to get additional or better control features. Exploring both the space of ECoG spectral features and cognitive tasks is important for designing and improving BCI systems. Deciding which brain features are best suited for which control applications and how to optimize those applications for the best results are key BCI questions yet to be answered. Understand the characteristics of brain features generated from different cognitive tasks in the context of applied BCI control helps inform these decisions.

The issue of false positives from control features is a major challenge to real world application of BCI devices and one that has not been sufficiently addressed by traditional screening with cued tasks. Since the focus has been on activating brain feature for control in short periods and not long term use, little is known about which brain features are easiest to keep 'off' when a user is not highly concentrated in a task. These features are likely to be more complex higher level mental concepts as opposed to low-level mental tasks such as motor control. High level concepts are thought to be encoded in a terms of transient relationships between cortical locations and not focal spectral features. Hence, feedback from the Brain Mirror system may be very important in being able to find such brain features.

In the context of long term BCI application, it is also important to note that the Brain Mirror was shown to generate functionally informative feedback from an implant at the high-density ECoG and micro-ECoG scales. While the large clinical grids provide a good platform for exploration, they are generally considered infeasible for long term implantation because of their large size. The Brain Mirror demonstrates that finer grain electrode density can discriminate complex finger movements, but how diverse the ECoG signal is on such a small scale needs, and how many different tasks can be discriminated, needs more exploration. The Brain Mirror system is especially important in investigating this direction because such micro-implants are even more limited in their use than the large scale grids, and there is more limited testing time.

5.2 The Brain Mirror as Brain Signal investigation tool

Functional Mapping is important part of clinical procedure and the Brain Mirror can be used as an additional tool in determining the functional organization of the cortex covered by the implanted electrodes. Mapping is hard because not all brains are the same and cannot be done based solely on anatomic location of the electrodes. Cortical Stimulus Mapping (CSM) shows electrode pairs that span areas essential for a given function, but results can be inconclusive

and are not the whole picture. Mapping based on ECoG frequency features can be a supplement to CSM. The Brain Mirror system provides several possible advantages in this context.

1. The Brain Mirror offers a more flexible platform for generating and identifying brain states associated with different mental tasks.
2. The Brain Mirror encodes for spectral networks that represent a robust description of brain state dynamics as measured by ECoG electrodes and the encoded networks can be inspected in terms of spatio-spectral content.
3. The Brain Mirror finds functionally relevant patterns even during resting state data. This offers the possibility for functional mapping when subject's condition makes it hard or impossible to actively participate in tasks.

Appendix A

Phoneme discriminant Core FSNs

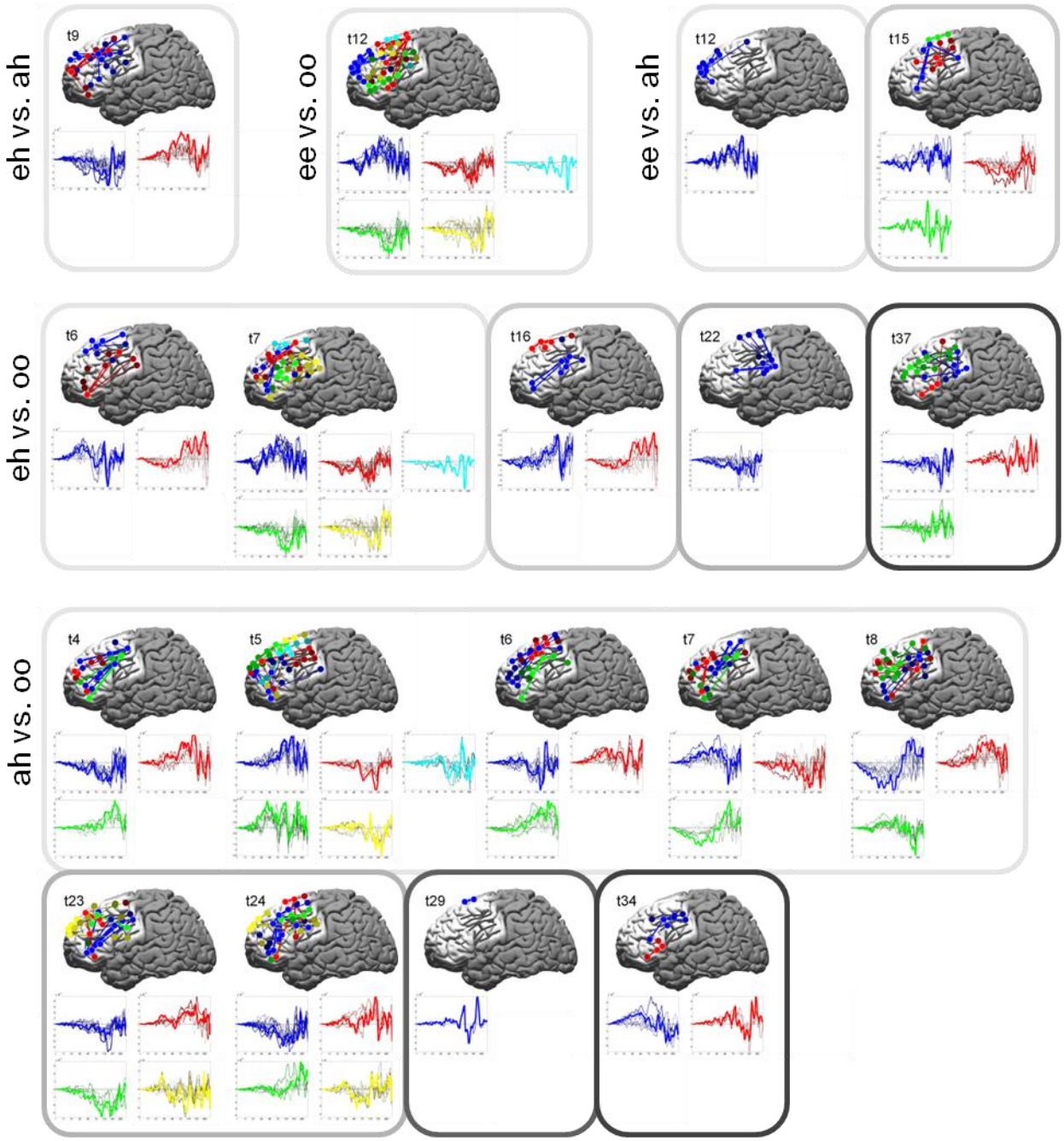

Figure A.1: Phoneme discriminant Core FSNs for subject 1 (see Figure 2.9 for figure description).

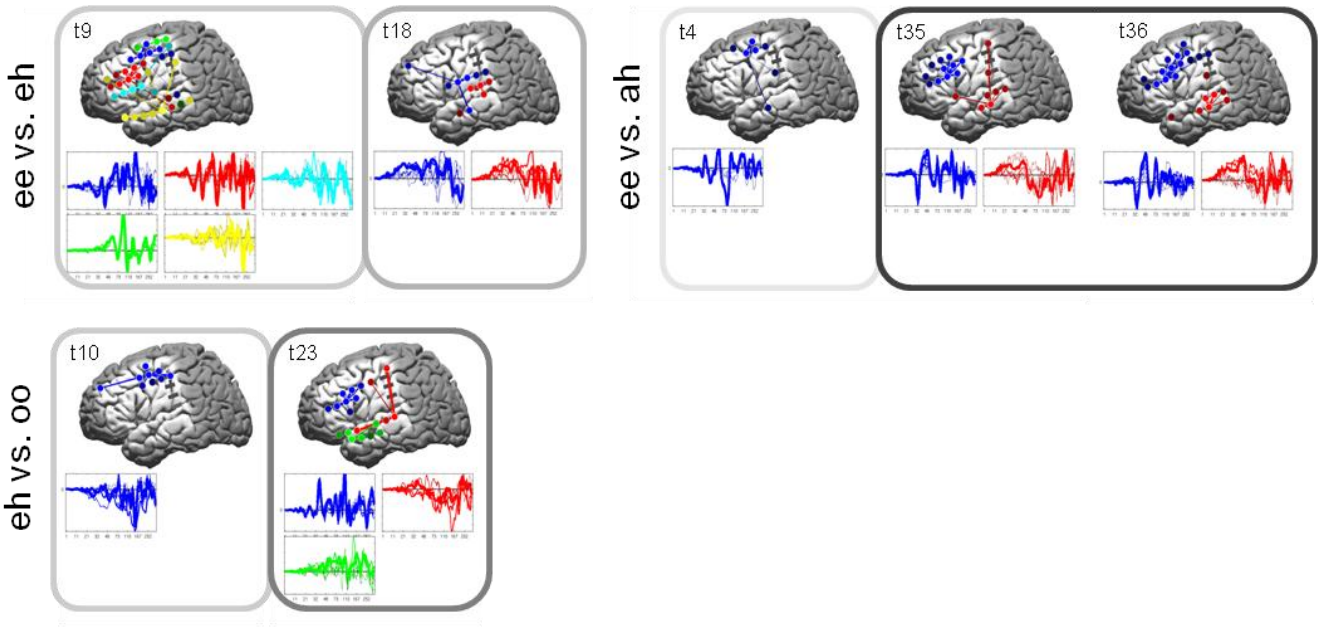

Figure A.2: Phoneme discriminant Core FSNs for subject 2.

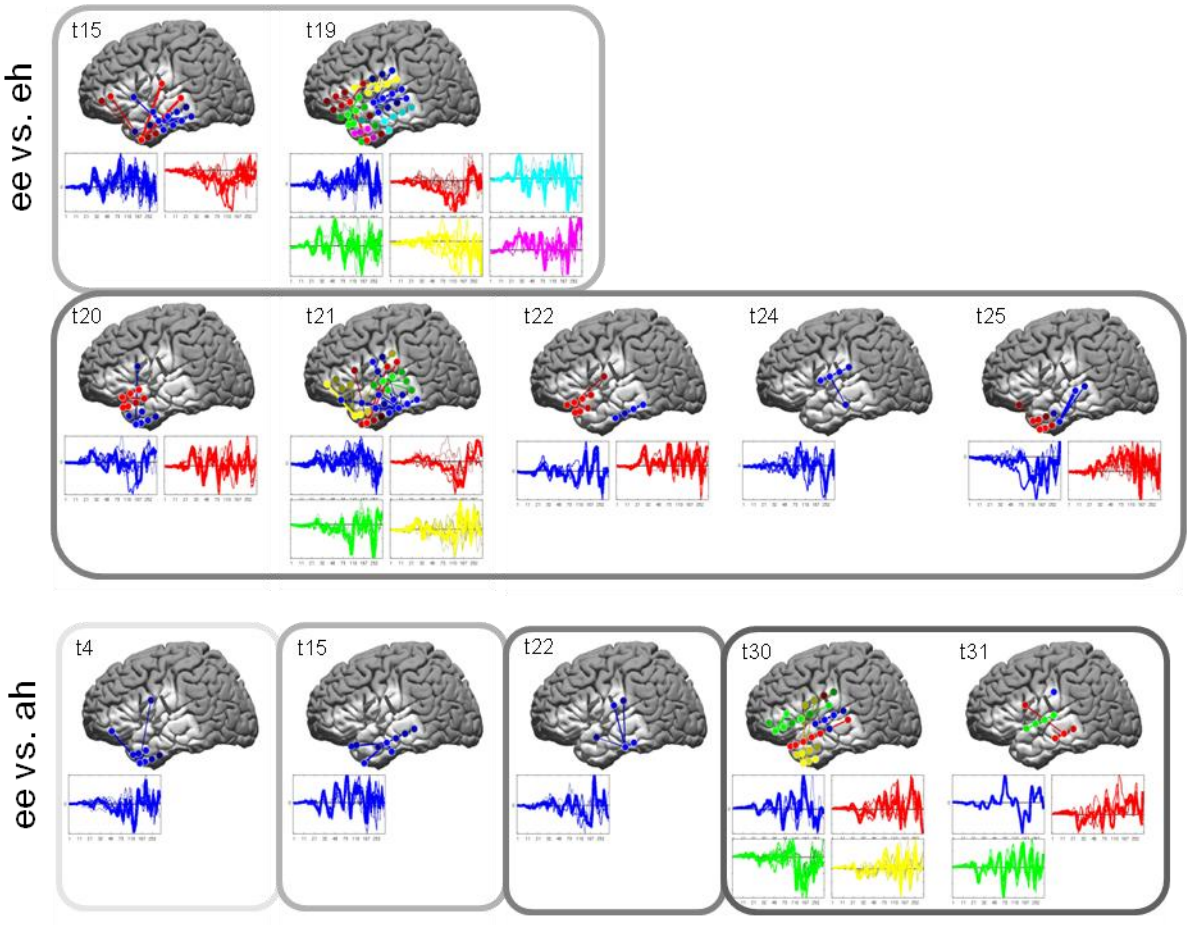

Figure A.3 Phoneme discriminant Core FSNs for subject 3 part 1.

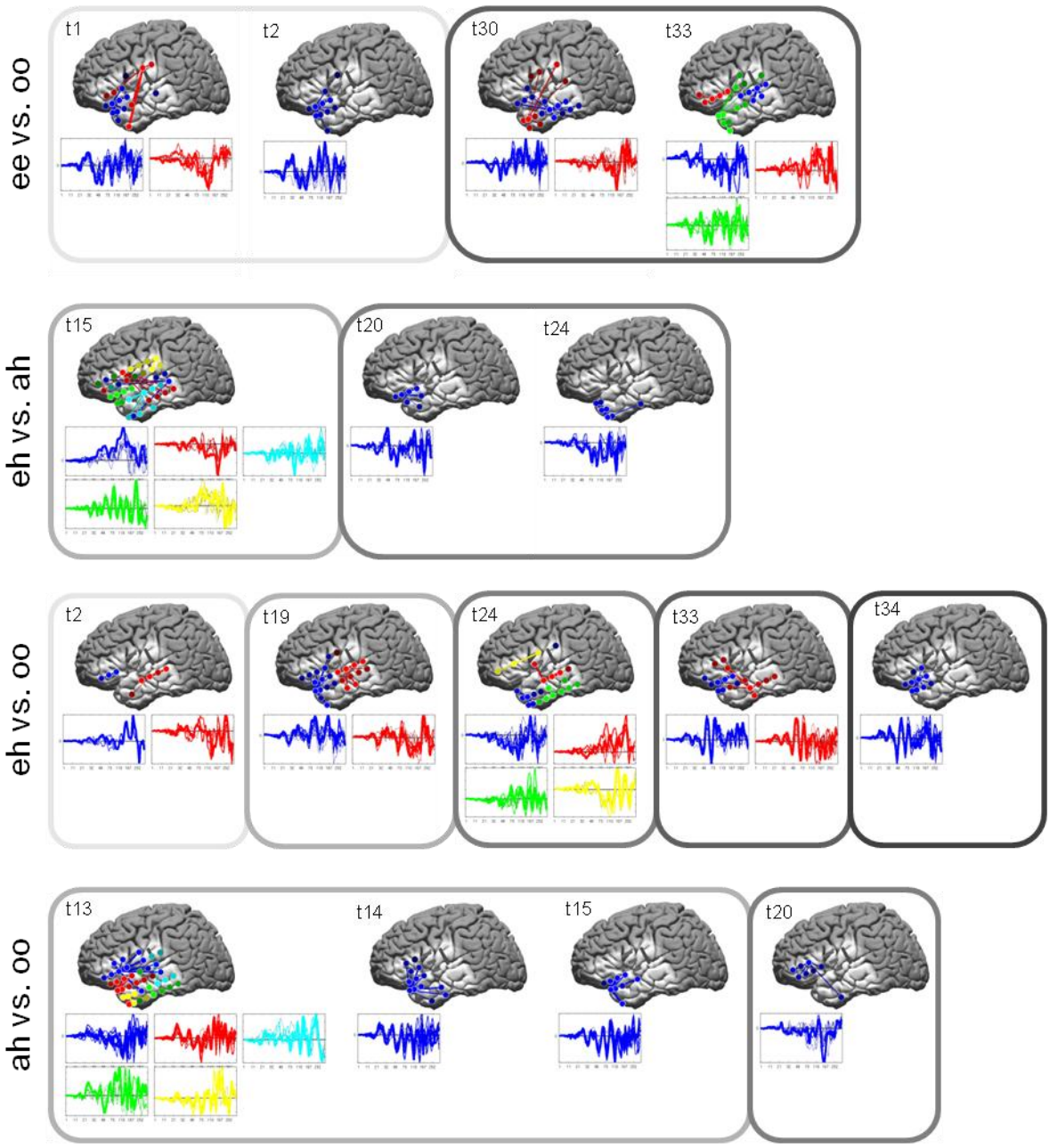

Figure A.4 Phoneme discriminant Core FSNs for subject 3 part 2.

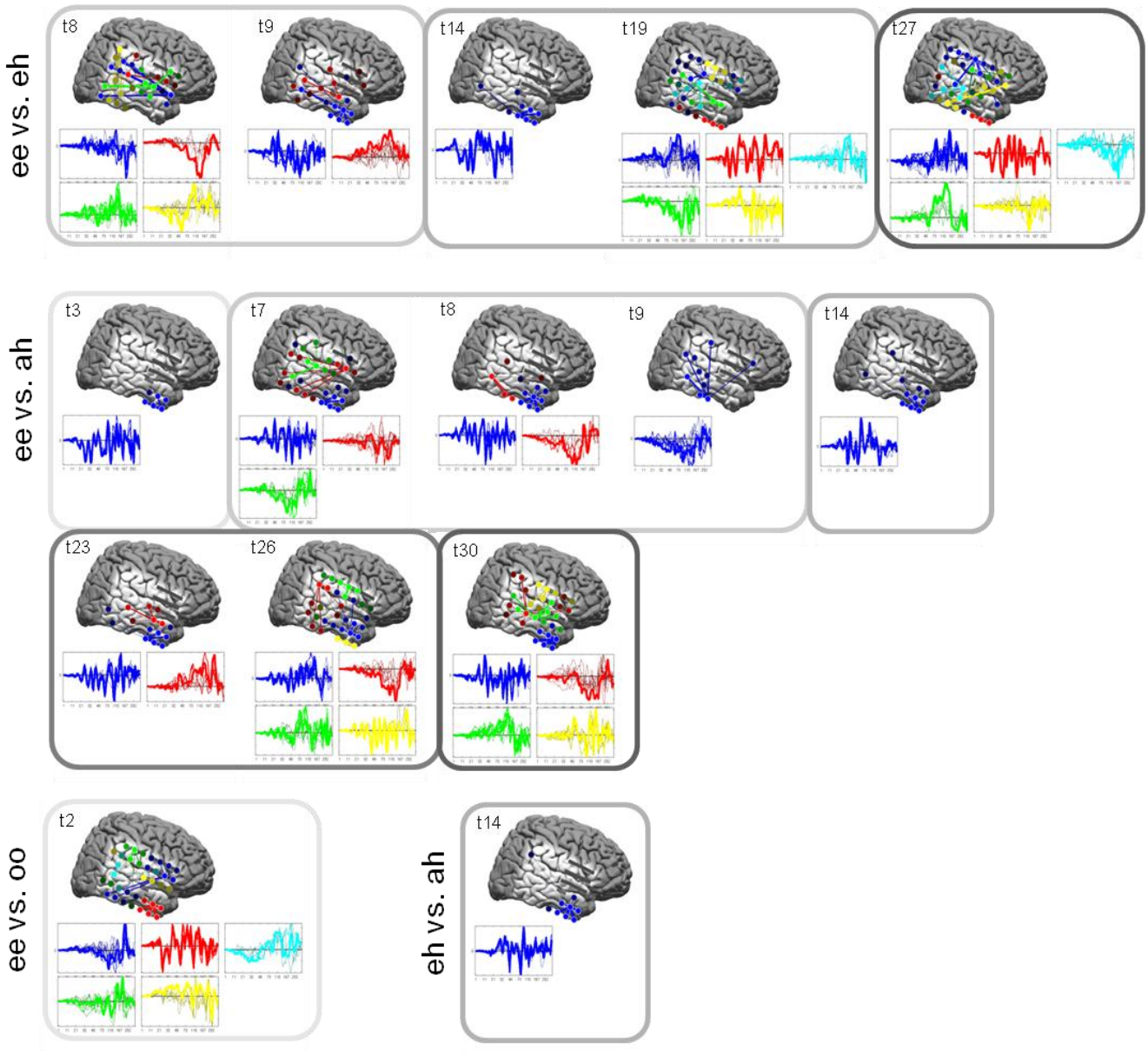

Figure A.5: Phoneme discriminant Core FSNs for subject 4 part 1.

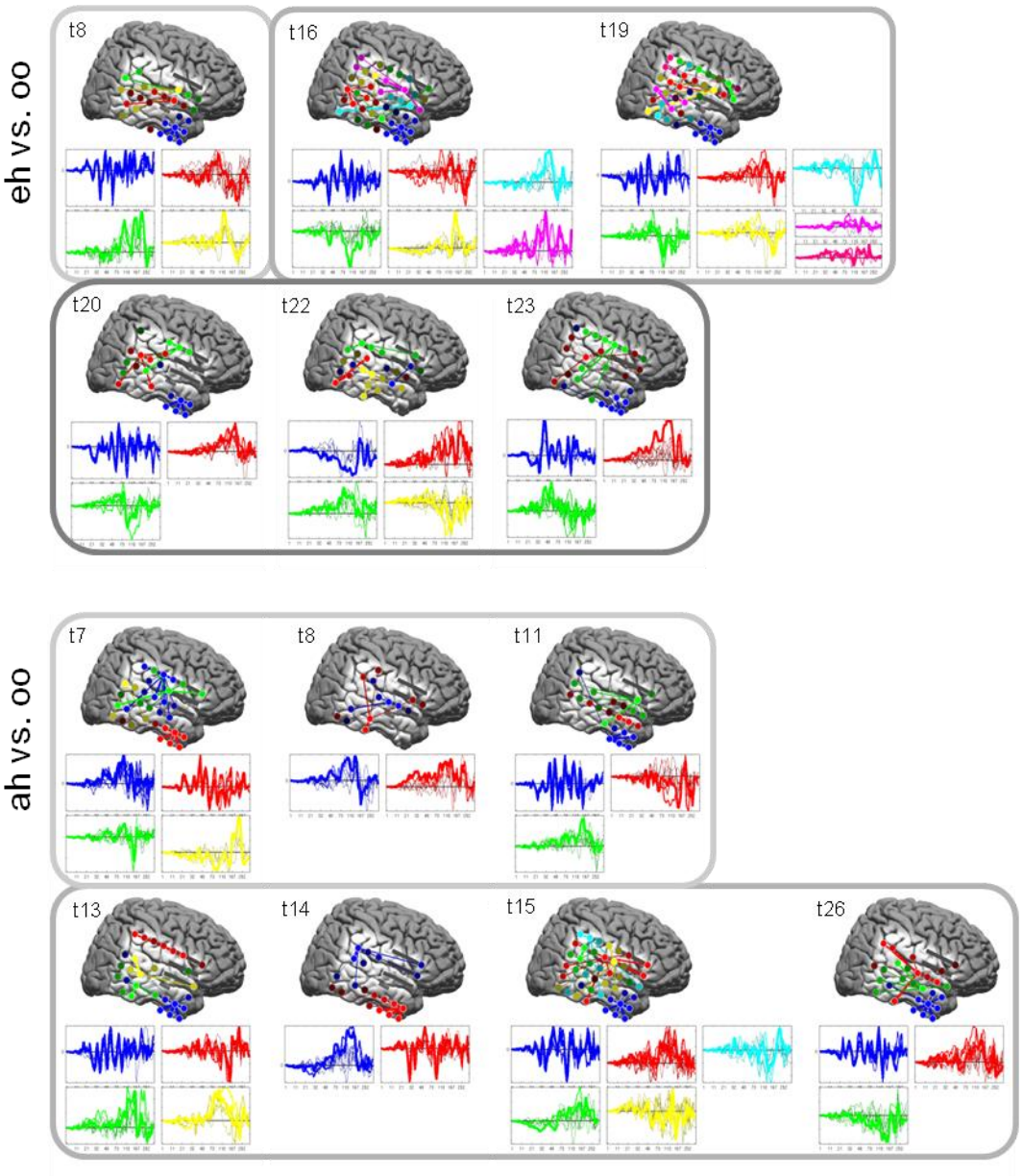

Figure A.6 Phoneme discriminant Core FSNs for subject 4 part 2.

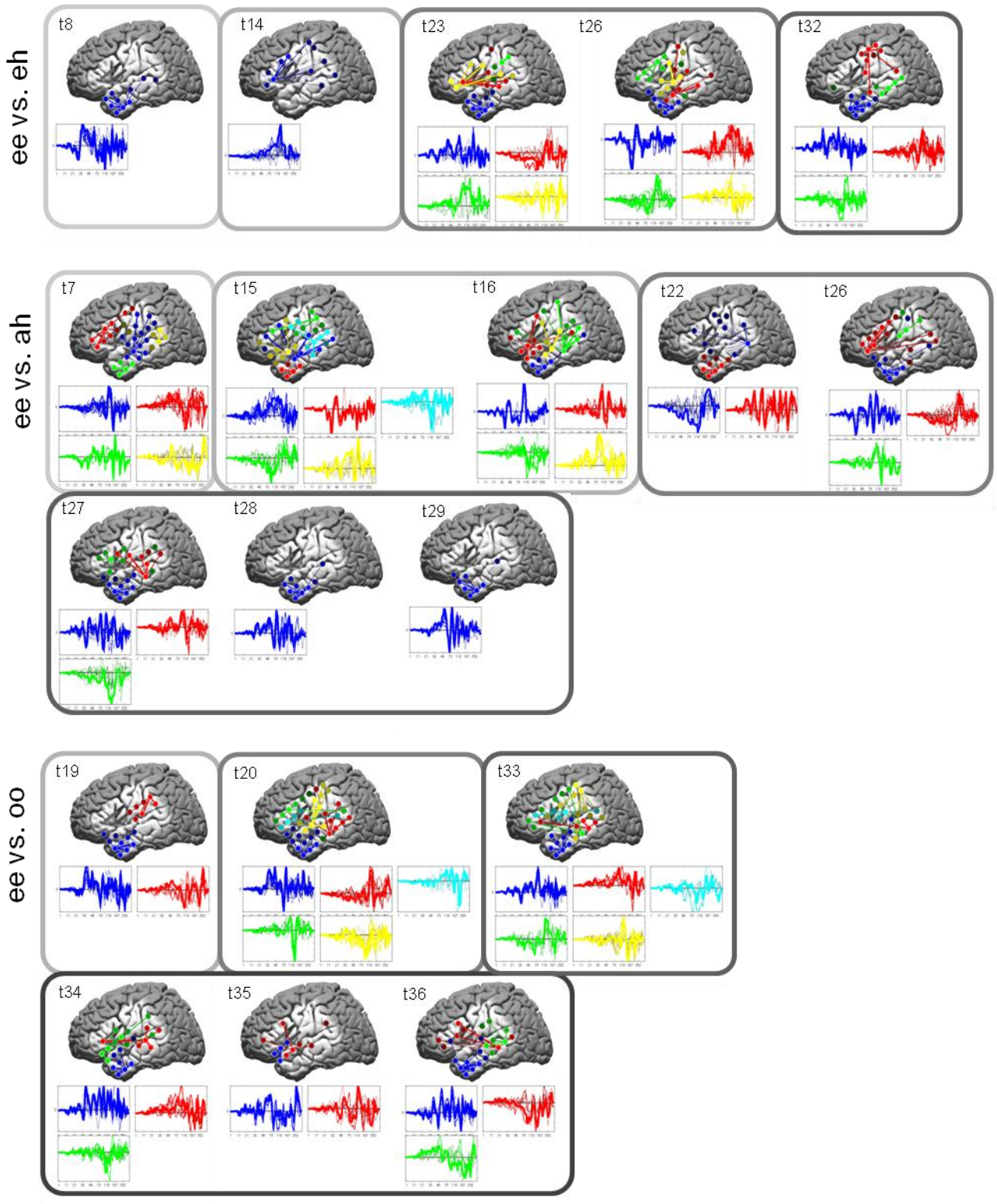

Figure A.7: Phoneme discriminant Core FSNs for subject 5 part 1.

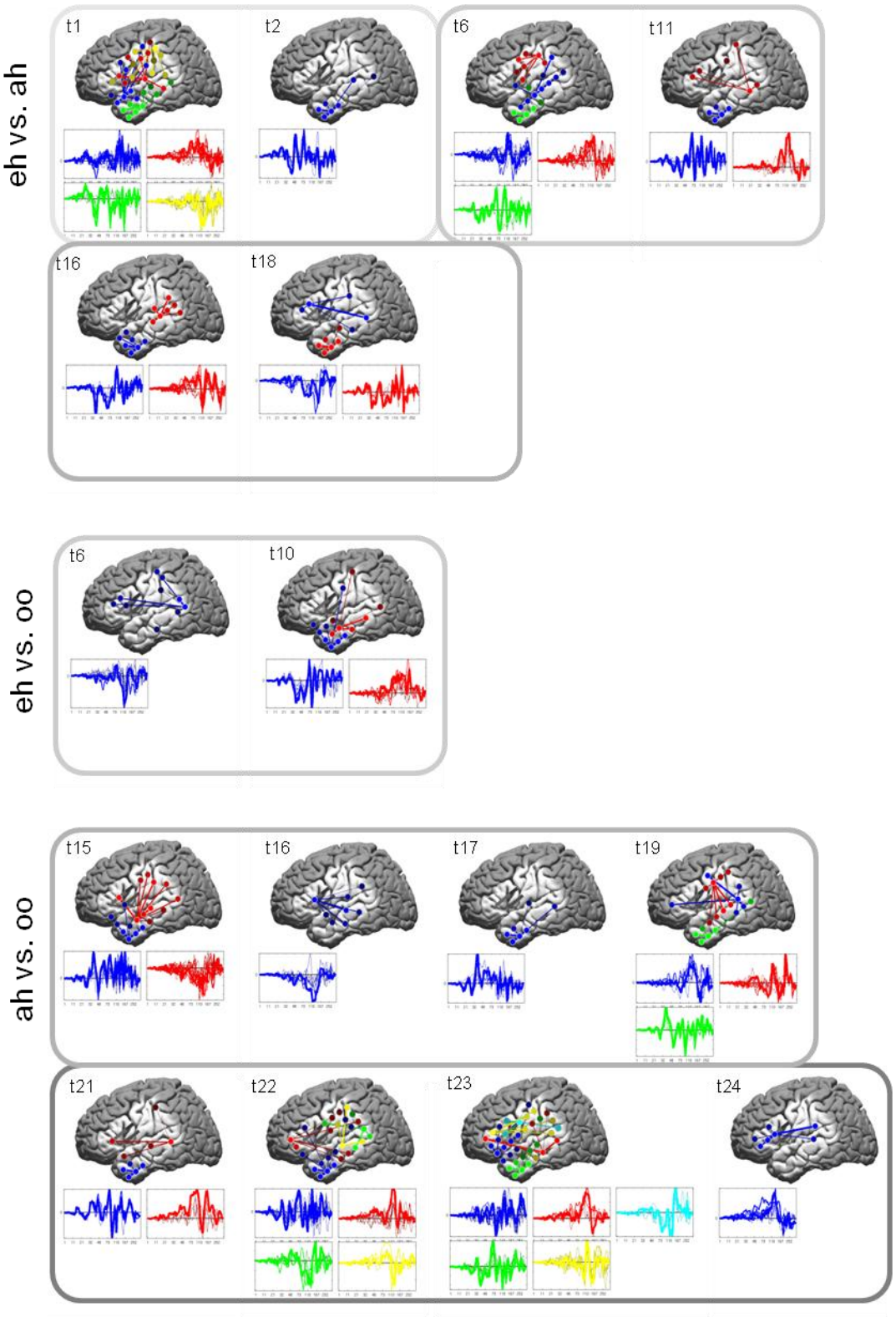

Figure A.8 Phoneme discriminant Core FSNs for subject 5 part 2.

References

1. Leuthardt, E.C., et al., *The emerging world of motor neuroprosthetics: a neurosurgical perspective.* Neurosurgery, 2006. **59**(1): p. 1-14; discussion 1-14.
2. Birbaumer, N., *Breaking the silence: brain-computer interfaces (BCI) for communication and motor control.* Psychophysiology, 2006. **43**(6): p. 517-32.
3. Birbaumer, N. and K. Haagen, *Restoration of Movement and Thought from Neuroelectric and Metabolic Brain Activity: Brain-Computer Interfaces (BCIs)*, in *Intelligent Computing Everywhere*, A.J. Schuster, Editor. 2007, Springer London: London, UK. p. 129-152.
4. saypeople.com. Available from: http://saypeople.com/wp-content/uploads/2011/12/Cortex.jpg.
5. Kyriakopoulos, M., et al., *Diffusion tensor imaging in schizophrenia.* Eur Psychiatry, 2008. **23**(4): p. 255-73.
6. Friston, K.J., et al., *Functional topography: multidimensional scaling and functional connectivity in the brain.* Cereb Cortex, 1996. **6**(2): p. 156-64.
7. Haemaelaeinen, M., et al., *Magnetoencephalography---theory, instrumentation, and applications to noninvasive studies of the working human brain.* Reviews of Modern Physics, 1993. **65**: p. 413-497.
8. Dale, N., et al., *Listening to the brain: microelectrode biosensors for neurochemicals.* Trends Biotechnol, 2005. **23**(8): p. 420-8.
9. Hubel, D.H. and T.N. Wiesel, *Receptive fields and functional architecture of monkey striate cortex.* J Physiol, 1968. **195**(1): p. 215-43.
10. Georgopoulos, A.P., A.B. Schwartz, and R.E. Kettner, *Neuronal population coding of movement direction.* Science, 1986. **233**(4771): p. 1416-9.
11. O'Keefea, J. and J. Dostrovsky, *The hippocampus as a spatial map. Preliminary evidence from unit activity in the freely-moving rat.* Brain Research, 1971. **34**(1): p. 171-175.
12. Seymour, J.P. and D.R. Kipke, *Neural probe design for reduced tissue encapsulation in CNS.* Biomaterials, 2007. **28**(25): p. 3594-607.
13. Vidal, J.J., *Real-time detection of brain events in EEG.* Special Issue Biological Signal Processing Analysis, 1977. **65**(5): p. 633-664.
14. Kramis, R., C.H. Vanderwolf, and B.H. Bland, *Two types of hippocampal rhythmical slow activity in both the rabbit and the rat: relations to behavior and effects of atropine, diethyl ether, urethane, and pentobarbital.* Exp Neurol, 1975. **49**(1 Pt 1): p. 58-85.
15. Crone, N.E., et al., *Functional mapping of human sensorimotor cortex with electrocorticographic spectral analysis - I. Alpha and beta event-related desynchronization.* Brain, 1998. **121**: p. 2271-2299.
16. Crone, N.E., et al., *Functional mapping of human sensorimotor cortex with electrocorticographic spectral analysis - II. Event-related synchronization in the gamma band.* Brain, 1998. **121**: p. 2301-2315.
17. Miller, K.J., et al., *Spectral changes in cortical surface potentials during motor movement.* J Neurosci, 2007. **27**(9): p. 2424-32.
18. Shah, A.S., et al., *Neural dynamics and the fundamental mechanisms of event-related brain potentials.* Cereb Cortex, 2004. **14**(5): p. 476-83.
19. Ng, E.H., et al., *Endometrial and subendometrial blood flow measured during early luteal phase by three-dimensional power Doppler ultrasound in excessive ovarian responders.* Hum Reprod, 2004. **19**(4): p. 924-31.
20. Rubehn, B., P. Fries, and T. Stieglitz. *MEMS-Technology for Large-Scale, Multichannel ECoG-Electrode Array Manufacturing.* in *4th European Conference of the International Federation for Medical and Biological Engineering*. 2008. Antwerp, Belgium: Springer Berlin Heidelberg.
21. Yamamoto, T., et al., *Recording of corticospinal evoked potential for optimum placement of motor cortex stimulation electrodes in the treatment of post-stroke pain.* Neurol Med Chir (Tokyo), 2007. **47**(9): p. 409-14.
22. Velasco, F., et al., *Motor cortex electrical stimulation applied to patients with complex regional pain syndrome.* Pain, 2009. **147**(1-3): p. 91-8.
23. Yanagisawa, T., et al., *Neural decoding using gyral and intrasulcal electrocorticograms.* Neuroimage, 2009. **45**(4): p. 1099-106.

24. Ojemann, J.G., E.C. Leuthardt, and K.J. Miller, *Brain-machine interface: restoring neurological function through bioengineering.* Clin Neurosurg, 2007. **54**: p. 134-6.
25. Leuthardt, E.C., et al., *Electrocorticography-based brain computer interface--the Seattle experience.* IEEE Trans Neural Syst Rehabil Eng, 2006. **14**(2): p. 194-8.
26. Gaona, C.M., et al., *Nonuniform high-gamma (60-500 Hz) power changes dissociate cognitive task and anatomy in human cortex.* J Neurosci, 2011. **31**(6): p. 2091-100.
27. Jacobs, J. and M.J. Kahana, *Direct brain recordings fuel advances in cognitive electrophysiology.* Trends Cogn Sci, 2010. **14**(4): p. 162-71.
28. Leuthardt, E.C., et al., *A brain-computer interface using electrocorticographic signals in humans.* J Neural Eng, 2004. **1**(2): p. 63-71.
29. Engel, A.K., P. Fries, and W. Singer, *Dynamic predictions: oscillations and synchrony in top-down processing.* Nat Rev Neurosci, 2001. **2**(10): p. 704-16.
30. Fries, P., D. Nikolic, and W. Singer, *The gamma cycle.* Trends Neurosci, 2007. **30**(7): p. 309-16.
31. Fries, P., *Neuronal gamma-band synchronization as a fundamental process in cortical computation.* Annu Rev Neurosci, 2009. **32**: p. 209-24.
32. Singer, W. and C.M. Gray, *Visual feature integration and the temporal correlation hypothesis.* Annu Rev Neurosci, 1995. **18**: p. 555-86.
33. Rotermund, D., et al., *Attention improves object representation in visual cortical field potentials.* J Neurosci, 2009. **29**(32): p. 10120-30.
34. Ray, S., et al., *High-frequency gamma activity (80-150Hz) is increased in human cortex during selective attention.* Clin Neurophysiol, 2008. **119**(1): p. 116-33.
35. Jensen, O., J. Kaiser, and J.P. Lachaux, *Human gamma-frequency oscillations associated with attention and memory.* Trends Neurosci, 2007. **30**(7): p. 317-24.
36. Pfurtscheller, G. and C. Andrew, *Event-Related changes of band power and coherence: methodology and interpretation.* J Clin Neurophysiol, 1999. **16**(6): p. 512-9.
37. McFarland, D.J., et al., *Mu and beta rhythm topographies during motor imagery and actual movements.* Brain Topogr, 2000. **12**(3): p. 177-86.
38. Wolpaw, J.R., et al., *Brain-computer interfaces for communication and control.* Clin Neurophysiol, 2002. **113**(6): p. 767-91.
39. Fabiani, G.E., et al., *Conversion of EEG activity into cursor movement by a brain-computer interface (BCI).* IEEE Trans Neural Syst Rehabil Eng, 2004. **12**(3): p. 331-8.
40. Pfurtscheller, G., et al., *Mu rhythm (de)synchronization and EEG single-trial classification of different motor imagery tasks.* Neuroimage, 2006. **31**(1): p. 153-9.
41. Gevins, A., et al., *Monitoring working memory load during computer-based tasks with EEG pattern recognition methods.* Hum Factors, 1998. **40**(1): p. 79-91.
42. Low, A., et al., *Determining working memory from ERP topography.* Brain Topogr, 1999. **12**(1): p. 39-47.
43. Sederberg, P.B., et al., *Theta and gamma oscillations during encoding predict subsequent recall.* J Neurosci, 2003. **23**(34): p. 10809-14.
44. Ramsey, N.F., et al., *Towards human BCI applications based on cognitive brain systems: an investigation of neural signals recorded from the dorsolateral prefrontal cortex.* IEEE Trans Neural Syst Rehabil Eng, 2006. **14**(2): p. 214-7.
45. Vansteensel, M.J., et al., *Brain-computer interfacing based on cognitive control.* Ann Neurol, 2010. **67**(6): p. 809-16.
46. Singer, W., *Understanding the brain. How can our intuition fail so fundamentally when it comes to studying the organ to which it owes its existence?* EMBO Rep, 2007. **8 Spec No**: p. S16-9.
47. Amari, S., *Dynamics of pattern formation in lateral-inhibition type neural fields.* Biol Cybern, 1977. **27**(2): p. 77-87.
48. Wang, X.J. and G. Buzsaki, *Gamma oscillation by synaptic inhibition in a hippocampal interneuronal network model.* J Neurosci, 1996. **16**(20): p. 6402-13.
49. Salinas, E. and T.J. Sejnowski, *Correlated neuronal activity and the flow of neural information.* Nat Rev Neurosci, 2001. **2**(8): p. 539-50.
50. Nir, Y., et al., *Coupling between neuronal firing rate, gamma LFP, and BOLD fMRI is related to interneuronal correlations.* Curr Biol, 2007. **17**(15): p. 1275-85.
51. Freeman, W.J., *The physiology of perception.* Sci Am, 1991. **264**(2): p. 78-85.

52. Jacobs, J. and M.J. Kahana, *Neural representations of individual stimuli in humans revealed by gamma-band electrocorticographic activity.* J Neurosci, 2009. **29**(33): p. 10203-14.
53. Lachaux, J.P., et al., *Measuring phase synchrony in brain signals.* Hum Brain Mapp, 1999. **8**(4): p. 194-208.
54. Tanji, K., et al., *High-frequency gamma-band activity in the basal temporal cortex during picture-naming and lexical-decision tasks.* J Neurosci, 2005. **25**(13): p. 3287-93.
55. Manning, J.R., et al., *Broadband shifts in local field potential power spectra are correlated with single-neuron spiking in humans.* J Neurosci, 2009. **29**(43): p. 13613-20.
56. Milstein, J., et al., *Neuronal shot noise and Brownian 1/f2 behavior in the local field potential.* PLoS One, 2009. **4**(2): p. e4338.
57. He, B.J. and M.E. Raichle, *The fMRI signal, slow cortical potential and consciousness.* Trends Cogn Sci, 2009. **13**(7): p. 302-9.
58. He, B.J. and M.E. Raichle, *Response to Koch: Elaborations on the SCP hypothesis.* Trends Cogn Sci, 2009. **13**(9): p. 368-369.
59. Breshears, J.D., et al., *Mapping Sensorimotor Cortex Using Slow Cortical Potential Resting-State Networks While Awake and Under Anesthesia.* Neurosurgery, 2012.
60. Rizzuto, D.S., et al., *Reset of human neocortical oscillations during a working memory task.* Proc Natl Acad Sci U S A, 2003. **100**(13): p. 7931-6.
61. Tallon-Baudry, C., O. Bertrand, and C. Fischer, *Oscillatory synchrony between human extrastriate areas during visual short-term memory maintenance.* J Neurosci, 2001. **21**(20): p. RC177.
62. Sehatpour, P., et al., *A human intracranial study of long-range oscillatory coherence across a frontal-occipital-hippocampal brain network during visual object processing.* Proc Natl Acad Sci U S A, 2008. **105**(11): p. 4399-404.
63. Gaillard, R., et al., *Converging intracranial markers of conscious access.* PLoS Biol, 2009. **7**(3): p. e61.
64. Canolty, R.T., et al., *High gamma power is phase-locked to theta oscillations in human neocortex.* Science, 2006. **313**(5793): p. 1626-8.
65. Schroeder, C.E., et al., *Neuronal oscillations and visual amplification of speech.* Trends Cogn Sci, 2008. **12**(3): p. 106-13.
66. Tort, A.B., et al., *Dynamic cross-frequency couplings of local field potential oscillations in rat striatum and hippocampus during performance of a T-maze task.* Proc Natl Acad Sci U S A, 2008. **105**(51): p. 20517-22.
67. Darvas, F., et al., *Nonlinear phase-phase cross-frequency coupling mediates communication between distant sites in human neocortex.* J Neurosci, 2009. **29**(2): p. 426-35.
68. He, B.J., et al., *The temporal structures and functional significance of scale-free brain activity.* Neuron, 2010. **66**(3): p. 353-69.
69. Schalk, G., et al., *Two-dimensional movement control using electrocorticographic signals in humans.* J Neural Eng, 2008. **5**(1): p. 75-84.
70. Ojemann, J.G., G.A. Ojemann, and E. Lettich, *Cortical stimulation mapping of language cortex by using a verb generation task: effects of learning and comparison to mapping based on object naming.* J Neurosurg, 2002. **97**(1): p. 33-8.
71. Talairach, J. and P. Tournoux, *Co-planar Stereotaxic Atlas of the Human Brain: 3-Dimensional Proportional System - an Approach to Cerebral Imaging.* 4 ed. Vol. 39. 1988, New York, NY: Thieme Medical Publishers.
72. Miller, K.J., et al., *Cortical electrode localization from X-rays and simple mapping for electrocorticographic research: The "Location on Cortex" (LOC) package for MATLAB.* J Neurosci Methods, 2007. **162**(1-2): p. 303-8.
73. Leuthardt, E.C., et al., *Using the electrocorticographic speech network to control a brain-computer interface in humans.* J Neural Eng, 2011. **8**(3): p. 036004.
74. Schalk, G., et al., *BCI2000: a general-purpose brain-computer interface (BCI) system.* IEEE Trans Biomed Eng, 2004. **51**(6): p. 1034-43.
75. McFarland, D.J., A. Toddlefkowicz, and J.R. Wolpaw, *Design and operation of an EEG-based brain-computer interface with digital signal processing technology.* Behavior Research Methods, Instruments, & Computers, 1997. **29**(3): p. 337-345.
76. McFarland, D.J., W.A. Sarnacki, and J.R. Wolpaw, *Brain-computer interface (BCI) operation: optimizing information transfer rates.* Biol Psychol, 2003. **63**(3): p. 237-51.
77. Birbaumer, N., et al., *The thought translation device (TTD) for completely paralyzed patients.* IEEE Trans Rehabil Eng, 2000. **8**(2): p. 190-3.

78. Donchin, E., K.M. Spencer, and R. Wijesinghe, *The mental prosthesis: assessing the speed of a P300-based brain-computer interface*. IEEE Trans Rehabil Eng, 2000. **8**(2): p. 174-9.
79. McFarland, D.J. and J.R. Wolpaw, *EEG-based communication and control: speed-accuracy relationships*. Appl Psychophysiol Biofeedback, 2003. **28**(3): p. 217-31.
80. Guger, C., et al., *How many people are able to operate an EEG-based brain-computer interface (BCI)?* IEEE Trans Neural Syst Rehabil Eng, 2003. **11**(2): p. 145-7.
81. Zhu, X., et al., *Expectation-Maximization Method for EEG-Based Continuous Cursor Control*. EURASIP Journal on Advances in Signal Processing, 2007. **2007**: p. 1-10.
82. Blankertz, B., et al., *The non-invasive Berlin Brain-Computer Interface: fast acquisition of effective performance in untrained subjects*. Neuroimage, 2007. **37**(2): p. 539-50.
83. Taylor, D.M., S.I. Tillery, and A.B. Schwartz, *Direct cortical control of 3D neuroprosthetic devices*. Science, 2002. **296**(5574): p. 1829-32.
84. Serruya, M.D., et al., *Instant neural control of a movement signal*. Nature, 2002. **416**(6877): p. 141-2.
85. Hochberg, L.R., et al., *Neuronal ensemble control of prosthetic devices by a human with tetraplegia*. Nature, 2006. **442**(7099): p. 164-71.
86. Hatsopoulos, N.G. and J.P. Donoghue, *The Science of Neural Interface Systems*. Annu Rev Neurosci, 2009.
87. Hochberg, L.R., et al., *Reach and grasp by people with tetraplegia using a neurally controlled robotic arm*. Nature, 2012. **485**(7398): p. 372-5.
88. Wisneski, K.J., et al., *Unique cortical physiology associated with ipsilateral hand movements and neuroprosthetic implications*. Stroke, 2008. **39**(12): p. 3351-9.
89. Breshears, J.D., et al., *Decoding motor signals from the pediatric cortex: implications for brain-computer interfaces in children*. Pediatrics, 2011. **128**(1): p. e160-8.
90. Miller, K.J., et al. *Correlation in paired one-dimensional, closed loop, overt, motor controlled BCI*. in *3rd International Brain-Computer Interface Workshop and Training Course*. 2006. Graz University of Technology, Austria.
91. Miller, K.J., et al., *Three cases of feature correlation in an electrocorticographic BCI*. Conf Proc IEEE Eng Med Biol Soc, 2008. **2008**: p. 5318-21.
92. Dat, T.H., L. Shue, and C. Guan. *Electrocorticographic signal classification based on time-frequency decomposition and nonparametric statistical modeling*. in *28th IEEE EMBS Annual International Conference*. 2006. New York City, NY: IEEE.
93. Ince, N.F., F. Goksu, and A.H. Tewfik, *An ECoG Based Brain Computer Interface with Spatially Adapted Time Frequency Patterns*, in *Int. Conf.(BIOSTEC)*. 2008.
94. Leuthardt, E.C., et al., *Microscale recording from human motor cortex - implications for a minimally invasive electrocorticographic brain computer interface (ECoG BCIs)*. Journal of Neurosurgery (in review), 2009.
95. Blakely, T., et al., *Localization and classification of phonemes using high spatial resolution electrocorticography (ECoG) grids*. Conf Proc IEEE Eng Med Biol Soc, 2008. **2008**: p. 4964-7.
96. Shenoy, P., et al., *Generalized features for electrocorticographic BCIs*. IEEE Trans Biomed Eng, 2008. **55**(1): p. 273-80.
97. Towle, V.L., et al., *ECoG gamma activity during a language task: differentiating expressive and receptive speech areas*. Brain, 2008. **131**(Pt 8): p. 2013-27.
98. Schalk, G., et al., *Decoding two-dimensional movement trajectories using electrocorticographic signals in humans*. J Neural Eng, 2007. **4**(3): p. 264-75.
99. Pistohl, T., et al., *Prediction of arm movement trajectories from ECoG-recordings in humans*. J Neurosci Methods, 2008. **167**(1): p. 105-14.
100. Shenoy, P., et al. *Finger Movement Classification for an Electrocorticographic BCI*. in *3rd International IEEE EMBS Conference on Neural Engineering*. 2007. Kohala Coast, HI: IEEE.
101. Miller, K.J., et al., *Decoupling the cortical power spectrum reveals real-time representation of individual finger movements in humans*. J Neurosci, 2009. **29**(10): p. 3132-7.
102. Wang, W., et al. *Human motor cortical activity recorded with Micro-ECoG electrodes, during individual finger movements*. in *Engineering in Medicine and Biology Society, EMBC 2009.* . 2009. Minneapolis, MN, USA.
103. Zanos, S., K.J. Miller, and J.G. Ojemann, *Electrocorticographic spectral changes associated with ipsilateral individual finger and whole hand movement*. Conf Proc IEEE Eng Med Biol Soc, 2008. **2008**: p. 5939-42.

104. Pei, X., et al., *Decoding vowels and consonants in spoken and imagined words using electrocorticographic signals in humans.* J Neural Eng, 2011. **8**(4): p. 046028.
105. Pei, X., et al., *Spatiotemporal dynamics of electrocorticographic high gamma activity during overt and covert word repetition.* Neuroimage, 2011. **54**(4): p. 2960-72.
106. Felton, E.A., et al., *Electrocorticographically controlled brain-computer interfaces using motor and sensory imagery in patients with temporary subdural electrode implants. Report of four cases.* J Neurosurg, 2007. **106**(3): p. 495-500.
107. Thampratankul, L., et al., *Cortical gamma oscillations modulated by word association tasks: intracranial recording.* Epilepsy Behav, 2010. **18**(1-2): p. 116-8.
108. Schalk, G., et al., *Brain-computer interfaces (BCIs): detection instead of classification.* J Neurosci Methods, 2008. **167**(1): p. 51-62.
109. Brunner, P., et al., *A practical procedure for real-time functional mapping of eloquent cortex using electrocorticographic signals in humans.* Epilepsy Behav, 2009. **15**(3): p. 278-86.
110. Jerbi, K., et al., *Watching brain TV and playing brain ball exploring novel BCI strategies using real-time analysis of human intracranial data.* Int Rev Neurobiol, 2009. **86**: p. 159-68.
111. Woolsey, T.A. and H. Van der Loos, *The structural organization of layer IV in the somatosensory region (SI) of mouse cerebral cortex. The description of a cortical field composed of discrete cytoarchitectonic units.* Brain Res, 1970. **17**(2): p. 205-42.
112. Georgopoulos, A.P., R.E. Kettner, and A.B. Schwartz, *Primate motor cortex and free arm movements to visual targets in three-dimensional space. II. Coding of the direction of movement by a neuronal population.* J Neurosci, 1988. **8**(8): p. 2928-37.
113. Quiroga, R.Q., et al., *Invariant visual representation by single neurons in the human brain.* Nature, 2005. **435**(7045): p. 1102-7.
114. Bitterman, Y., et al., *Ultra-fine frequency tuning revealed in single neurons of human auditory cortex.* Nature, 2008. **451**(7175): p. 197-201.
115. Price, C.J., *The anatomy of language: contributions from functional neuroimaging.* J Anat, 2000. **197 Pt 3**: p. 335-59.
116. John, E.R., A.L. Leiman, and E. Sachs, *An exploration of the functional relationship between electroencephalographic potentials and differential inhibition.* Ann N Y Acad Sci, 1961. **92**: p. 1160-82.
117. Fries, P., et al., *Oscillatory neuronal synchronization in primary visual cortex as a correlate of stimulus selection.* J Neurosci, 2002. **22**(9): p. 3739-54.
118. Ghazanfar, A.A., C.R. Stambaugh, and M.A. Nicolelis, *Encoding of tactile stimulus location by somatosensory thalamocortical ensembles.* J Neurosci, 2000. **20**(10): p. 3761-75.
119. von Stein, A. and J. Sarnthein, *Different frequencies for different scales of cortical integration: from local gamma to long range alpha/theta synchronization.* Int J Psychophysiol, 2000. **38**(3): p. 301-13.
120. Riehle, A., et al., *Spike synchronization and rate modulation differentially involved in motor cortical function.* Science, 1997. **278**(5345): p. 1950-3.
121. Steinmetz, P.N., et al., *Attention modulates synchronized neuronal firing in primate somatosensory cortex.* Nature, 2000. **404**(6774): p. 187-90.
122. Fries, P., et al., *Modulation of oscillatory neuronal synchronization by selective visual attention.* Science, 2001. **291**(5508): p. 1560-3.
123. Cabeza, R. and L. Nyberg, *Neural bases of learning and memory: functional neuroimaging evidence.* Curr Opin Neurol, 2000. **13**(4): p. 415-21.
124. McIntosh, A.R., *Mapping cognition to the brain through neural interactions.* Memory, 1999. **7**(5-6): p. 523-48.
125. Bassett, D.S. and E. Bullmore, *Small-world brain networks.* Neuroscientist, 2006. **12**(6): p. 512-23.
126. Fanselow, E.E., A.P. Reid, and M.A. Nicolelis, *Reduction of pentylenetetrazole-induced seizure activity in awake rats by seizure-triggered trigeminal nerve stimulation.* J Neurosci, 2000. **20**(21): p. 8160-8.
127. Chong, L., et al. *Classification of ECoG signals for motor imagery tasks*. in *2nd International Conference on Signal Processing Systems (ICSPS)* 2010. Dalian, China.
128. Zhao, H.B., et al., *Channel Selection and Feature Extraction of ECoG-Based Brain-Computer Interface Using Band Power.* Applied Mechanics and Materials, 2010. **44 - 47**: p. 3564-3568.
129. Ombao, H., et al., *Spatio-spectral analysis of brain signals.* Statistica Sinica, 2008. **18**: p. 1465-1482.
130. Branco, D.M., et al., *Functional variability of the human cortical motor map: electrical stimulation findings in perirolandic epilepsy surgery.* J Clin Neurophysiol, 2003. **20**(1): p. 17-25.

131. Bruns, A., *Fourier-, Hilbert- and wavelet-based signal analysis: are they really different approaches?* J Neurosci Methods, 2004. **137**(2): p. 321-32.
132. Johnson, R.A. and D.W. Wichern, *Applied multivariate statistical analysis*. 5th ed. 2002, Upper Sadle River, NJ: Prentice Hall.
133. Friman, O., et al., *Detection of neural activity in fMRI using maximum correlation modeling.* Neuroimage, 2002. **15**(2): p. 386-95.
134. Muller, H.P., et al., *New methods in fMRI analysis. Hierarchical cluster analysis for improved signal-to-noise ratio compared to standard techniques.* IEEE Eng Med Biol Mag, 2002. **21**(5): p. 134-42.
135. Fucsek, M., et al., *[Rare case of congenital transsphenoidal meningoencephalocele causing respiratory problems].* Orv Hetil, 2004. **145**(9): p. 483-9.
136. Pohar, M., M. Blas, and S. Turk, *Comparison of Logistic Regression and Linear Discriminant Analysis: A Simulation Study* Metodološki zvezki, 2004. **1**(1): p. 143-161.
137. Maris, E., Oostenveld, R., *Nonparametric statistical testing of EEG- and MEG-data.* J. of Neuro. Sci. Methods, 2007(164): p. 177-190.
138. Frey, B.J. and D. Dueck, *Clustering by passing messages between data points.* Science, 2007. **315**(5814): p. 972-6.
139. Schalk, G., et al., *Real-time detection of event-related brain activity.* Neuroimage, 2008. **43**(2): p. 245-9.
140. Fransson, P., *Spontaneous low-frequency BOLD signal fluctuations: an fMRI investigation of the resting-state default mode of brain function hypothesis.* Hum Brain Mapp, 2005. **26**(1): p. 15-29.
141. Laurienti, P.J., *Deactivations, global signal, and the default mode of brain function.* J Cogn Neurosci, 2004. **16**(9): p. 1481-3.
142. Gusnard, D.A., et al., *Medial prefrontal cortex and self-referential mental activity: relation to a default mode of brain function.* Proc Natl Acad Sci U S A, 2001. **98**(7): p. 4259-64.
143. Raichle, M.E., et al., *A default mode of brain function.* Proc Natl Acad Sci U S A, 2001. **98**(2): p. 676-82.
144. De Luca, M., et al., *fMRI resting state networks define distinct modes of long-distance interactions in the human brain.* Neuroimage, 2006. **29**(4): p. 1359-67.
145. Pizoli, C.E., et al., *Resting-state activity in development and maintenance of normal brain function.* Proc Natl Acad Sci U S A, 2011. **108**(28): p. 11638-43.
146. van den Heuvel, M.P. and H.E. Hulshoff Pol, *Exploring the brain network: a review on resting-state fMRI functional connectivity.* Eur Neuropsychopharmacol, 2010. **20**(8): p. 519-34.
147. Raichle, M.E. and A.Z. Snyder, *A default mode of brain function: a brief history of an evolving idea.* Neuroimage, 2007. **37**(4): p. 1083-90; discussion 1097-9.
148. Smith, S.M., et al., *Correspondence of the brain's functional architecture during activation and rest.* Proc Natl Acad Sci U S A, 2009. **106**(31): p. 13040-5.
149. Mantini, D., et al., *Electrophysiological signatures of resting state networks in the human brain.* Proc Natl Acad Sci U S A, 2007. **104**(32): p. 13170-5.
150. He, B.J., et al., *Electrophysiological correlates of the brain's intrinsic large-scale functional architecture.* Proc Natl Acad Sci U S A, 2008. **105**(41): p. 16039-44.
151. Hinton, G.E., S. Osindero, and Y.W. Teh, *A fast learning algorithm for deep belief nets.* Neural Comput, 2006. **18**(7): p. 1527-54.
152. Hinton, G.E. and R.R. Salakhutdinov, *Reducing the dimensionality of data with neural networks.* Science, 2006. **313**(5786): p. 504-7.
153. Brand, M. *Incremental Singular Value Decomposition of Uncertain Data with Missing Values*. in *European Conference on Computer Vision*. 2002.

Vita

Zachary Voges Freudenburg

Degrees

Ph.D. Computer Science, August 2012
M.S. Computer Science, December 2004
B.S. Physics, May 2001

Professional Societies

Society of Neuroscience
IEEE

Publications

Freudenburg, Z. V., Anderson, N., Pless, R. Smart, W. D., Leuthardt, E. C. (2008) Advantages of a gabor wavelet dictionary in ECoG signal analysis. *Abstract for Socety for Neuroscience Annual Conferences 2008*.

Freudenburg, Z. V., Ghosh, B. K., Ulinski, P. S. (2009) Synaptic adaptation and sustained generation of waves in a model of turtle visual cortex, *IEEE Trans. Biomed. Eng.* 56(5): 1277-1286.

Freudenburg, Z. V., Pless, R. Smart, W. D., Leuthardt, E. C. (2009) Evaluation of task driven anatomic-frequency networks using multivariate analysis of electrocorticographic (ECoG) signals. *Abstract for Socety for Neuroscience Annual Conferences 2009*.

Liu, Y., Sharma, M., Gaona, C. M., Breshears, J. D., Roland, J., Z. V. Freudenburg, Weinberger, K. Q., Eric C. Leuthardt, E. C. (2010) Decoding Ipsilateral Finger Movements from ECoG Signals in Humans. *Advances in Neural Information Processing* Systems *(NIPS).* 23: pages 1468-1476.

Breshears, J. D., Roland, J. L., Sharma, M., Gaona, C. M., Freudenburg, Z. V., Tempelhoff, R., Avidan, M. S., Leuthardt, E. C. (2010) Stable and dynamic cortical electrophysiology of induction and emergence with propofol anesthesia. Proc. Natl. Acad. Sci. U S A. 107(49): 21170-21175.

Freudenburg, Z. V., Ramsey, N. F., Wronkiewicz, M., Smart, W. D., Pless, R., Leuthardt (2011) Real-time Naive Learning of Neural Correlates in ECoG Electrophysiology. *Int. J. of Machine Learning and Computing.* 1(3): 269-278.

Freudenburg, Z. V., Vansteensel, M., Bleichner, M., Aarnoutse, E., Leijten, F., Ramsey, N. (2011) Phoneme decoding using high-density ECoG signal from the mouth region of motor cortex. *Abstract for Socety for Neuroscience Annual Conferences 2011.*

Breshears, J. D., Gaona, C. M., Roland, J. L., Sharma, M., Anderson, N. R., Bundy, D. T., Freudenburg, Z. V., Smyth, M. D., Zempel, J., Limbrick, D. D., Smart, W. D. Leuthardt, E. C. (2011) Decoding motor signals from the pediatric cortex: implications for brain-computer interfaces in children. *Pediatrics.* 128(1): e160-8.

Roland, J., Miller, K., Freudenburg, Z., Sharma, M., Smyth, M., Gaona, C., Breshears, J., Corbetta, M., Leuthardt, E. C. (2011) The effect of age on human motor electrocorticographic signals and implications for brain-computer interface applications. *J. Neural Eng.* 8(4): 046013.

Gaona, C. M., Sharma, M., Freudenburg, Z. V., Breshears, J. D., Bundy, D. T., Roland, J., Barbour, D. L., Schalk, G., Leuthardt, E. C. (2011) Nonuniform high-gamma (60-500 Hz) power changes dissociate cognitive task and anatomy in human cortex. *J Neurosci.* 31(6): 2091-2100.

Freudenburg, Z. V., Vansteensel, M., Bleichner, M., Aarnoutse, E., Gaona, C., Sharma, M., Bundy, D., Breshears, J., Pless, R. B., Ramsey, N. F., Leuthardt, E. C. (2012) Extracting functional brain networks from human resting state electrocorticography using spatio-spectral deep belief network analysis *Abstract for Socety for Neuroscience Annual Conferences 2012.*

August 2012

Visualization Of Neural Signals, Freudenburg, Ph.D., 2012